

# A Verified Compiler for Quantum Simulation

LIYI LI, Iowa State University, USA

FENFEN AN, Iowa State University, USA

FEDERICO ZAHARIEV, Iowa State University, USA

ZHI XIANG CHONG, Iowa State University, USA

AMR SABRY, Indiana University, USA

MARK S. GORDON, Iowa State University, USA

Hamiltonian simulation is a central application of quantum computing, with significant potential in modeling physical systems and solving complex optimization problems. Existing compilers for such simulations typically focus on low-level representations based on Pauli operators, limiting programmability and offering no formal guarantees of correctness across the compilation pipeline. We introduce QBLUE, a high-level, formally verified framework for compiling Hamiltonian simulations. QBLUE is based on the formalism of second quantization, which provides a natural and expressive way to describe quantum particle systems using creation and annihilation operators. To ensure safety and correctness, QBLUE includes a type system that tracks particle types and enforces Hermitian structure. The framework supports compilation to both digital and analog quantum circuits and captures multiple layers of semantics, from static constraints to dynamic evolution. All components of QBLUE, including its language design, type system, and compilation correctness, are fully mechanized in the Rocq proof framework, making it the first end-to-end verified compiler for second-quantized Hamiltonian simulation.

## 1 Introduction

Quantum simulation is a flagship application of quantum computing, promising to model physical systems [Du and Vary 2023; Kreshchuk et al. 2021; Zhang et al. 2021], chemical reactions [Cao et al. 2019; Evangelista and Batista 2023; Lanyon et al. 2010; McArdle et al. 2020], and materials [Emani et al. 2021; Fedorov and Gelfand 2021; Outeiral et al. 2021] with precision beyond classical capabilities [Feynman 1982]. Yet programming such simulations remains precarious. Current compilers for Hamiltonian simulation operate at low-level abstractions, often directly manipulating Pauli strings or untyped tensor expressions, and provide no formal guarantees about the correctness of the resulting circuits [Cao et al. 2024; Lao and Browne 2022; Li et al. 2022b; Peng et al. 2024]. This disconnect between high-level physical intent and low-level implementation risks silent errors, miscompiled models, and untrustworthy scientific outcomes.

We present QBLUE, the first *formally verified compiler* for quantum simulation based on the formalism of *second quantization*. QBLUE allows users to express Hamiltonians in terms of creation and annihilation operators, enforcing Hermiticity and physical validity through a high-level type system. Programs written in QBLUE are compiled into executable quantum circuits or analog schedules with *end-to-end formal guarantees*: every compilation path is verified using a mechanized proof system, and all generated artifacts preserve the intended quantum dynamics within proven error bounds.

To support this, QBLUE employs a three-tiered semantic architecture:

- **Constraint semantics** defines symbolic, well-typed Hamiltonians using second-quantized expressions subject to constraints such as Hermiticity and particle type;
- **Dynamic semantics** interprets the simulation operator  $\exp(-ir e)$  as the time evolution of the Hamiltonian  $e$  over a duration  $r$ ;

- **Application semantics** compiles the simulation operator into backend-specific execution artifacts, such as gate-based circuits via Trotterization or QDrift, or weighted interaction graphs for analog Ising platforms.

These layers are connected via a *type-indexed compilation pipeline*, verified in the RocQ proof framework [Bertot and Castéran 2013]. Each transformation is guided by types that track not just dimensions and modes (e.g., bosonic<sup>1</sup> vs. fermionic<sup>2</sup>), but also matrix kinds (plain, Hermitian, unitary), ensuring that the semantics of quantum simulation is preserved throughout. The type system plays a central role, as it enforces anti-commutation for fermions, validates that matrix expressions are well-formed and Hermitian where required, and ensures that exponentiated Hamiltonians yield unitary operators. Equational rules, canonicalization procedures, and symbolic rewrites are all type-preserving and fully mechanized.

QBLUE supports *multiple backends*, each with distinct compilation paths and correctness theorems. For digital platforms, QBLUE emits standard gate sequences with Trotterized simulation of Pauli terms. For stochastic simulation, it supports QDrift-based sampling. For analog devices, it produces native Ising Hamiltonians for direct scheduling. All paths are type-preserving and formally linked to the semantics of the original program.

We prove a central *compilation correctness theorem*: for any Hermitian-typed Hamiltonian expression  $e$  and simulation time  $r$ , the compiled program  $U$  simulates  $\exp(-ire)$  within a formally derived error bound  $\epsilon$ . These bounds are computed symbolically as part of the compiler and are backend-specific, capturing, for instance, differences between first-order Trotterization and QDrift. Backend-specific optimizations (e.g., analog graph emission) are verified to preserve semantics modulo these error bounds.

**Summary of Contributions.** This paper contributes:

- A typed second-quantization quantum programming language supporting bosonic and fermionic modes, symbolic operators, and physically meaningful type-indexed semantics;
- A verified compilation pipeline that spans constraint, dynamic, and application semantics targeting multiple backends (gate-based, stochastic, and analog) with certified error bounds;
- A mechanized metatheory, including type soundness, anti-commutation preservation, equational correctness, and end-to-end compilation theorems;
- A complete example of typed, verified Hamiltonian simulation, illustrating how symbolic physics programs can be compiled and executed with formal confidence.

**Paper Roadmap.** Section 2 introduces the two-site Hubbard model as a running example, showcasing how QBLUE encodes physical systems via typed creation and annihilation operators. Section 3 reviews mathematical preliminaries from quantum simulation and second quantization. Section 4 presents the core formal system of QBLUE, including syntax, type system, and equational theory. Section 5 describes the compilation pipeline in detail, including canonicalization, backend-specific transformations, and certified error bounds. Section 6 discusses related work across quantum simulation languages and verified compilers. Finally, Section 7 summarizes contributions and outlines future directions in verified quantum programming.

The RocQ proofs mentioned in the paper are available on Zenodo <https://zenodo.org/records/15852130>, anonymously. We additionally include eight appendices: Appendix A provides in-depth background; Appendix B collects lemmas on Trotterization error bounds; Appendix D analyzes the perturbative gadget construction; Appendix E surveys other particle transformation methods;

<sup>1</sup>More precisely, we model finite “boson-like” systems as representing a real boson needs an infinite Hilbert space state.

<sup>2</sup>For simplicity, we restrict fermions in one system to be of the same kind and the same spin.

Appendix F presents a Hubbard model for hydrogen chains; and Appendix G outlines other physical models definable in QBlue.

## 2 A Guided Example: QBLUE on a Two-Site Hubbard Model

To illustrate how QBLUE expresses, compiles, and verifies quantum models, we present a complete example: the fermionic Hubbard model on two lattice sites. This minimal system captures key features of many-body quantum mechanics, including particle motion, local interactions, and coherent evolution, while remaining compact enough to explore in a single section. Conceptually, it models a simple chemical reaction in which electrons tunnel between orbitals and repel each other when co-located, offering a physically grounded yet abstractly expressive setting for quantum programming and formal verification.

**Model Setup and Physical Operators.** The fermionic Hubbard model captures essential features of strongly correlated systems, such as quantum tunneling and on-site repulsion. Although originally formulated for extended lattices, even a two-site version reveals the core phenomena of many-body dynamics. We consider a one-dimensional lattice with two fermionic sites, labeled site 0 and site 1. Each site may be either *unoccupied* or *occupied* by a single fermion. The occupation number at each site is given by a value in  $\{0, 1\}$  (for bosons, the occupation number can be bigger than 1, see Section 4), where 0 means no particle and 1 means a particle is present. These values describe physical quantum states, not Boolean truth values, and are distinct from the numeric indices labeling the sites.

The total Hilbert space is  $\mathbb{C}^2 \otimes \mathbb{C}^2$ , with computational basis states  $|m\rangle |n\rangle$ , where  $m$  and  $n$  indicate the occupation of site 0 and site 1, respectively. Three standard fermionic operators define the system’s dynamics. The *creation operator*  $a^\dagger(j)$  adds a particle to site  $j$  if it is unoccupied: for instance,  $a^\dagger(0)|0\rangle|0\rangle = |1\rangle|0\rangle$ , and  $a^\dagger(1)|m\rangle|0\rangle = (-1)^m|m\rangle|1\rangle$ . Applying  $a^\dagger(j)$  to an occupied site yields the vacuous state  $O$ . The *annihilation operator*  $a(j)$  removes a particle if one is present: for example,  $a(0)|1\rangle|0\rangle = |0\rangle|0\rangle$  and  $a(1)|m\rangle|1\rangle = (-1)^m|m\rangle|0\rangle$ . Again, acting on an unoccupied site yields  $O$ . The *number operator*  $\mathbb{1}(j) = a^\dagger(j) \circ a(j)$  (and its complement  $\mathbb{0}(j) = a(j) \circ a^\dagger(j)$ ) projects onto the subspace where site  $j$  is occupied (or unoccupied, respectively).<sup>3</sup> This composition first annihilates a particle if present and then recreates it, preserving the state. For instance,  $\mathbb{1}(0)|1\rangle|0\rangle = |1\rangle|0\rangle$ , while  $\mathbb{1}(0)|0\rangle|0\rangle = O$ .

**Constraint Semantics: Hamiltonian as a Typed Expression.** The physical behavior of the system is captured as a constraint-level expression in QBLUE:

$$\hat{H} = - \left( a^\dagger(0) \circ a(1) + a^\dagger(1) \circ a(0) \right) + 2 \cdot \mathbb{1}(0) \circ \mathbb{1}(1).$$

The first component models coherent *tunneling* of a fermion between the two sites. The term  $a^\dagger(0) \circ a(1)$  removes a particle from site 1 and creates it at site 0, and vice versa for the mirror term. Together, they ensure symmetric transition amplitudes and reversible evolution. The second term models *on-site repulsion*: the state  $|1\rangle|1\rangle$ , where both sites are occupied, incurs an energy cost of 2.

Typing ensures this expression is well-formed. The type system classifies particle operators by the types of the sites ( $i$ ) they act on. Here, each site has type  $t^{\mathbb{N}}(2)$ , representing a spinless fermionic mode. The creation and annihilation operators act on single  $t^{\mathbb{N}}(2)$ -typed sites, and compositions like  $a^\dagger(0) \circ a(1)$  act over  $t^{\mathbb{N}}(2) \otimes t^{\mathbb{N}}(2)$ , two sites each typed as  $t^{\mathbb{N}}(2)$  ( $\otimes$  is marked blue when referring to type operators). The entire Hamiltonian is typed as  $\mathcal{F}^h(t^{\mathbb{N}}(2) \otimes t^{\mathbb{N}}(2))$ , meaning it is a

<sup>3</sup>In traditional literature, the number operator is denoted  $n(j) = a^\dagger(j)a(j)$ ; here, we write it as  $\mathbb{1}(j)$  to emphasize its role as a projector onto the occupied subspace.

Hermitian constraint-level expression over fermionic types. This forms the *constraint semantics* of the program: a typed specification of allowable physical interactions.

Note that a single QBLUE operator,  $a^\dagger$  or  $a$ , is not Hermitian. QBLUE utilizes a *kind flag* to identify expressions as Hermitian (h) or non-Hermitian (p), e.g.,  $a^\dagger$  is typed as  $\mathcal{F}^p(t^{\mathbb{N}}(2))$ . We then utilize type-guided equational theory to identify Hermitian constraint-level expressions. Via the QBLUE type soundness theorem, we unveil the following.

**PROPOSITION 2.1 (UNITARY EXISTENCE OF HERMITIAN CONSTRAINTS).** Given a Hamiltonian  $e$ , typed as  $\iota \vdash e \triangleright \mathcal{F}^h(\iota)$ , for all  $r$ , the  $\exp(-ir e)$  semantics is properly defined in QBLUE.

The lemmas are given in Section 4.6. The fact ensures that every h-kind expression can be simulated via our Hamiltonian simulation operator, explained shortly below.

**Dynamic Semantics: Mapping to Pauli Operators.** To simulate the model, QBLUE compiles constraint-level expressions into qubit-level operators using the Jordan-Wigner transformation. This yields the *dynamic semantics*, a.k.a., Hamiltonian simulation ( $\exp(-ir e)$ ), which governs unitary evolution on qubit registers.

The number operator maps to  $\mathbb{1}(j) = \frac{I-Z(j)}{2}$ <sup>4</sup>, where  $Z(j)$  is the Pauli-Z matrix. The tunneling term becomes  $\frac{1}{2}(X(0) \circ X(1) + Y(0) \circ Y(1))$ , where  $X(j)$  and  $Y(j)$  are Pauli-X and Y matrices. Substituting yields:

$$\hat{H} = -\frac{1}{2}(X(0) \circ X(1) + Y(0) \circ Y(1)) + 2 \cdot \left( \frac{I-Z(0)}{2} \right) \circ \left( \frac{I-Z(1)}{2} \right),$$

which simplifies to:

$$\hat{H} = -\frac{1}{2}(X(0) \circ X(1) + Y(0) \circ Y(1)) + \frac{1}{2}(I - Z(0) - Z(1) + Z(0) \circ Z(1)). \quad (2.1)$$

Dropping constant and local-field terms yields the effective Hamiltonian:

$$\hat{H}' = -\frac{1}{2}(X(0) \circ X(1) + Y(0) \circ Y(1)) + \frac{1}{2}Z(0) \circ Z(1). \quad (2.2)$$

Transforming  $\hat{H}$  to  $\hat{H}'$  introduces some system errors, explained shortly below. This form is used for digital simulation or direct execution on analog backends. In both cases, type-correctness ensures that the transformation preserves the intended physical behavior. Extending the result from our type soundness, we show that every h-kind constraint expression  $e$  can be rewritten into a Pauli-based expression with a canonicalized form, as follows.

**PROPOSITION 2.2 (ALWAYS CANONICALIZIBLE).** Given a  $n$ -site Hamiltonian  $e$ , typed as  $\iota \vdash e \triangleright \mathcal{F}^h(\iota)$ ,  $e$  can be canonicalized to a Pauli-string-based Hamiltonian  $\hat{H} = \sum_j r_j \cdot (\bigotimes_{k=0}^{n-1} \mathcal{P}_{j,k})$  with  $\mathcal{P} \in \{X, Y, Z, I\}$ .

The lemmas are shown in Sections 5.1 and 5.2. We show that the canonicalized Pauli-string-based Hamiltonian can always be in the form of a sum of pairs of a real-number amplitude with a Pauli string of single-Pauli operators.

**Application Semantics: Target-Specific Execution.** The final step assigns meaning to the Hamiltonian through backend-specific execution—the *application semantics*. On gate-based quantum devices, QBLUE applies Trotterization to approximate time evolution. For  $r = \frac{\pi}{4}$ , we obtain<sup>5</sup>:

$$\exp(-ir\hat{H}') \approx \exp(-i\frac{-\pi}{8}X(0) \circ X(1)) \circ \exp(-i\frac{-\pi}{8}Y(0) \circ Y(1)) \circ \exp(-i\frac{\pi}{8}Z(0) \circ Z(1)). \quad (2.3)$$

<sup>4</sup>We use a single  $I$  without any indices to indicate a tensor of identity operations applied to all sites.

<sup>5</sup>Hamiltonian simulation  $\exp(-ir\hat{H})$  typically requires  $r$  to be positive, while negative time simulation can be done by inverting the circuit. The restriction is on the analog schedule generation, as we require  $r$  to be positive in every step.

Each exponential is implemented using standard gate patterns:

- $X(0) \circ X(1)$ : Hadamard basis change, CNOT–Rz–CNOT, undo basis.
- $Y(0) \circ Y(1)$ : rotate via  $S^\dagger$  and Hadamards, then same as above.
- $Z(0) \circ Z(1)$ : directly synthesized using CNOT–Rz–CNOT.

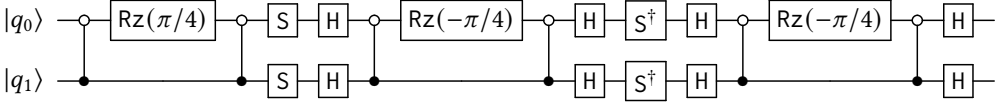


Fig. 1. Quantum circuit for one Trotter step of evolution under  $\hat{H}^\theta$ , with  $\theta = \pi/8$ . Terms are applied in the order  $Z(0) \circ Z(1)$ ,  $Y(0) \circ Y(1)$ ,  $X(0) \circ X(1)$ .

In QBLUE, we permit different compilation paths, e.g., users can select a different Trotterization algorithm, QDrift, to compile the Hamiltonian simulation. We also permit analog-based compilation. For analog platforms such as the IBM [Alexander et al. 2020] and Indiana [Richerme 2025] machines, the compiler targets native Ising models. For the IBM machine model, these are of the form  $\sum_j r_j \cdot X(j) + \sum_k r_k \cdot Z(k) + \sum_{j < k} \theta_{jk} \cdot Z(j) \circ Z(k)$  [Peng et al. 2024]. The interaction term  $Z(0) \circ Z(1)$  is directly compatible with the native couplers. In this case, QBLUE emits a weighted interaction graph suitable for analog scheduling.

**Correctness Across the Stack.** At each stage—constraint, dynamic, and application—QBLUE guarantees correctness through types. The constraint semantics ensure well-formed expressions; the dynamic semantics preserve physical behavior; and the application semantics respect hardware constraints. These guarantees are enforced and verified in RocQ, the logical backend that ensures semantic alignment between typed programs and their denotations. In this way, QBLUE provides an end-to-end framework for writing, reasoning about, and executing quantum programs grounded in both physical intuition and formal correctness.

Our compilation correctness ensures that the compiled circuit, simulating a Hamiltonian  $\hat{H}$  with time  $r$ , is within error bound  $\epsilon$  of the dynamic semantics  $\exp(-ir\hat{H})$ . For example, when simulating the above two-site Hubbard model, in the trotterization step, the error of compiling  $\hat{H}$  in Eq. 2.2 to  $\exp(-ir\hat{H}')$  in Eq. 2.3 has been calculated by our certified compiler. In the standard Trotterization method, the error bound is  $\pi^2/16$  following Eq. 5.4.1. The QBLUE compiler implements different compilation algorithms for different use cases. By selecting QDrift-based Trotterization, our compiler produces an error bound of  $3\pi^2/16$  following Eq. 5.4.2. Note that the error introduced by dropping the constant and local-field terms in Eq. 2.1 has been naturally included in the calculation. We list our main compilation theorem (simplified version) below.

**PROPOSITION 2.3 (COMPILATION CORRECTNESS).** Given a Hamiltonian  $e$ , typed as  $\iota \vdash e \triangleright \mathcal{F}^h(\iota)$ , and a time period  $r$ , the simulation  $\exp(-ir e)$  is correctly compiled to quantum circuit, via the pipeline  $\mathcal{F}^h(\iota) \vdash (e, r) \gg U : \mathcal{F}^u(\iota')$ , with a verified error bound  $\epsilon$  between  $U$  and  $\exp(-ir e)$ .

### 3 Mathematical Background

This section reviews the mathematical foundations used throughout the paper, focusing on the representation of quantum states, operators, and their algebraic manipulation. These form the basis for our compilation and simulation framework, particularly as it relates to encoding Hamiltonians, managing particle types, and enforcing structural constraints during circuit generation.

**Quantum States and Superposition.** In quantum computing, the state of a system is described by a unit vector in a Hilbert space. We adopt Dirac (bra-ket) notation [Dirac 1939] to express such vectors compactly. For a system of dimension  $m$ , a state in the Hilbert space  $\mathcal{H}_m$  is written as  $z_0 |0\rangle + \dots + z_{m-1} |m-1\rangle$ , where each  $|j\rangle$  is a computational basis vector, such as  $|0\rangle = [1\ 0\ \dots]^T$  and  $|1\rangle = [0\ 1\ \dots]^T$ , and  $z_j$  is a complex-number amplitude. When more than one amplitude  $z_j$  is nonzero, the state is said to be in a *superposition* [Nielsen and Chuang 2011], such as the state  $\frac{1}{\sqrt{2}}(|0\rangle + |1\rangle)$ . Quantum systems can be composed via the tensor product. For instance, the two-qubit state  $|0\rangle \otimes |1\rangle$  (also written as  $|0\rangle |1\rangle$ ) corresponds to the vector  $[0\ 1\ 0\ 0]^T$ . However, not all joint states can be decomposed into tensor products. Such states exhibit non-classical correlations between particles and are called *entangled*. A canonical example is the Bell pair  $\frac{1}{\sqrt{2}}(|0\rangle |0\rangle + |1\rangle |1\rangle)$ .

**Hamiltonian Simulation and Pauli Strings.** To simulate physical systems, quantum computers approximate the unitary time evolution  $\exp(-ir\hat{H})$  generated by a Hamiltonian  $\hat{H}$ . Here,  $\hat{H}$  is a Hermitian operator ( $\hat{H} = \hat{H}^\dagger$ ), and  $r$  is a time or interaction parameter. A standard compilation strategy involves Trotterization, which rewrites  $\hat{H}$  as a weighted sum of local terms:  $\hat{H} = \sum_j z_j \hat{P}_j$ , where each  $\hat{P}_j$  is a tensor product of operators and  $z_j$  are typically real scalars.<sup>6</sup> In many cases, the  $\hat{P}_j$  terms are drawn from the Pauli group, forming what are called *Pauli strings*. For an  $n$ -site system, a Pauli string takes the form  $\hat{P}_j = \mathcal{P}_n \otimes \dots \otimes \mathcal{P}_1$ , where each  $\mathcal{P}_k \in \{I, X, Y, Z\}$  acts on a qubit Hilbert space  $\mathcal{H}_2$ .

**Second Quantization and Tensor Strings.** More expressive Hamiltonians (particularly those modeling fermionic or bosonic systems) are naturally represented using the formalism of second quantization. Instead of Pauli operators, the building blocks here are creation ( $a^\dagger$ ) and annihilation ( $a$ ) operators. A typical Hamiltonian term is expressed as a composition  $\bar{\alpha} = \alpha_1 \circ \dots \circ \alpha_j$  with  $\alpha_j \in \{a, a^\dagger\}$  and  $\circ$  denoting matrix multiplication. To represent spatial structure, such operator sequences are tensorized across sites, forming what we call *tensor strings*:  $\bar{\alpha}_n \otimes \dots \otimes \bar{\alpha}_1$ <sup>7</sup>. For convenience, we write indexed notation such as  $a(j)$  or  $a^\dagger(j)$  to insert an operator at site  $j$  with identities elsewhere. For example,  $a(j) = \bigotimes_{k=0}^{j-1} I \otimes a \otimes \bigotimes_{k=j+1}^{n-1} I$ .

**Fermionic Ladder Semantics.** To reason formally about tensor strings in second quantization, it helps to instantiate the algebra of creation and annihilation operators to a concrete setting. We focus on a simplified, two-dimensional model that behaves like a boson system but preserves key properties shared with fermions (particularly the notion of occupancy constraints). In this model, the ladder operators act on a two-level system with basis  $\{|0\rangle, |1\rangle\}$ , corresponding to the absence or presence of a particle. The annihilation operator is defined as  $a = \begin{pmatrix} 0 & 1 \\ 1 & 0 \end{pmatrix}$  and the creation operator as  $a^\dagger = \begin{pmatrix} 0 & 0 \\ 1 & 0 \end{pmatrix}$ . These matrices satisfy the following behavior  $a^\dagger |0\rangle = |1\rangle$ ,  $a^\dagger |1\rangle = 0$ ,  $a |1\rangle = |0\rangle$ , and  $a |0\rangle = 0$ . From these, we define two compound operations:  $\mathbb{1} = a^\dagger \circ a$ , which acts as a projector onto the occupied state  $|1\rangle$ , and  $\mathbb{0} = a \circ a^\dagger$ , which projects onto the unoccupied state  $|0\rangle$ . These projections are not unitary but are useful for expressing static constraints on particle presence within a state. Such projectors can be applied across multiple sites. For instance, the operator  $\mathbb{1} \otimes \mathbb{0}$  preserves the state  $|1\rangle |0\rangle$  and maps all other basis states to  $0$ . This mechanism enables local constraints to be embedded compositionally within a larger quantum system. For example,  $a^\dagger \circ a \otimes a \circ a^\dagger |1\rangle |0\rangle = |1\rangle |0\rangle$  but vanishes on other basis states. This semantics serve as the foundation for the constraint-based interpretation of programs in QBLUE, distinct from their dynamic (unitary) semantics.

<sup>6</sup>Any Hermitian Hamiltonian can be rewritten in a Pauli string form with real coefficients; see Section 5.2.

<sup>7</sup>When it occurs as part of a tensor structure, the identity  $I$  refers to a single site.

Nat. Num	$m, n, j, k, g \in \mathbb{N}$	Real Number	$\theta, r \in \mathbb{R}$	Complex Number	$z \in \mathbb{C}$	Variable	$x, y, f$
	Single-Site Basis Vector in $\mathcal{H}_m$	$\eta$	$::=  k\rangle$		$k \in [0, m)$		
	$n$ -Site Basis-ket State	$w$	$::= \bigotimes_{k=0}^{n-1} \eta_k$				
	Quantum State Type	$\iota$	$::= t^{[\mathfrak{N}]}(m)  $	$\iota \otimes \iota$			
	Quantum State	$\psi$	$::= \sum_j z_j w_j  $	$0$			

Fig. 2. QBLUE state structure for particles. A  $t(m)$ -typed basis vector  $|j\rangle$  can have  $j \in [0, m)$ . We abbreviate  $z \cdot \bigotimes_{k=0}^0 \eta_k \equiv z \eta_0$  and  $z_1 \eta_1 \otimes z_2 \eta_2 \equiv (z_1 * z_2) \eta_1 \eta_2$ .  $[\mathfrak{N}]$  means an operational  $\mathfrak{N}$  flag.

**Pauli Operators as Ladder Composites.** The creation and annihilation operators not only express physical processes like particle addition and removal, but they also provide a basis for reconstructing familiar gate-level abstractions. In particular, the standard Pauli matrices can be algebraically derived as composites of these ladder operations:  $I = 0 + \mathbb{1}$ ,  $X = a^\dagger + a$ ,  $Y = ia - ia^\dagger$ , and  $Z = 0 - \mathbb{1}$ . These definitions not only reproduce the expected matrix representations of the Pauli group but also clarify how Pauli strings (as used in quantum simulation) can be viewed as special cases of more general tensor strings involving creators and annihilators. This relationship reinforces the idea that the Pauli operators can be interpreted as expressive but coarse-grained encodings of particle-level dynamics. In the QBLUE framework, this makes it possible to derive constraint-oriented operations from lower-level semantics while retaining compatibility with gate-based formulations. However, it is important to emphasize that the resulting operators are interpreted as symbolic constraints, not necessarily as executable quantum gates.

**Typing and Compilation in QBLUE.** In QBLUE, quantum programs are enriched with a type system that classifies each site according to particle type. For example,  $t^{\mathfrak{N}}(2)$  denotes a two-dimensional fermionic state, while  $t(2)$  is used for standard qubit or two-dimensional bosonic sites. These types are essential for interpreting the semantics of Hamiltonians correctly and guiding their compilation into circuits. Typing becomes particularly useful when translating systems across representations. For example, a two-site system typed as  $t(m) \otimes t(m)$  can be compiled to a qubit system by expressing each state  $j \in [0, m)$  as a bitstring of length  $N = \lceil \log(m) \rceil$ , yielding a system with  $2N$  qubits of type  $t(2)$ . Such translations are captured by higher-order functions ( $\bigotimes^2 t(m) \rightarrow \bigotimes^2 t(m) \rightarrow (\bigotimes^{2N} t(2) \rightarrow \bigotimes^{2N} t(2))$ ). This flexible typing and compilation infrastructure supports our goal of modeling diverse quantum systems within a unified symbolic and operational framework.

## 4 Formalism

This section discusses QBLUE's syntax, type system, semantics, and equivalence relations on typed programs.

### 4.1 Quantum Particle System State Representation

In QBLUE, we model quantum systems as collections of *sites*, where each site is associated with a local Hilbert space. In typical qubit-based systems, each site corresponds to a two-dimensional Hilbert space  $\mathcal{H}_2$ . More generally, however, sites may have different dimensionalities to account for distinct particle types (such as bosons and fermions), which require different local state spaces. For example, a three-site system might assign  $\mathcal{H}_3$  to the first site,  $\mathcal{H}_4$  to the second, and  $\mathcal{H}_5$  to the

DataType Kind	$\zeta$	::= p   h   u
Quantum Operation Type	$\tau$	::= $\mathcal{F}^\zeta(\iota)$
Constraint Expression	$\hat{H}, e$	::= $z a : t^{[\aleph]}(m) \mid I : t^{[\aleph]}(m) \mid e^\dagger \mid e \otimes e \mid e + e \mid e \circ e$
Unitary Expression	$U$	::= $\exp(-i\hat{H}) \mid U \circ U$

Fig. 3. QBLUE syntax. Both  $e$  and  $\hat{H}$  range over programs; we reserve  $\hat{H}$  to Hamiltonian programs. Blue type annotations are optional in the syntax.

third, yielding a composite Hilbert space  $\mathcal{H}_{60} = \mathcal{H}_3 \otimes \mathcal{H}_4 \otimes \mathcal{H}_5$ . In this tensor product, each factor encodes the quantum state of an individual site.

Figure 2 defines the quantum state syntax used in QBLUE, which formalizes such systems using *computational basis vectors and basis kets*. A single-site basis vector of type  $t^{[\aleph]}(m)$ <sup>8</sup> is written as the ket  $\eta = |k\rangle$ , where  $k \in [0, m)$  identifies one of the  $m$  local basis vectors. A composite  $n$ -site basis-ket state is then expressed as  $w = \bigotimes_{k=0}^{n-1} \eta_k$ . For example, two sites of type  $t(3)$  in basis vectors  $|2\rangle$  and  $|1\rangle$  compose into the joint state  $|2\rangle \otimes |1\rangle$ , which we abbreviate as  $|2\rangle |1\rangle$ .

A single-site basis vector  $|k\rangle$  of type  $t(m)$  can be scaled by a complex amplitude  $z$ , forming a single-site state  $z|k\rangle$ . For an  $n$ -site system, we write basis-ket states as  $w = \bigotimes_{k=0}^{n-1} \eta_k$ , and associate amplitudes component-wise. For example, the state  $z_1\eta_1 \otimes z_2\eta_2$  can be abbreviated as  $(z_1 * z_2)\eta_1\eta_2$ . In general, a quantum superposition state is written canonically as  $\psi = \sum_j z_j w_j$ , where each  $w_j$  is a basis-ket term and  $z_j \in \mathbb{C}$ . We also include the zero vector  $0$  to represent the null state, which plays a role in the semantics of second quantization.

## 4.2 Program Syntax

Figure 3 defines the abstract syntax of QBLUE programs. A constraint expression  $e$  (or  $\hat{H}$  when explicitly Hermitian) denotes a symbolic Hamiltonian imposing user-defined constraints to a system, while a unitary expression  $U = \exp(-i\hat{H})$  represents compiled time evolution. The type constructor  $\mathcal{F}^\zeta(\iota)$  classifies program fragments over a typed state space  $\iota$  by kind  $\zeta$ : plain (p), Hermitian (h) or unitary (u). Hermitian terms correspond to physical Hamiltonians, while unitary terms represent compiled simulations executable on quantum hardware.

The term  $z a : t^{[\aleph]}(m)$  represents an annihilation operator, scaled by an amplitude  $z$ , acting on a site of type  $t^{[\aleph]}(m)$ ; the corresponding identity operator is  $I : t^{[\aleph]}(m)$ . The type annotation  $\aleph$  clarifies particle type (fermionic if  $\aleph$  is set, bosonic otherwise), but it is not part of the term syntax by itself; types are inferred and checked by the system. The conjugate transpose operator  $e^\dagger$  denotes the adjoint of  $e$ . In particular,  $(z a : t^{[\aleph]}(m))^\dagger$  desugars to  $z^\dagger a^\dagger : t^{[\aleph]}(m)$ , representing a creator. In QBLUE, expressions  $z a : t^{[\aleph]}(m)$  and  $z' a' : t^{[\aleph]}(m)$  are syntactically equal if  $z = z'$  for  $a \in \{a, a^\dagger\}$ .

Expressions include tensor compositions  $e \otimes e$  to represent operations on distinct sites, additive combinations  $e + e$  for linear combinations of terms (see Section A.3), and sequential compositions  $e \circ e$  for operator application. At the unitary level,  $\exp(-i\hat{H})$  performs Hamiltonian simulation and  $U \circ U$  represents unitary composition. Both sequential compositions  $e \circ e$  and  $U \circ U$  are matrix multiplications but they operate at distinct semantic levels, constraint and dynamic, respectively.

Programs often use indexed notation as syntactic sugar for tensor expressions. For a system with  $n$  sites, an indexed operator such as  $a^\dagger(j)$  denotes the tensor product of identity operators at all sites except for site  $j$ , where the operator  $a^\dagger$  is applied. For instance, the Hamiltonian of the two-site Hubbard model includes these terms:  $-z_t \sum_j (a^\dagger(j) \circ a(j+1) + a^\dagger(j+1) \circ a(j))$ . Here, each indexed term implicitly expands into a tensor product over the full system. Note that the

<sup>8</sup> $m$  in the site type can be conceptually understood as the maximum number of particles that can occupy a site.

**Expression Equivalence:**

$$\begin{aligned}
& \vdash (e_1 + e_2) \circ e \equiv (e_1 \circ e) + (e_2 \circ e) & \vdash e \circ (e_1 + e_2) \equiv (e \circ e_1) + (e \circ e_2) & \vdash (e_1 + e_2) \otimes e \equiv e_1 \otimes e + e_2 \otimes e \\
& \vdash e \otimes (e_1 + e_2) \equiv e \otimes e_1 + e \otimes e_2 & \vdash (e_1 \otimes e_2)^\dagger \equiv e_1^\dagger \otimes e_2^\dagger & \vdash (e_1 + e_2)^\dagger \equiv e_1^\dagger + e_2^\dagger & \vdash (e_1 \circ e_2)^\dagger \equiv e_2^\dagger \circ e_1^\dagger \\
& \vdash (e^\dagger)^\dagger \equiv e & \vdash I^\dagger \equiv I & \vdash I \circ e \equiv e & \vdash e \circ I \equiv e & \text{E-TEN} \\
& & & & & l^b \vdash (e_1 \otimes e_2) \circ (e_3 \otimes e_4) \equiv (e_1 \circ e_3) \otimes (e_2 \circ e_4)
\end{aligned}$$

**Typing Rules:**

$$\begin{array}{c}
\text{T-OPF} \\
\frac{}{t^{\mathfrak{N}}(2) \vdash z a \triangleright \mathcal{F}^p(t^{\mathfrak{N}}(2))} \\
\\
\text{T-OPB} \\
\frac{}{t(m) \vdash z a \triangleright \mathcal{F}^p(t(m))} \\
\\
\text{T-ID} \\
\frac{}{t^{[\mathfrak{N}]}(m) \vdash I \triangleright \mathcal{F}^h(t^{[\mathfrak{N}]}(m))} \\
\\
\text{T-DAG} \\
\frac{l \vdash e \triangleright \mathcal{F}^\zeta(l)}{l \vdash e^\dagger \triangleright \mathcal{F}^\zeta(l)} \\
\\
\text{T-HER} \\
\frac{l \vdash e^\dagger \equiv e \quad l \vdash e \triangleright \mathcal{F}^p(l)}{l \vdash e \triangleright \mathcal{F}^h(l)} \\
\\
\text{T-TEN} \\
\frac{l \vdash e \triangleright \mathcal{F}^\zeta(l) \quad l' \vdash e' \triangleright \mathcal{F}^\zeta(l')}{l \otimes l' \vdash e \otimes e' \triangleright \mathcal{F}^\zeta(l \otimes l')} \\
\\
\text{T-APP} \\
\frac{l \vdash e \triangleright \mathcal{F}^\zeta(l) \quad l \vdash e' \triangleright \mathcal{F}^{\zeta'}(l)}{l \vdash e \circ e' \triangleright \mathcal{F}^{\zeta \sqcup \zeta'}(l)} \\
\\
\text{T-SIM} \\
\frac{l \vdash e \triangleright \mathcal{F}^h(l)}{l \vdash \exp(-ie) \triangleright \mathcal{F}^u(l)} \\
\\
\text{T-PLUS} \\
\frac{l \vdash e \triangleright \mathcal{F}^\zeta(l) \quad l \vdash e' \triangleright \mathcal{F}^\zeta(l)}{l \vdash e + e' \triangleright \mathcal{F}^\zeta(l)} \\
\\
\text{T-UAPP} \\
\frac{l \vdash U \triangleright \mathcal{F}^u(l) \quad l \vdash U' \triangleright \mathcal{F}^u(l)}{l \vdash U \circ U' \triangleright \mathcal{F}^u(l)}
\end{array}$$

Fig. 4. Typing and equational rules.  $\equiv$  is the equivalence relation, assuming associativity and commutativity for  $+$ .  $h \sqcup p = p$  and  $u \sqcup p = p$  and type error otherwise.  $l^b$  means  $l$  has no fermionic type subterms ( $t^{\mathfrak{N}}(2)$ ).

identity operator  $I$  is type-sensitive; for a  $t(2)$  typed site,  $I = a^\dagger \circ a + a \circ a^\dagger$ , capturing both occupied and unoccupied projections.

**4.3 Typing Rules**

We now introduce the QBLUE typing system. Every well-typed QBLUE program, whether a Hamiltonian  $\hat{H}$  or a unitary  $U$ , is assigned a type of the form  $\mathcal{F}^\zeta(l)$ , where  $\zeta$  denotes the matrix kind and  $l$  specifies the type of the quantum state to which the program applies. For instance, a single-site operation might have type  $\mathcal{F}^\zeta(t(m))$ , meaning that it acts on a bosonic state space of dimension  $m$ . Such types can be viewed as abstractly denoting maps  $t(m) \rightarrow t(m)$  on single-site states. The kind  $\zeta$  tracks the nature of the matrix represented by a program: ordinary (p), Hermitian (h), or unitary (u). A Hamiltonian program  $\hat{H}$  must be Hermitian (i.e.,  $\hat{H} = \hat{H}^\dagger$ ), and a unitary program  $U$  must arise as a matrix exponential  $U = \exp(-i\hat{H})$ . This structure ensures that only unitary operators are considered executable on quantum hardware. To model multi-site systems, QBLUE includes tensor types of the form  $\mathcal{F}^\zeta(l_1 \otimes l_2)$ , used to separate sites (see Figure 2). These types track how a program composes across sites with heterogeneous particle types.

The typing judgment  $l \vdash e \triangleright \tau$  asserts that under input state type  $l$ , the expression  $e$  has type  $\tau$ . Figure 4 defines the typing rules and equivalence principles of QBLUE. The type system enforces two critical properties:

- Correct typing for each operator with respect to its local particle type.
- Kind soundness: Hermitian and unitary kinds are preserved and checked via rewrite equivalences.

QBLUE models particle systems with various state types  $t^{[\mathfrak{N}]}(m)$ , where the dimensionality  $m$  corresponds to the Hilbert space of a site, and the flag  $[\mathfrak{N}]$  distinguishes bosons (flag off) from

fermions (flag on). The type  $\iota$  denotes the full system's shape, constructed using tensor products  $\otimes$  across sites.

Rules T-OPF and T-OPB type a single annihilation operator applied to a fermionic or bosonic state, respectively. We assume fermions are modeled using a two-dimensional Hilbert space  $t^{\mathbf{N}}(2)$ <sup>9</sup>, while bosons may use arbitrary dimensions  $t(m)$ . Multi-site systems are typed using rule T-TEN, which constructs a composite operation over a system with type  $\iota = \iota_1 \otimes \iota_2$ . For example, a two-site system  $\eta_1 \otimes \eta_2$  has type  $t(m) \otimes t(j)$ , and a composite operator  $a \otimes a$  is well-typed if its components are typed as  $\mathcal{F}^\zeta(t(m))$  and  $\mathcal{F}^\zeta(t(j))$ . The resulting type is  $\mathcal{F}^\zeta(t(m) \otimes t(j))$ , making particle types explicit and analyzable in the type system. The typing rules also ensure well-formedness of other operations. For instance, rule T-PLUS types additive combinations  $e + e'$ , which represent quantum superpositions. The operands must have matching types and kinds; notably, additive composition is not permitted for unitary kinds, as quantum hardware does not support coherent superpositions of distinct unitaries.

Since QBLUE programs represent matrices, the kind system tracks how program fragments compose. Every physically realizable (i.e., executable) program must ultimately have unitary kind  $u$ , and this must arise through simulation of a Hamiltonian of kind  $h$  using  $\exp(-i\hat{H})$ . In second quantization, basic operators such as  $a$  and  $a^\dagger$  are not Hermitian. To promote an expression to kind  $h$ , rule T-HER requires that the expression be equivalent to its adjoint under the equational rules shown in Figure 4. For example, the Hubbard Hamiltonian in Section 2 includes the term  $a^\dagger(j) \circ a(j+1) + a^\dagger(j+1) \circ a(j)$ , which is Hermitian because it is equal to its own conjugate transpose under syntactic equivalence. Rule T-SIM enforces that the matrix exponential  $\exp(-ie)$  is only allowed when  $e$  is Hermitian, producing a unitary. Rule T-APP governs composition: the resulting kind is computed via a join operation  $\zeta \sqcup \zeta'$ , defined over the subtyping lattice  $h \sqsubseteq p$  and  $u \sqsubseteq p$ . This permits combining Hermitian or unitary operations with ordinary ones (defaulting to  $p$ ), but prohibits mixing  $h$  and  $u$  directly, which would result in a kinding error.

#### 4.4 Equational Theory

QBLUE includes a system of equational rules that define algebraic equivalences between programs. These equivalences are interpreted modulo commutativity for the  $+$  operation and associativity, which we assume implicitly throughout. The equational theory is primarily used to relate well-typed programs. We define this notion of equivalence formally below.

*Definition 4.1 (Well-Typed Equational Rewrites).* We write  $\iota \vdash e \equiv e'$  to mean that two well-typed QBLUE programs  $e$  and  $e'$  are equationally equivalent. That is,  $e \equiv e'$  can be derived using the equational rules, and both programs have the same type  $\tau$  under the same system shape  $\iota: \iota \vdash e \triangleright \tau$  and  $\iota \vdash e' \triangleright \tau$ . We denote  $\vdash e \equiv e' \text{ as } \forall \iota. \iota \vdash e \equiv e'$ .

Most of the equational rules in Figure 4 are valid for arbitrary types, with the exception of rule E-TEN, which is only valid for bosons. Specifically, the subterm  $t^b$  must not contain any component typed with  $t^\alpha(2)$ , as tensor operations involving fermions are not independent due to anti-commutation. This restriction is illustrated by the equation  $(I \otimes a^\dagger) \circ (a^\dagger \otimes I) = -(a^\dagger \otimes I) \circ (I \otimes a^\dagger)$  which exhibits fermionic anti-commutation. If E-TEN were allowed, the left-hand side could be rewritten as  $(I \circ a^\dagger) \otimes (a^\dagger \circ I) = a^\dagger \otimes a^\dagger$  while the right-hand side would become  $-(a^\dagger \circ I) \otimes (I \circ a^\dagger) = -a^\dagger \otimes a^\dagger$ . Clearly,  $a^\dagger \otimes a^\dagger$  and  $-a^\dagger \otimes a^\dagger$  are not equal but E-TEN would incorrectly equate them. This demonstrates the necessity of type sensitivity in our equational system.

Equational rewrites allow us to normalize programs into canonical forms, which serve as a foundation for both the semantics of QBLUE and the compilation procedure in Section 5. In particular,

<sup>9</sup>Due to the anti-commutation property, a fermionic site can have at most one particle.

they allow adjoint operators ( $\dagger$ ) to be pushed inward to atomic terms and linear sum (+) outward to the program top level, simplifying the structure of expressions and enabling structural comparison. This motivates the following notion of normal form.

*Definition 4.2 ( $\dagger$ -Canonical Form).* A well-typed program  $e$  is in  $\dagger$ -canonical form if:

- $e$  is written as a linear combination  $\sum_j z_j e_j$ , where each  $z_j$  is a scalar amplitude and each  $e_j$  contains no further sum operators;
- in every subterm of the form  $e_1^\dagger$ ,  $e_1$  is of the form  $z a : \iota$ , meaning the adjoint is applied only to atomic particle operators.

LEMMA 4.3 (CANONICALIZATION VIA REWRITING). For every Hamiltonian program  $e$ , there exists a  $\dagger$ -canonical program  $e'$  such that  $\iota \vdash e \equiv e'$ .

PROOF. By structural induction on the typing derivation of  $e$ , using the equational rewrite rules in Figure 4. All cases have been fully mechanized.  $\square$

This canonical form underlies the Hamiltonian constraint semantics developed in the next section. In Section 5.2, we introduce a second, more general canonicalization procedure (also defined via the equational theory of Figure 4) that applies to Hamiltonians expressed not in terms of second-quantized creation and annihilation operators, but using Pauli operators.

## 4.5 Semantics

The semantics of QBLUE is defined over  $\dagger$ -canonicalized programs (see Theorem 4.1) as presented in Figure 5. These programs describe finite  $n$ -site systems whose site states are typed by a shape  $\iota$ , with  $|\iota| = n$ . To interpret such programs, we begin with a typed quantum state  $\iota \vdash \psi$ , defined in terms of the Dirac notation introduced in Figure 2.

*Definition 4.4 (QBLUE Typed State).* Let  $\psi = \sum_j z_j w_j$  be a quantum state. We write  $\iota \vdash \psi$  to mean that for every  $j$ , term  $w_j$  is a well-typed basis ket under  $\iota$ : that is,  $\iota \vdash w_j$ :

- $\iota \otimes \iota' \vdash w \otimes w'$ , if  $\iota \vdash w$  and  $\iota' \vdash w'$ ;
- $t(m) \vdash |j\rangle$ , if  $j < m$ ;
- $t^{\mathbb{N}}(2) \vdash |j\rangle$ , if  $j \in \{0, 1\}$ .

Given a typed state, the semantics of QBLUE is defined denotationally as  $\llbracket \iota \vdash \square \triangleright \tau \rrbracket_g$ , where  $\square$  is a well-typed  $\dagger$ -canonicalized program (either a Hamiltonian  $e$  or a unitary  $U$ ), and  $g \in \mathbb{N}$  is a context parameter. As explained in Section 2, each QBLUE program simultaneously defines both constraint semantics (via Hamiltonians) and dynamic semantics (via unitary evolution).

The interpretation  $\llbracket \iota \vdash \square \triangleright \tau \rrbracket_0$  (with  $g = 0$ ) gives the core meaning of a Hamiltonian  $\hat{H}$  as a Hermitian operator, and a unitary program  $U$  as a unitary matrix, corresponding to the constraint and dynamic semantics, respectively. The context  $g$  is used to account for fermionic anti-commutation effects and is initialized to 0 during evaluation. More generally,  $\llbracket \iota \vdash \square \triangleright \tau \rrbracket_g$  defines a transformation on  $\iota$ -typed quantum states, i.e., a function  $\iota \rightarrow \iota$ .

Figure 5 presents the semantic rules using two complementary views. The rules S-TOP, S-OPB, S-OPF, and S-TEN adopt the function view, describing how programs act on specific basis kets or superpositions thereof. The rules S-PLUS, S-APP, S-SIM, and S-UAPP adopt the matrix view, interpreting programs as linear operators and expressing their composition explicitly. The context  $g$  plays a role in enforcing global constraints, particularly related to fermionic parity signs, as described next.

**Constraint Semantics.** The constraint-level semantics,  $\llbracket \iota \vdash e \triangleright \tau \rrbracket_g$ , begins with rule S-TOP, which lifts the semantics of  $e$  pointwise over a superposition  $\sum_j z_j w_j$ . The rules S-OPB and S-OPF

## Single Ket Semantics:

$$\llbracket a^\dagger \rrbracket(m) |k\rangle := \sqrt{k+1} |k+1\rangle \quad \text{if } k \neq m \quad \llbracket a^\dagger \rrbracket(m) |m\rangle := 0 \quad \llbracket a \rrbracket(m) |k\rangle := \sqrt{k} |k-1\rangle \quad \text{if } k \neq 0 \quad \llbracket a \rrbracket(m) |0\rangle := 0$$

## Semantics Rules:

$$\begin{array}{l} \text{S-TOP} \\ \llbracket \iota \vdash e \triangleright \tau \rrbracket_g \sum_j z_j w_j := \sum_j z_j (\llbracket \iota \vdash e \triangleright \tau \rrbracket_g w_j) \end{array} \quad \begin{array}{l} \text{S-OPB} \\ \llbracket t(m) \vdash z a^{[\dagger]} \triangleright \tau \rrbracket_g |j\rangle := z (\llbracket a^{[\dagger]} \rrbracket(m) |j\rangle) \end{array}$$

$$\begin{array}{l} \text{S-OPF} \\ \llbracket t^{\text{N}}(2) \vdash z a^{[\dagger]} \triangleright \tau \rrbracket_g |j\rangle := ((-1)^g * z) (\llbracket a^{[\dagger]} \rrbracket(2) |j\rangle) \end{array} \quad \begin{array}{l} \text{S-ID} \\ \llbracket t^{\text{N}}(m) \vdash I \triangleright \tau \rrbracket_g |j\rangle := |j\rangle \end{array}$$

$$\text{S-TEN} \quad \llbracket \frac{\iota \vdash e \triangleright \mathcal{F}^\zeta(\iota) \quad \iota' \vdash e' \triangleright \mathcal{F}^\zeta(\iota')}{\iota \otimes \iota' \vdash e \otimes e' \triangleright \mathcal{F}^\zeta(\iota \otimes \iota')} \rrbracket_g (w_1 \otimes w_2) := \llbracket \iota \vdash e \triangleright \mathcal{F}^\zeta(\iota) \rrbracket_g w_1 \otimes \llbracket \iota' \vdash e' \triangleright \mathcal{F}^\zeta(\iota') \rrbracket_{(g+S(\iota)(w_1))} w_2$$

$$\text{S-APP} \quad \llbracket \frac{\iota \vdash e \triangleright \mathcal{F}^\zeta(\iota) \quad \iota \vdash e' \triangleright \mathcal{F}^{\zeta'}(\iota)}{\iota \vdash e \otimes e' \triangleright \mathcal{F}^{\zeta \cup \zeta'}(\iota)} \rrbracket_g := \llbracket \iota \vdash e \triangleright \mathcal{F}^\zeta(\iota) \rrbracket_g (\llbracket \iota \vdash e' \triangleright \mathcal{F}^{\zeta'}(\iota) \rrbracket_g)$$

$$\text{S-PLUS} \quad \llbracket \frac{\iota \vdash e \triangleright \mathcal{F}^\zeta(\iota) \quad \iota \vdash e' \triangleright \mathcal{F}^\zeta(\iota)}{\iota \vdash e + e' \triangleright \mathcal{F}^\zeta(\iota)} \rrbracket_g := \llbracket \iota \vdash e \triangleright \mathcal{F}^\zeta(\iota) \rrbracket_g + \llbracket \iota \vdash e' \triangleright \mathcal{F}^\zeta(\iota) \rrbracket_g$$

$$\text{S-SIM} \quad \llbracket \frac{\iota \vdash e \triangleright \mathcal{F}^h(\iota)}{\iota \vdash \exp(-ie) \triangleright \mathcal{F}^u(\iota)} \rrbracket_g := \sum_{n=0}^{\infty} \frac{(-i \llbracket \iota \vdash e \triangleright \mathcal{F}^h(\iota) \rrbracket_g)^n}{n!}$$

$$\text{S-UAPP} \quad \llbracket \frac{\iota \vdash U \triangleright \mathcal{F}^u(\iota) \quad \iota \vdash U' \triangleright \mathcal{F}^u(\iota)}{\iota \vdash U \circ U' \triangleright \mathcal{F}^u(\iota)} \rrbracket_g := \llbracket \iota \vdash U \triangleright \mathcal{F}^u(\iota) \rrbracket_g (\llbracket \iota \vdash U' \triangleright \mathcal{F}^u(\iota) \rrbracket_g)$$

$$S(t^{\text{N}}(m))(|j\rangle) = j \quad S(t(m))(|j\rangle) = 0 \quad S(\iota \otimes \iota')(\eta \otimes \eta') = S(\iota)(\eta) + S(\iota')(\eta')$$

Fig. 5. QBLUE semantics for  $\dagger$ -canonicalized program.  $a^{[\dagger]}$  means either a creator  $a^\dagger$  or an annihilator  $a$ . Terms inside  $\llbracket - \rrbracket$  are QBlue operators. For terms outside  $\llbracket - \rrbracket$ , black  $*$  and  $+$  are scalar multiplication and addition, purple items are quantum state vector operations, and  $\llbracket - \rrbracket (\llbracket - \rrbracket)$  is matrix multiplication.

define the effect of bosonic and fermionic single-site operators, using the primitive definitions at the top of Figure 5. Each operator is scaled by  $z$ , or  $(-1)^g * z$  in the fermionic case.

In rule S-OPF, the natural-numbered context  $g$  enforces fermionic anti-commutation: applying a fermionic operator introduces a sign  $(-1)^g$ , where  $g$  is the number of occupied fermion sites (i.e.,  $|1\rangle$  basis kets) before the target site. We assume a fixed total ordering of the sites in shape  $\iota$ . For example, applying an annihilation operator  $a$  to the third site in the state  $|1\rangle |1\rangle |1\rangle |0\rangle$  (where the first is bosonic and the second fermionic) yields  $-|1\rangle |1\rangle |0\rangle |0\rangle$ , due to one prior fermionic excitation. The sign correction is propagated via the accumulated context  $g$  using the function  $S$  defined in rule S-TEN. Rule S-TEN defines the semantics of tensor composition. Given two subterms and a tensor product input state  $w_1 \otimes w_2$ , the semantics applies the two subterms recursively and combines the results using  $\otimes$ . Note that zero vectors propagate through tensor products:  $0 \otimes w = 0$  and  $w \otimes 0 = 0$ . A zero-valued basis ket anywhere in the tensor string collapses the entire state. Rules S-PLUS and S-APP define semantic interpretations of sum and application. A sum

corresponds to a linear combination of operators, while a sequential composition corresponds to matrix multiplication or function composition.

**Dynamic Semantics.** The rules S-SIM and S-UAPP define the dynamic semantics of QBLUE. Rule S-SIM interprets the expression  $\exp(-ie)$  as the matrix exponential, where  $e$  is Hermitian. The exponential is defined via its standard power series expansion, which converges to a unitary operator when  $e$  is Hermitian. We interpret this construct as the least fixed point of the matrix exponential series, approximated computationally as needed. Rule S-UAPP interprets sequential composition of unitaries as standard matrix multiplication. Thus, dynamic programs in QBLUE are built by composing unitary evolutions, each derived from a Hamiltonian constraint via simulation.

#### 4.6 Metatheory

We present the QBLUE theorems that connect the semantics and the type system. These results highlight how the type system enforces the anti-commutation property for fermions.

Lemma 4.5 below connects Hamiltonians and unitaries, stating that a type guided equivalence Hamiltonian  $\hat{H}'$  has the same quantum simulation behavior as the original Hamiltonian  $\hat{H}$ .

LEMMA 4.5 (HAMILTONIAN EQUIVALENCE CORRECTNESS). Given  $\hat{H}$  and  $\hat{H}'$ , such that  $\iota \vdash \hat{H} \equiv \hat{H}'$ , for every  $r$ ,  $\llbracket \iota \vdash \exp(-i\hat{H}) \triangleright \mathcal{F}^u(\iota) \rrbracket_g = \llbracket \iota \vdash \exp(-i\hat{H}') \triangleright \mathcal{F}^u(\iota) \rrbracket_g$ .

PROOF. Fully mechanized proofs were done by induction on semantic rules, with the extra lemma that our equational theory is an equivalence relation (reflective, symmetric, and transitive).  $\square$

We prove the QBLUE type soundness theorem, which states that a well-typed QBLUE program, when applied to a well-typed quantum state, produces a result that is also well-typed.

THEOREM 4.6 (TYPE SOUNDNESS). If  $\iota \vdash \square \triangleright \mathcal{F}^\zeta(\iota)$ , with  $\square$  being  $\hat{H}$  or  $U$ , and  $\iota \vdash \psi$ , then  $\llbracket \iota \vdash \square \triangleright \mathcal{F}^\zeta(\iota) \rrbracket_g$  well-defines a  $\zeta$ -kind matrix, and for all  $\psi'$ ,  $\llbracket \iota \vdash \square \triangleright \tau \rrbracket_g(\psi) = \psi'$ , then  $\iota \vdash \psi'$ .

PROOF. Fully mechanized proofs were done by induction on the QBLUE type system.  $\square$

One utility of the type soundness theorem is to guarantee the anti-commutation property of fermion operations in QBLUE, stated as follows.

COROLLARY 4.7 (GUARANTEE ANTI-COMMUTATION). If  $\bigotimes^n t^{\mathbb{N}}(2) \vdash \hat{H} \triangleright \mathcal{F}^h(\bigotimes^n t^{\mathbb{N}}(2))$ ,  $\hat{H}'$ 's interpretation  $\llbracket \bigotimes^n t^{\mathbb{N}}(2) \vdash \hat{H}' \triangleright \mathcal{F}^h(\bigotimes^n t^{\mathbb{N}}(2)) \rrbracket_0$  preserves fermions' anti-commutation property.

PROOF. Fully mechanized proofs were done by induction on the QBLUE semantics for well-typed programs with the assumption that all sites are fermions ( $t^{\mathbb{N}}(2)$ ).  $\square$

The type soundness theorem indicates the existence of a compilation to quantum circuits and is used in our compilation correctness in Section 5.

## 5 The QBlue Compilation Procedure

This section presents the QBLUE compilation steps (Figure 6) along with correctness proofs for each step. The compiler transforms a Hamiltonian simulation expression  $\exp(-ir e)$ , where  $e$  is a QBLUE Hamiltonian program and  $r$  is a time parameter, into a quantum circuit executable on quantum hardware. We model compilation as a judgment of the form  $\mathcal{F}^h(\iota) \vdash (e, r) \gg U : \mathcal{F}^u(\iota')$ , which extends the typing judgment  $\iota \vdash e \triangleright \mathcal{F}^h(\iota)$  introduced in Section 4.2. The QBLUE compiler supports multiple compilation paths, allowing users to choose among different strategies. The perturbative gadget transformation (Section 5.3) is optional. We also provide two Trotterization algorithms and three different synthesis methods. The main theorem in Section 5.6 assumes a compilation path that omits the perturbative gadget, but it is general enough to handle both Trotterization variants.

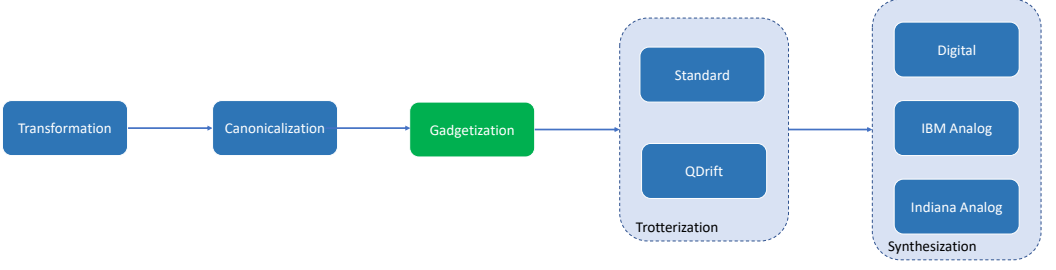


Fig. 6. Hamiltonian Simulation Compilation Flow

$$\begin{array}{l}
 \text{PT-PLUS} \\
 \frac{l \vdash_n e_1 \gg_t \hat{H}_1 \triangleright l' \quad l \vdash_n e_2 \gg_t \hat{H}_2 \triangleright l'}{l \vdash_n e_1 + e_2 \gg_t \hat{H}_1 + \hat{H}_2 \triangleright l'} \\
 \\
 \text{PT-TEN} \\
 \frac{|l_1|^N = m \quad l_1 \vdash_n e_1 \gg_t \hat{H}_1 \triangleright l'_1 \quad l_2 \vdash_{n+m} e_2 \gg_t \hat{H}_2 \triangleright l'_2}{l_1 \otimes l_2 \vdash_n e_1 \otimes e_2 \gg_t \hat{H}_1 \otimes \hat{H}_2 \triangleright l'_1 \otimes l'_2} \\
 \\
 \text{PT-FEUP} \\
 t^N(2) \vdash_n (za)^\dagger \gg_t z^\dagger \left( \bigotimes_{k=0}^n Z \right) \otimes (X - iY) \triangleright t(2) \\
 \\
 \text{PT-BoUP} \\
 \frac{B'(j) = \bigotimes_{k=0}^{\lceil \log(m) \rceil - 1} \mathcal{A}^k(j, j+1)}{t(m) \vdash_n (za)^\dagger \gg_t z^\dagger \sum_{j=0}^{m-2} \sqrt{j+1} B'(j) \triangleright \bigotimes_{k=0}^{\lceil \log(m) \rceil} t(2)} \\
 \\
 \text{PTS-SUM} \\
 \frac{\forall j. l \vdash w_j \gg_t w'_j \triangleright l'}{l \vdash \sum_j w_j \gg_t \sum_j w'_j \triangleright l'} \\
 \\
 \text{PTS-Bo} \\
 \frac{l \vdash w \gg_t w' \triangleright l'}{t(m) \otimes l \vdash z |j\rangle \otimes w \gg_t z |j\rangle_{\lceil \log(m) \rceil} \otimes w' \triangleright \bigotimes_{k=0}^{\lceil \log(m) \rceil} t(2) \otimes l'} \\
 \\
 \text{PT-APP} \\
 \frac{l \vdash_n e_1 \gg_t \hat{H}_1 \triangleright l' \quad l \vdash_n e_2 \gg_t \hat{H}_2 \triangleright l'}{l \vdash_n e_1 \circ e_2 \gg_t \hat{H}_1 \circ \hat{H}_2 \triangleright l'} \\
 \\
 \text{PT-FELOW} \\
 t^N(2) \vdash_n za \gg_t z \left( \bigotimes_{k=0}^n Z \right) \otimes (X + iY) \triangleright t(2) \\
 \\
 \text{PT-BoLow} \\
 \frac{B(j) = \bigotimes_{k=0}^{\lceil \log(m) \rceil - 1} \mathcal{A}^k(j, j-1)}{t(m) \vdash_n za \gg_t z \sum_{j=1}^{m-1} \sqrt{j} B(j) \triangleright \bigotimes_{k=0}^{\lceil \log(m) \rceil} t(2)} \\
 \\
 \text{PTS-FE} \\
 \frac{l \vdash w \gg_t w' \triangleright l'}{t^N(2) \otimes l \vdash z \eta \otimes w \gg_t z \eta \otimes w' \triangleright t(2) \otimes l'} \\
 \\
 \mathcal{A}^k(j, m) = \frac{1}{2}(X - iY) \text{ if } \llbracket j \rrbracket[k] = 0 \wedge \llbracket m \rrbracket[k] = 1 \quad \mathcal{A}^k(j, m) = \mathbb{1} \text{ if } \llbracket j \rrbracket[k] = \llbracket m \rrbracket[k] = 1 \\
 \mathcal{A}^k(j, m) = \frac{1}{2}(X + iY) \text{ if } \llbracket j \rrbracket[k] = 1 \wedge \llbracket m \rrbracket[k] = 0 \quad \mathcal{A}^k(j, m) = 0 \text{ if } \llbracket j \rrbracket[k] = \llbracket m \rrbracket[k] = 0
 \end{array}$$

Fig. 7. Particle transformation rules.  $|l|^N$  collects the # of fermions ( $t^N(2)$ ) in  $l$ .  $\llbracket j \rrbracket$  converts  $j$  to bitstring.

The correctness of compilation paths that include the perturbative gadget is addressed in Section D. We begin by describing the individual compilation steps and then state the theorem covering the entire pipeline.

## 5.1 Particle Transformation

The first compilation step is particle transformation, transforming the second quantization program in Figure 3 to a  $t(2)$ -typed qubit-based Hamiltonian program  $\hat{H}$  in a Pauli-string-based form. For

clarity, we list below the Pauli string program syntax, as a syntactic sugar extension of the QBLUE syntax in Figure 3, with all the sites being  $t(2)$ -typed.

$$\mathcal{P} ::= X \mid Y \mid Z \mid I \qquad \hat{H} ::= z \mathcal{P} \mid \hat{H} + \hat{H} \mid \hat{H} \otimes \hat{H}$$

The particle transformation compilation can be expressed as the flow-sensitive judgment  $\iota \vdash_n e \gg_{\mathfrak{t}} \hat{H} \triangleright l'$ , as an extension of the QBLUE typing rules. Here,  $e$  is the input h-kind Hamiltonian program in the second quantization form with the type  $\mathcal{F}^h(\iota)$ ,  $\hat{H}$  is the Pauli string Hamiltonian (syntax defined above) with the type  $\mathcal{F}^h(\iota')$ , and  $n$  is the flow sensitive context. A Hamiltonian program describes constraints for a finite number of quantum particles. Without losing generality, for any program  $e$ , we assume that  $e$  can be canonicalized as its operations ordered as a list structure describing a one dimensional list of applications to the sites, and the flag  $n$  indicates that the current compilation is processing the  $n+1$ -th element in the list as  $n$  is the previous site adjacent to the  $n+1$ -th site.

Figure 7 shows the transformation rules. The transformation for fermion particles is based on Jordan-Wigner transformation [Jordan and Wigner 1928b], while the boson transformation is based on Holstein-Primakoff transformation [Veis et al. 2016]. We show an alternative transformation in Section E. Rules PT-PLUS and PT-APP deal with linear sum and sequence operations; such operation transformations depend on the subterm transformations. In transforming tensor operations in PT-TEN, we ensure that  $e_1$ 's type is  $\mathcal{F}^h(\iota_1)$ . Without losing generality, we also find the site application length (the site number of applied operations in  $e_1$ ) to be  $m$ , as  $|\iota_1| = m$ . Recall that we assume the sites of  $e_1$  and  $e_2$  applied to are canonicalized as an ordered list, so  $e_2$ 's flow-sensitive context is set to  $n + m$ , as  $n + m + 1$  represents the first site position  $e_2$  applies to.

Rules PT-FELow and PT-FEUP describe the transformation for fermion annihilators and creators. As we mentioned, fermions are always  $t^{\mathbb{N}}(2)$  typed. To compile fermion particle simulations, we apply  $Z$  operations to all the sites before the  $n$ -th site. For the current site ( $n + 1$ ), we apply a lowering ( $X + iY$ ) or a raising ( $X - iY$ ) operation. The resulting type is  $\mathcal{F}^h(t(2))$ , representing that the compiled result is a single qubit operation, i.e., a qubit is enough to describe a fermion site state.

Rules PT-BoLow and PT-BoUP describe the binary compilation scheme to transform boson annihilators and creators. In compiling the particle simulation, we use  $\lceil \log(m) \rceil$  qubits to represent a  $t(m)$  typed boson state, as the compilation results in a  $\mathcal{F}^h(\otimes^{\lceil \log(m) \rceil} t(2))$  typed operation. Generally, applying a creator  $a^\dagger$  to  $|j\rangle$  results in  $|j+1\rangle$  and applying an annihilator  $a$  to  $|j\rangle$  results in  $|j-1\rangle$ . The compiled system produces a sum of all  $j$ -th Pauli strings turning  $|j\rangle$  to  $|j+1\rangle$  (or  $|j-1\rangle$  for  $a$ ). For each  $j$ , we examine  $j$ 's binary representation, compare  $j$  and  $j+1$  bitwise (or  $j-1$  for  $a$ ), and then apply a proper Pauli operation ( $\mathcal{A}^k(j, m)$ ). For example, if we compiled a  $t(5)$  boson state  $|3\rangle$  as  $|1\rangle |1\rangle |0\rangle |0\rangle$  (LSB form), applying a creator to the state results in  $|0\rangle |0\rangle |1\rangle |0\rangle$  ( $|4\rangle$ ); Such behavior is captured by  $B'(3)$  in PT-BoUP, where we use a lowering operation ( $X + iY$ ) to remove the two  $|1\rangle$  bits and apply a raising operation on the third qubit. Note that in the case both bits ( $[j][k]$  and  $[m][k]$ ) are the same, we need to apply  $\mathbb{1}$  or  $\mathbb{0}$  operations, corresponding to the Pauli operations  $\frac{1}{2}(I - Z)$  and  $\frac{1}{2}(I + Z)$ , respectively.

Rules PTS-SUM, PTS-FE, and PTS-Bo describe the transformation of states for a particle system state to a state in the qubit system. The transformation judgment is  $\iota \vdash \psi \gg_{\mathfrak{t}} \psi' \triangleright l'$ , where we transform the typed  $\iota$  state  $\psi$  to type  $\iota'$  state  $\psi'$ . Rules PTS-FE and PTS-Bo transform fermion and boson states, described above.

LEMMA 5.1 (PARTICLE TRANSFORMATION CORRECTNESS). Given  $\iota \vdash_0 e \gg_{\mathfrak{t}} \hat{H} \triangleright l'$ , for any  $\psi_1$ , such that  $\iota \vdash \psi_1$ , with the compiled state  $\psi'_1$ , denoted as  $\iota \vdash \psi_1 \gg_{\mathfrak{t}} \psi'_1 \triangleright l'$ ,  $\psi_2 = \llbracket \iota \vdash e \triangleright \mathcal{F}^h(\iota) \rrbracket_0(\psi_1)$  and  $\psi'_2 = \llbracket \iota \vdash \hat{H} \triangleright \mathcal{F}^h(\iota) \rrbracket_0(\psi'_1)$ ; thus,  $\iota \vdash \psi_2 \gg_{\mathfrak{t}} \psi'_2 \triangleright l'$ .

PROOF. Fully mechanized proofs were done by induction on the particle transformation rules in Figure 7.  $\square$

**Example Transformation.** We show the compilation of a bosonic particle system to quantum computers (not the QBLUE boson-like system). Bosons are a special particle and typically require an infinite-dimensional Hilbert space to describe a particle site, e.g., a boson is typed  $t(\infty)$ . A typical way of approximating a bosonic system [Veis et al. 2016] utilizes  $2^n$  dimensional Hilbert space, i.e., we use a length  $n$  basis vector to track  $2^n - 2$  basis-vector state from  $|0\rangle$  to  $|2^n - 2\rangle$ . The extra  $n+1$ -th basis-vector  $|2^n - 1\rangle$  acts as an overflow bit, indicating if a maximal orbital is reached.

We now apply the transformation to a two-site bosonic system, with  $m = 4$ . We use the Hubbard model  $\hat{H}$  in Section 2 to describe the superconducting behaviors of bosons. We focus on transforming the sub-expression  $a^\dagger(0): t(4) \circ a(1): t(4) + a(0): t(4) \circ a^\dagger(1): t(4)$  to Pauli-string-based Hamiltonian. It is enough to show the transformation for a single creator and annihilator applying to different  $|j\rangle$  basis-vectors, e.g., examining the cases of applying  $a^\dagger$  to  $|0\rangle$  getting  $|1\rangle$  and applying  $a$  to  $|2\rangle$  outputting  $|1\rangle$ .

$a^\dagger$	$ j\rangle$ transition	$ 0\rangle \rightarrow  1\rangle$	$ 1\rangle \rightarrow  2\rangle$	$ 2\rangle \rightarrow  3\rangle$
	Binary transition	$ 0\rangle 0\rangle \rightarrow  1\rangle 0\rangle$	$ 1\rangle 0\rangle \rightarrow  0\rangle 1\rangle$	$ 0\rangle 1\rangle \rightarrow  1\rangle 1\rangle$
	Pauli String	$\frac{1}{2}(X - iY) \otimes \frac{1}{2}(I + Z)$	$\frac{1}{2}(X + iY) \otimes \frac{1}{2}(X - iY)$	$\frac{1}{2}(X - iY) \otimes \frac{1}{2}(I - Z)$
$a$	$ j\rangle$ transition	$ 3\rangle \rightarrow  2\rangle$	$ 2\rangle \rightarrow  1\rangle$	$ 1\rangle \rightarrow  0\rangle$
	Binary transition	$ 1\rangle 1\rangle \rightarrow  0\rangle 1\rangle$	$ 0\rangle 1\rangle \rightarrow  1\rangle 0\rangle$	$ 1\rangle 0\rangle \rightarrow  0\rangle 0\rangle$
	Pauli String	$\frac{1}{2}(X + iY) \otimes \frac{1}{2}(I - Z)$	$\frac{1}{2}(X - iY) \otimes \frac{1}{2}(X + iY)$	$\frac{1}{2}(X + iY) \otimes \frac{1}{2}(I + Z)$

The above table shows different cases for  $a^\dagger$  and  $a$ . In each case, we first show the desired basis-vector transitions, the binary-based basis-vector transitions, and then the Pauli string encoding of the transitions. The transformation for the  $t(4)$  typed creators and annihilators are the sum of the three cases listed above, e.g.,  $a^\dagger: t(4)$  is transformed to  $\frac{1}{2}(X - iY) \otimes \frac{1}{2}(I + Z) + \frac{1}{2}(X + iY) \otimes \frac{1}{2}(X - iY) + \frac{1}{2}(X - iY) \otimes \frac{1}{2}(I - Z)$ . The transformation of the whole sub-expression  $(a^\dagger(0): t(4) \circ a(1): t(4) + a(0): t(4) \circ a^\dagger(1): t(4))$  replaces each of the creators and annihilators with the transformed sum terms above.

## 5.2 Canonicalization

The compiled Pauli-string-based Hamiltonian program  $\hat{H}$  in Section 5.1 can have a complicated structure, which can be canonicalized to a standard form via the use of the equational rules in Section 4.5. We define the canonical form as follows.

*Definition 5.2 (Pauli Canonical Form).* Let  $\mathcal{P} \in \{I, X, Y, Z\}$ , a program  $\hat{H}$ , typed as  $\bigotimes^n t(2) \vdash \hat{H} \triangleright \mathcal{F}^h(\bigotimes^n t(2))$ , is called Pauli Canonical  $\sum_j r_j \hat{P}_j$ , where  $\hat{P}_j = \bigotimes_{k=0}^{n-1} \mathcal{P}_{j,k}$  ( $r_j$  is a real number).

Theorem 5.2 states that every program  $\hat{H}$  typed as  $\bigotimes^n t(2) \vdash \hat{H} \triangleright \mathcal{F}^h(\bigotimes^n t(2))$ , where  $|\bigotimes^n t(2)| = n$ , can be rewritten as a two-dimensional list. The outer list corresponds to a sum  $\sum_j r_j \hat{P}_j$ , and each inner element  $\hat{P}_j$  is a fixed-length tensor product  $\bigotimes_{k=0}^{n-1} \mathcal{P}_k$ , representing a list of  $n$  Pauli operations. Each of these inner lists (i.e., tensor factors) has fixed size  $n$ , matching the type length  $|t| = n$  in the typing judgment  $\iota \vdash \hat{H} \triangleright \mathcal{F}^h(\iota)$ . The  $k$ -th element of the tensor list corresponds to the operation applied to the  $k$ -th site.

Another key simplification is Pauli operation sequence applications ( $\mathcal{P} \in \{I, X, Y, Z\}$ ) in a single site can be merged into a single Pauli operation, i.e.,  $\mathcal{P}_1 \circ \mathcal{P}_2$  can be

	$X$	$Y$	$Z$
$X$	$I$	$iZ$	$-iY$
$Y$	$-iZ$	$I$	$iX$
$Z$	$iY$	$-iX$	$I$

Fig. 8. Pauli Merging

rewritten as a single Pauli operation. Applying an identity  $I$  with a  $\mathcal{P}$  results in  $\mathcal{P}$ . The application results of other Pauli operations ( $\mathcal{P}_1$  and  $\mathcal{P}_2$ ) are defined in Figure 8. The two Pauli applications represent simplification, where a sequence of Pauli group applications results in a single Pauli operation with a certain real number amplitude. We have the following canonicalization correctness lemma.

LEMMA 5.3 (CANONICAL COMPILATION CORRECTNESS). Given  $\hat{H}$ , typed  $\bigotimes^n t(2) \vdash \hat{H} \triangleright \mathcal{F}^h(\bigotimes^n t(2))$ , there is  $\hat{H}'$ , such that  $\bigotimes^n t(2) \vdash \hat{H} \equiv \hat{H}'$  and  $\hat{H}'$  is Pauli canonical in Theorem 5.2.

PROOF. Fully mechanized proofs were done via the equational theory in Section 4.4 and the assumption of a  $\dagger$ -canonical program, with the extra lemma stated in Theorem 5.4.  $\square$

LEMMA 5.4 (GUARANTEED CANONICALIZATION). Given a  $\dagger$ -canonical program (Theorem 4.2)  $e = \sum_j z_j e_j$ , typed as  $\bigotimes^n t(2) \vdash e \triangleright \mathcal{F}^h(\bigotimes^n t(2))$ , for every  $z_j e_j$ , either  $z_j$  is a real number, or we can find another  $z_k e_k$  in  $e$ , such that  $e_j = e_k^\dagger$ , and  $z_j = z_k^\dagger$ .

With the Theorem 4.5, we can show that the Hamiltonian simulation of  $\hat{H}$  and its equivalent canonical form  $\hat{H}'$  produce the same result.

### 5.3 Gadgetization

The *gadgetization* step is defined as the transformation of a canonicalized Pauli-string-based Hamiltonian  $\hat{H}$  to another Hamiltonian  $\hat{H}'$ , with each Pauli string in  $\hat{H}'$  being two-local – a  $k$ -local Pauli string refers to that the number of non-identity Pauli operations (not equal to  $I$ ) is at most  $k$ . This step might happen before or after Trotterization.

The simplest solution is to perform a unitary synthesization [Whitfield et al. 2011] in the synthesization stage (Section 5.5), which were performed by most previous compiler works [Cao et al. 2024; Peng et al. 2024], as these works hid the step as a subroutine of their Trotterization algorithms. However, there are quantum algorithms for performing the transformation, such as the perturbative gadget algorithms. We believe that it is necessary to substantiate it as a step in our certified compiler, and clarify that there is a key component in compiling a Hamiltonian simulation that transforms a higher local Pauli-string-based Hamiltonian to a two-local Hamiltonian, with the note that this step might happen in the synthesization, which is why the step is marked **green** in Figure 6.

The rest of the section provides an example demonstrating the *perturbative gadget* algorithm [Jordan and Farhi 2008], which is formalized in Section D. We start with the  $\mathcal{F}^h(\bigotimes^n t(2))$  typed canonicalized Pauli-string-based Hamiltonian  $\hat{H} = \sum_j r_j \hat{P}_j$ , canonicalized in Section 5.2, and produce a two-local Hamiltonian via the algorithm. Assume that we have a 4-local Hamiltonian with two Pauli strings, as  $\hat{H} = r_1 \hat{P}_1 + r_2 \hat{P}_2$ ;  $\hat{P}_1$  and  $\hat{P}_2$  are defined on six different Pauli operations  $\{\mathcal{P}_1, \dots, \mathcal{P}_6\}$  as follows, demonstrated as left in Figure 9.

$$\hat{P}_1 = \mathcal{P}_1 \otimes \mathcal{P}_2 \otimes \mathcal{P}_3 \otimes \mathcal{P}_4 \otimes I \otimes I \quad \hat{P}_2 = I \otimes I \otimes \mathcal{P}_3 \otimes \mathcal{P}_4 \otimes \mathcal{P}_5 \otimes \mathcal{P}_6$$

As shown in Figure 9, for each Pauli string  $\hat{P}_j$  ( $j \in [0, 1]$ ) in a  $k$ -local Hamiltonian, we assume that  $k$  ancilla qubits are provided. To generate the result  $H_{\text{gad}}$  Hamiltonian, we are given 4 extra qubits for each Pauli string. For each Pauli string  $\hat{P}_j$ , the algorithm generates a connection Hamiltonian  $\hat{H}^{\text{anc}}$  to connect the ancilla qubits corresponding to the non- $I$  terms in  $\hat{P}_j$ , and a behavioral Hamiltonian  $\hat{H}^{\text{v}}$  to capture the constraints in  $\hat{P}_j$  from the ancilla qubits back to the original qubits. To generate the connection Hamiltonians, we produce the following two Hamiltonians for the Pauli strings  $\hat{P}_1$  and  $\hat{P}_2$ :

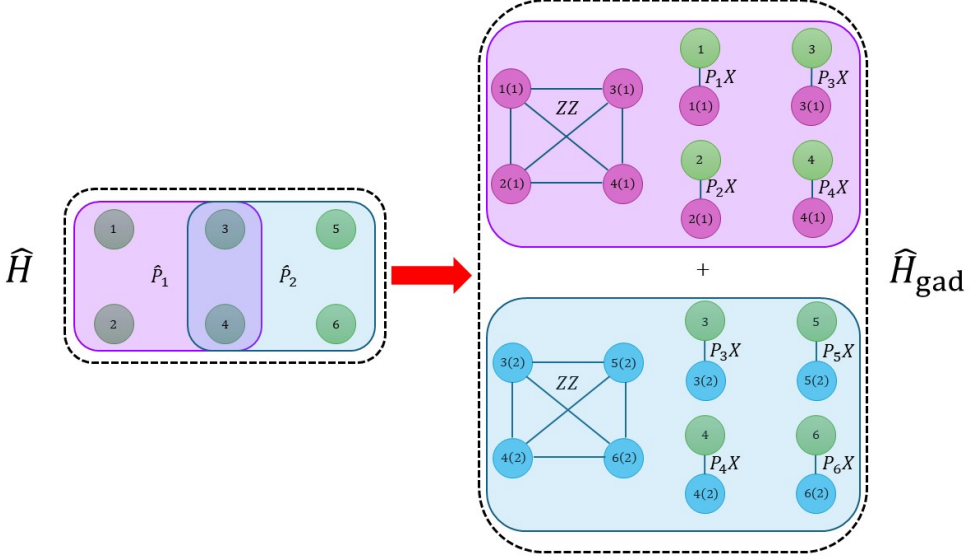


Fig. 9. Perturbative gadget for a sum (the dashed areas) of two 4-local Pauli strings. The green numbered nodes are the original qubits; the purple (e.g., 3(1)) and blue (e.g., 5(2)) nodes are ancilla qubits.

$$\hat{H}_1^{\text{anc}} = \sum_{m=1}^3 \sum_{n=m+1}^4 (I - Z(m(1)) \circ Z(n(1))) \quad \hat{H}_2^{\text{anc}} = \sum_{m=3}^5 \sum_{n=m+1}^6 (I - Z(m(2)) \circ Z(n(2)))$$

We use  $\mathcal{P}(j(k))$  to denote applying the Pauli operation  $\mathcal{P}$  to the  $j$ -th site in a  $k$ -th Pauli string  $\hat{P}_k$ . Hence  $Z(j(1))$  and  $Z(j(2))$  represent the application of  $Z$  operation to the ancilla qubit for the  $j$ -th site in the first and second Pauli string, respectively. To generate the behavior Hamiltonians, we produce the following two Hamiltonians for the Pauli strings  $\hat{P}_1$  and  $\hat{P}_2$ :

$$\hat{H}_1^{\text{v}} = \sum_{n=1}^4 r'_n \mathcal{P}_n(n) \circ X(n(1)) \quad \text{where } r'_1 = r_1 \wedge (n \neq 1 \Rightarrow r'_n = 1)$$

$$\hat{H}_2^{\text{v}} = \sum_{n=3}^6 r'_n \mathcal{P}_n(n) \circ X(n(2)) \quad \text{where } r'_3 = r_3 \wedge (n \neq 3 \Rightarrow r'_n = 1)$$

Similarly,  $X(j(1))$  and  $X(j(2))$  represent the application of  $X$  operation to the ancilla qubit for the  $j$ -th site in the first and second Pauli strings, respectively. The result Hamiltonian  $\hat{H}_{\text{gad}}$  is the sum of the four Hamiltonians  $\theta_1 \hat{H}_1^{\text{anc}}$ ,  $\theta_2 \hat{H}_2^{\text{anc}}$ ,  $\theta_3 \hat{H}_1^{\text{v}}$  and  $\theta_4 \hat{H}_2^{\text{v}}$ , with some amplitude values ( $\theta_j$  for  $j \in [1, 4]$ ). The simulation of  $\hat{H}_{\text{gad}}$  approximates the simulation of the original Hamiltonian  $\hat{H}$ ; the algorithm, the approximation lemma, and the whole compiler pipeline theorem including perturbative gadget are given in Section D.

#### 5.4 Trotterization

Trotterization [Lloyd 1996] is the step to turn the Hamiltonian simulation operator of a sum of Pauli strings to a sequence of Pauli string simulations, each corresponding to a unitary operation, executable in a quantum computer. Trotterization is based on the Lie-Trotter product formula (left below) [Lie 1880] and the approximated formula, on the right, developed by Suzuki [Suzuki 1991].

$$\exp(A + B) = \lim_{m \rightarrow \infty} (\Pi^m \exp(\frac{A}{m}) \circ \exp(\frac{B}{m})) \quad \exp(\delta(A + B)) = \exp(\delta(A)) \circ \exp(\delta(B)) + O(\delta^2)$$

The Suzuki approximation above suggests that the error rate  $O(\delta^2)$  is related to the square of the variable term  $\delta$ . Thus, to simulate a quantum system  $\exp(-ir\hat{H})$  with respect to a time period  $r$ , one can select a large  $m$  to consecutively apply the exponential  $\exp(\frac{A}{m}) \circ \exp(\frac{B}{m})$  to the state  $m$  times, so  $\frac{r}{m}$  diminishes such that the error rate  $O((\frac{r}{m})^2)$  is negligible. Such tactics can be generalized to an arbitrary number of summation terms.

Through Trotterization, given a time period  $r$  and an  $n$ -qubit Pauli-string-based Hamiltonian  $\hat{H} = \sum_{j=0}^{d-1} \theta_j \hat{P}_j$  (with  $\hat{P}_j = \bigotimes_{k=0}^{n-1} P_{j,k}$ ), there is  $m$  such that  $\Pi^m \exp(-i\frac{r}{m} \theta_0 \hat{P}_0) \circ \dots \circ \Pi^m \exp(-i\frac{r}{m} \theta_j \hat{P}_j) \circ \dots$  approximating  $\exp(-ir\hat{H})$ , where  $\Pi^m U = U \circ \dots \circ U$ , repeating  $m$  times of  $U$ . Each matrix exponential operation, a.k.a., Hamiltonian simulation operation, generates a unitary, and Trotterization makes all these generated small unitaries in sequence. The error is related to  $r$  and  $\theta_j$ , detailed below.

In QBLUE, we enable two kinds of Trotterization algorithms, the standard algorithm and QDrift [Campbell 2019]. The standard algorithm uses the Lie-Trotter method. The QDrift method randomizes the sequence of exponential operations, allowing a faster Hamiltonian simulation. We first state the general theorem based on an error bound  $\epsilon$  (specialized to the two algorithms), then discuss it individually, unveiling the error bounds in different settings.

LEMMA 5.5 (TROTTERIZATION CORRECTNESS). Given  $\hat{H} = \sum_{j=0}^{d-1} \theta_j \hat{P}_j$  and time  $r$ , typed as  $\bigotimes^n t(2) \vdash \hat{H} \triangleright \mathcal{F}^h(\bigotimes^n t(2))$ , there is  $m$  and  $N$ , such that,  $\exp(-ir\hat{H})$ 's Trotterization procedure results in  $\Pi^N U(d, m, n, r)$ , the error is bound by,

$$\| \left\| \bigotimes^n t(2) \vdash \exp(-i\theta\hat{H}) \triangleright \mathcal{F}^u(\bigotimes^n t(2)) \right\|_0 - \left\| \bigotimes^n t(2) \vdash \Pi_{k=0}^{N-1} U(d, m, n, r) \triangleright \mathcal{F}^u(\bigotimes^n t(2)) \right\|_0 \| < \epsilon.$$

PROOF. To show Theorem 5.5 for the standard Trotterization and QDrift, our Coq proof performs induction on  $N$ , with key error bound lemmas discussed below.  $\square$

As a running example, we use the following simple Ising model and show its Trotterized results along with the two algorithms' descriptions.

$$\hat{H}_{I1} = \sum_j r_h X(j) + \sum_j Z(j) \circ Z(j+1)$$

**The Standard Algorithm.** In the standard form, for each Pauli string  $\theta_j \hat{P}_j$ , we construct an application sequence  $\Pi^m \exp(-i\frac{r}{m} \theta_j \hat{P}_j)$ , i.e., we repeat the simulation of  $\theta_j \hat{P}_j$  for  $m$  times with a scaled time slot  $\frac{r}{m}$ . Formally,  $U(d, m, n, r)$  is defined as  $\exp(-i\frac{r}{m} \theta_j \hat{P}_j)$  with  $N = d * m$ , i.e.,  $m$  being a splitting number of each Pauli string and  $d$  being the number of Pauli strings in  $\hat{H}$ . Thus, the whole procedure produces an application sequence, explained below.

For example, to simulate the Pauli-string-based Hamiltonian  $\hat{H}_{I1}$  with a time slot  $r$  and splitting number  $m$ , we compute the approximation of the exponent  $\exp(-ir\hat{H}_{I1})$  as follows.

$$\begin{aligned} \exp(-ir\hat{H}_{I1}) &= \Pi^m \left( \exp(-i\frac{r}{m} (\sum_j Z(j) \circ Z(j+1) + r_h \sum_j X(j))) \right) \\ &= \Pi^m \left( \exp(-i\frac{r}{m} Z(0) \circ Z(1)) \circ \exp(-i\frac{r}{m} Z(1) \circ Z(2)) \circ \dots \circ \exp(-i\frac{r}{m} r_h X(0)) \circ \exp(-i\frac{r}{m} r_h X(1)) \circ \dots \right) \end{aligned}$$

Let  $\hat{H} = \sum_{j=0}^{d-1} \theta_j \hat{P}_j$  with  $N = d * m$ , if we list all the trotted Hamiltonian simulation sequences by listing all Pauli strings, we form an  $N$ -element set as  $\hat{H}_k \in \{ \frac{\theta_0}{m} \hat{P}_0, \frac{\theta_0}{m} \hat{P}_0, \dots, \frac{\theta_j}{m} \hat{P}_j, \frac{\theta_j}{m} \hat{P}_j, \dots, \frac{\theta_{d-1}}{m} \hat{P}_{d-1} \}$ .  $\hat{H}$  can be viewed as a sum of  $N$  different element Hamiltonians  $\hat{H}_k$  in the set. We estimate the error bound  $\epsilon$  related to  $O(r^2)$ , and the exact formula is listed below [Childs et al. 2021].

$$\begin{aligned} \exp(-i\theta X) = \text{RX}(2\theta) &= \begin{pmatrix} \cos \theta & -i \sin \theta \\ -i \sin \theta & \cos \theta \end{pmatrix} & \exp(-i\theta Y) = \text{RY}(2\theta) &= \begin{pmatrix} \cos \theta & -\sin \theta \\ \sin \theta & \cos \theta \end{pmatrix} \\ \exp(-i\theta Z) = \text{RZ}(2\theta) &= \begin{pmatrix} \exp(-i\theta) & 0 \\ 0 & \exp(i\theta) \end{pmatrix} \end{aligned}$$

Fig. 10. Pauli matrices simulated to rotation gates.  $\exp(-i\theta \mathcal{P})$  can be thought as simulating  $\mathcal{P}$  on time  $\theta$ .

$$\epsilon = \frac{r^2}{2} \sum_{k=1}^N \left\| \left( \sum_{j=k+1}^N \hat{H}_j \right) \circ \hat{H}_k - \hat{H}_k \circ \left( \sum_{j=k+1}^N \hat{H}_j \right) \right\|. \quad (5.4.1)$$

The Coq proof relies on a key error bound lemma (Section B) based on the error bound in Equation (5.4.1).

**QDrift.** We manage the Pauli strings in  $\hat{H} = \sum_{k=0}^{d-1} \theta_k \hat{P}_k$  as a set  $\{\theta_0 \hat{P}_0, \dots, \theta_{d-1} \hat{P}_{d-1}\}$ . Let  $\lambda = \sum_{k=0}^{d-1} |\theta_k|$ , we probabilistically pick a Pauli string in the set and repeat the process  $N$  times; such picks are listed as a sequence  $m_0, \dots, m_k, \dots, m_{N-1}$ , each  $m_k \in [0, d)$ . The QDrift procedure produces an application sequence  $\prod_{k=0}^{N-1} \exp(-i \frac{r\lambda}{N} \theta_{m_k} \hat{P}_{m_k})$ , i.e., the  $U(d, m, n, r)$  is set to  $\exp(-i \frac{r\lambda}{N} \theta_{m_k} \hat{P}_{m_k})$ . Here the parameter  $m$  in  $U(d, m, n, r)$  is not explicitly used but it satisfies  $N = d * m$ .

We demonstrate the key difference of QDrift with respect to the standard Trotterization using the  $\hat{H}_{I1}$  example above. To approximate the exponential  $\exp(-ir\hat{H}_{I1})$ , we randomly choose  $N$  Pauli strings in the set  $\{r_h X(0), r_h X(1), \dots, Z(0) \circ Z(1), Z(1) \circ Z(2), \dots\}$ , and then construct the trottered sequence. One example choice is as follows.

$$\exp(-ir\hat{H}_{I1}) = \exp(-i \frac{r\lambda}{N} Z(j) \circ Z(j+1)) \circ \exp(-i \frac{r\lambda}{N} Z(k) \circ Z(k+1)) \circ \dots \circ \exp(-i \frac{r\lambda}{N} r_h X(k)) \circ \exp(-i \frac{r\lambda}{N} r_h X(0)) \circ \dots$$

Let  $\hat{H} = \sum_{k=0}^{d-1} \theta_k \hat{P}_k$  and  $\lambda = \sum_{k=0}^{d-1} |\theta_k|$ , QDrift randomly picks  $N$  different Pauli strings for simulation, the error rate  $\epsilon$  is related to  $O(\frac{r^2}{N})$ , with the exact bound listed below [Campbell 2019].

$$\epsilon = \frac{2\lambda^2 r^2}{N} \quad (5.4.2)$$

The Coq proof relies on a key error bound lemma (Section B) based on the error bound in Equation (5.4.2).

## 5.5 Synthesization

Synthesization applies the application sequence of matrix exponentials of Pauli strings generated from Trotterization to quantum circuits, either digital or analog. In synthesizing an application sequence  $\prod_j \exp(-i\theta_j \hat{P}_j)$ , it is enough to describe the synthesization of a single matrix exponential term  $\exp(-i\theta_j \hat{P}_j)$ . We discuss the digital and analog-based synthesization below.

**Digital Synthesization.** The digital synthesization synthesized the simulation of a Pauli string,  $\exp(-i\theta_j \hat{P}_j)$ , to elementary quantum gates, e.g., single-qubit gates, such as H, Rz, Ry, and Rx gates, as well as two qubit controlled-not gate CX ( $\text{CX}(x, y)$  controlling on  $x$  and applying  $X$  gate on  $y$ ).

The procedure focuses on the non- $I$  terms in a Pauli string  $\hat{P} = \bigotimes_{j=0}^{n-1} \mathcal{P}_j$ . If  $\hat{P}$  has only one non- $I$  term, the compilation generates a rotation gate, listed in Figure 10. In the Bloch qubit sphere interpretation [Nielsen and Chuang 2011], the rotation gate Rx, Ry, Rz can be expressed as some Hamiltonian simulations of Pauli matrices ( $\text{Rz}(2\theta)(j)$  applies a  $Z$ -axis rotation in the  $j$ -th qubit), which essentially suggests that the simulation of singleton Pauli  $X$ ,  $Y$ , and  $Z$  terms are the above phase rotation gates. For example, the gate synthesis of  $\exp(-i \frac{2\pi}{n} X(j))$  generates an Rx gate, as  $\text{Rx}(\frac{2\pi}{n})(j)$ . We describe the algorithm in Figure 10 for a Pauli string with more than one non- $I$  term, i.e., a  $k$ -local Pauli string with  $k > 1$ .

**Algorithm 1** Digital Synthesization of  $U = \exp(-i\theta\hat{P})$  for a Pauli string  $\hat{P}$ 

- 
- 1: **Input:** Pauli string  $\hat{P} = \bigotimes_{k=0}^{n-1} \mathcal{P}_k$ , time period  $\theta$
  - 2: **Output:** Digital circuit  $U = \exp(-i\theta\hat{P})$
  - 3:
  - 4: Collect sites  $\{m_1, m_2, \dots, m_l\}$  where  $\mathcal{P}_{m_j} \neq I$ , with  $l \leq n$
  - 5:  $U \leftarrow \text{Rz}(2\theta)(m_1)$
  - 6:  $j = m_1$
  - 7: **for**  $m_j \in \{m_2, \dots, m_l\}$  **do**
  - 8:    $U \leftarrow \text{CX}(m_{j-1}, m_j) \circ U \circ \text{CX}(m_{j-1}, m_j)$
  - 9: **end for**
  - 10: **for**  $m_j \in \{m_1, \dots, m_l\}$  **do**
  - 11:   **if**  $\mathcal{P}_{m_j} = Y$  **then**
  - 12:      $U \leftarrow \text{Rz}(\frac{\pi}{2})(m_j) \circ \text{H}(m_j) \circ U \circ \text{H}(m_j) \circ \text{Rz}(-\frac{\pi}{2})(m_j)$
  - 13:   **else if**  $\mathcal{P}_{m_j} = X$  **then**
  - 14:      $U \leftarrow \text{H}(m_j) \circ U \circ \text{H}(m_j)$
  - 15:   **end if**
  - 16: **end for**
  - 17: **Return**  $U$
- 

$$\exp(-i\theta ZZ(j) \circ Z(j+1)) = \begin{array}{c} \bullet \\ \oplus \\ \text{---} \\ \oplus \\ \bullet \end{array} \begin{array}{c} \bullet \\ \text{---} \\ \oplus \\ \text{---} \\ \oplus \\ \bullet \end{array} \begin{array}{c} \text{Rz}(2\theta) \\ \text{---} \\ \oplus \\ \text{---} \\ \oplus \\ \bullet \end{array} \quad \exp(-i\theta ZZ) = \begin{pmatrix} \exp(-i\frac{\theta}{2}) & 0 & 0 & 0 \\ 0 & \exp(i\frac{\theta}{2}) & 0 & 0 \\ 0 & 0 & \exp(i\frac{\theta}{2}) & 0 \\ 0 & 0 & 0 & \exp(-i\frac{\theta}{2}) \end{pmatrix}$$

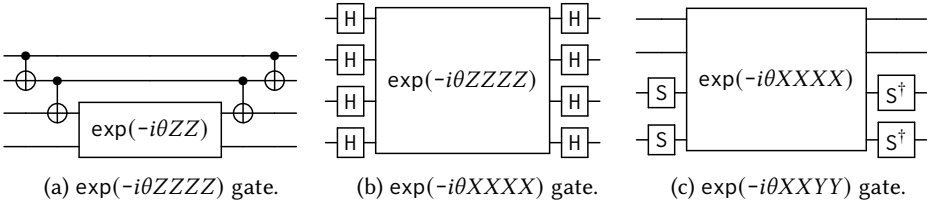
Fig. 11. Circuit and unitary for ZZ Interaction. The left circuit applies on  $j$  and  $j+1$  qubits.

Fig. 12. Synthesized circuits for some long Pauli strings.

We first show the gate synthesization of the simple  $t(2)$  typed Ising model  $\hat{H}_{I1}$  in Section 5.4, which produces a sequence of  $\exp(-i\frac{t}{n}Z(j) \circ Z(j+1))$  and  $\exp(-i\frac{t}{n}r_h X(j))$  operations (the sequence length is related to  $n$ ). If  $n$  is large enough, the operation sequence is a good approximation to  $\exp(-ir\hat{H}_{I1})$ . The  $\exp(-i\frac{t}{n}r_h X(j))$  operation produces a Rx gate [Nielsen and Chuang 2011], while  $\exp(-i\frac{t}{n}Z(j) \circ Z(j+1))$  produces a digital circuit as the left in Figure 11, performing two controlled-not gates and an  $\text{Rz}(2\frac{t}{n})$  gate in the middle for the  $j$ -th and  $j+1$ -th qubits, i.e.,  $\text{Rz}(2\theta)$  is an  $z$ -axis phase rotation gate.

The above assumes a two-local Pauli string with non- $I$  terms being  $Z$ . If we do not perform a perturbative gadget, we might have  $k$ -local Pauli strings with  $k > 2$ . The general algorithm is described in Algorithm 1.

We show an example of a long Pauli string synthesization in Figure 12. Such long Pauli strings might appear in the Hamiltonian simulation of many systems, such as the bosonic system  $\hat{H}$  in Section 5.1. After applying Trotterization on the  $\hat{H}$  for boson systems, we generate a sequence of Hamiltonian simulations of Pauli strings. Some possible Pauli string terms might be 4-local, as  $Z \otimes Z \otimes Z \otimes Z$  (abbreviated as ZZZZ),  $X \otimes X \otimes X \otimes X$  (abbreviated as XXXX) and  $X \otimes X \otimes Y \otimes Y$

---

**Algorithm 2** IBM-based Analog Synthesization of  $U = \exp(-i\theta\hat{P})$  for 2-Local Pauli Strings
 

---

```

1: Input: 2-local Pauli string  $\hat{P} = \bigotimes_{k=0}^{n-1} \mathcal{P}_k$ , time period  $\theta$ 
2: Output: Analog Hamiltonian simulation  $U = \Pi^m \exp(-ir\hat{P})$ 
3:
4: Identify non-identity sites  $m_1$  and  $m_2$  where  $\mathcal{P}_{m_j} \neq I$ 
5:  $U \leftarrow \exp(-i\theta Z(m_1)) \circ Z(m_2)$ 
6: for  $m_j \in \{m_1, m_2\}$  do
7:   if  $\mathcal{P}_{m_j} \neq Z$  then
8:     let  $U_1 = \exp(-i\frac{\pi}{4}X(m_j)) \circ \exp(-i\frac{\pi}{4}Z(m_j)) \circ \exp(-i\frac{\pi}{4}X(m_j))$  in
9:      $U \leftarrow U_1 \circ U \circ U_1$ 
10:   end if
11:   if  $\mathcal{P}_{m_j} = Y$  then
12:      $U \leftarrow \exp(-i\frac{\pi}{4}Z(m_j)) \circ U \circ \exp(-i\frac{\pi}{4}Z(m_j))$ 
13:   end if
14: end for
15: Return  $U$ 

```

---

(abbreviated as  $XXYY$ ). The simulation of the  $ZZZZ$  term results in a quadruple  $Z$  interaction in Figure 12a, containing a  $ZZ$  interaction application in the middle, shown in Figure 11, with the surrounding of controlled-not gates. The digital gate synthesization of  $\exp(-i\theta XXXX)$  and  $\exp(-i\theta XXYY)$  is based on the quadruple  $Z$  interaction with reapirs for  $X$  and  $Y$  conversion, which results in the circuits in Figures 12b and 12c. We show the correctness lemma below.

LEMMA 5.6 (DITIGAL SYNTHESIZATION CORRECTNESS).  $\exp(-i\theta\hat{P})$  can be synthesized as a sequence of unitary operations as  $\Pi_k U_k$ , based on the elementary gates,  $\{H, Rx, Ry, Rz, CX\}$ .

PROOF. Fully mechanized proofs were done by induction on the Pauli canonical forms. By applying Algorithm 1, we produce a unitary  $U$  for  $\exp(-i\theta\hat{P})$ . Then, we interpret the two terms as matrix representations in VOQC [Hietala et al. 2023] and equate the two interpretations.  $\square$

**Analog Synthesization.** Many quantum computers provide backends to perform analog quantum computation, i.e., we can view a quantum computer as a Hamiltonian simulator to simulate small Hamiltonians in sequence. Each simulation step in a quantum simulator takes in a positive real number  $\theta$  and a Pauli string  $\hat{P}$ , and produce the simulation result as  $\exp(-i\theta\hat{P})$ . The procedure is machine-dependent. For example, an IBM machine permits the simulation of one or two-local Pauli strings in the set  $\{X, Z, ZZ\}$  ( $ZZ$  means a two-local Pauli string with only  $Z$  Pauli operations). Another machine (Indiana), developed by Richerme *et al.* [Kyprianidis et al. 2024; Richerme 2025], permits the simulation of  $k$ -local Pauli strings in the set  $\{Z, X^*\}$ , where  $X^*$  permits a Pauli string simulation with an arbitrary number of  $X$  Paulis. We show two analog synthesization algorithms in Algorithms 2 and 3 to compile our Pauli strings to the IBM and Indiana machines, respectively.

To perform analog synthesization for the IBM machine, we assume that a two-local Hamiltonian is achieved by applying a perturbative gadget. The simulation of a one-local Pauli can be dealt with by the matrix exponential formulas in Figure 10. The Indiana machine permits the simulation of a  $k$ -local Pauli string, i.e., we do not need perturbative gadget to generate two-local Pauli strings.

As an example, to simulate a simple Ising system  $\hat{H}_{I1}$  above, we can directly perform the simulation  $\exp(-i\frac{t}{n}Z(j) \circ Z(k))$  and  $\exp(-i\frac{t}{n}r_h X(j))$  for sites  $j$  and  $k$ , in the IBM setting. If  $\frac{t}{n}$  is negative, we can instead simulate a positive number  $\frac{t}{n} + 2m\pi$ . The direct Hamiltonian simulation permits a more efficient circuit compilation. The above analog synthesization step essentially implements

**Algorithm 3** Indiana Analog Synthesization of  $U = \exp(-i\theta\hat{P})$ 


---

```

1: Input: Pauli string  $\hat{P} = \bigotimes_{k=0}^{n-1} \mathcal{P}_k$ , time period  $\theta$ 
2: Output: Analog circuit  $U = \exp(-i\theta\hat{P})$ 
3:
4: Collect sites  $\{m_1, m_2, \dots, m_k\}$  where  $\mathcal{P}_{m_j} \neq I$ , with  $l \leq n$ 
5:  $\hat{P}' = I$ 
6: for  $m_j \in \{m_1, \dots, m_k\}$  do
7:    $\hat{P}' \leftarrow \hat{P}' \circ X(m_j)$ 
8: end for
9:  $U \leftarrow \exp(-i\theta \hat{P}')$ 
10: for  $m_j \in \{m_1, \dots, m_k\}$  do
11:   if  $\mathcal{P}_{m_j} = Y$  then
12:      $U \leftarrow \exp(-i\frac{\pi}{4}Z(m_j)) \circ U \circ \exp(-i\frac{7\pi}{4}Z(m_j))$ 
13:   else if  $\mathcal{P}_{m_j} = Z$  then
14:     let  $U_1 = \exp(-i\frac{\pi}{4}X(m_j)) \circ \exp(-i\frac{\pi}{4}Z(m_j)) \circ \exp(-i\frac{\pi}{4}X(m_j))$  in
15:      $U \leftarrow U_1 \circ U \circ U_1$ 
16:   end if
17: end for
18: Return  $U$ 

```

---

the ZZ-interaction gate in Figure 11, and also shows the reason for some interaction gates being much more efficient than elementary gates in IBM machines, evidenced in Peng et al. [2024].

To perform the simulation  $\exp(-i\theta XXYY)$  in the Indiana machine, we can construct the simulation procedures (Algorithm 3) as follows: We construct the simulation operation  $\exp(-i\theta XXXX)$ , with the single qubit simulations  $\exp(-i\frac{\pi}{4}Z)$  and  $\exp(i\frac{7\pi}{4}Z)$  around the last two qubits.

Other quantum machines might have different permitted Pauli string sets, such as Quera machines [QuEra 2024]. Consequently, the machine Hamiltonian analog synthesization step must employ different analog synthesization methods for each quantum machine. We show the correctness lemma for the two machines below.

LEMMA 5.7 (ANALOG SYNTHESIZATION CORRECTNESS).  $\exp(-i\theta\hat{P})$  can be synthesized as a sequence of unitary operations as  $\Pi_k U_k$ , based on the simulations of Pauli strings permitted in the IBM machine ( $\{X, Z, ZZ\}$ ) and the Indiana machine ( $\{Z, X^*\}$ ).

PROOF. Fully mechanized proofs were done by the same methodology as proving Theorem 5.6. Here, we equate the two matrix interpretations of  $\exp(-i\theta\hat{P})$  and the unitaries generated via Algorithms 2 and 3.  $\square$

## 5.6 The Whole Pipeline Theorem

Below, we show the correctness theorem for compiling a Hamiltonian simulation of a constraint expression  $e$ , typed as  $\iota \vdash e \triangleright \mathcal{F}^h(\iota')$ , to quantum circuits. We first show the correctness theorem below for the compilation pipeline in Figure 6, without the perturbative gadget step; such a pipeline is modeled as  $\mathcal{F}^h(\iota) \vdash (e, r) \gg U : \mathcal{F}^u(\iota')$ . Such a compilation is split into the four steps above. The theorem is a complete version of Theorem 2.3.

THEOREM 5.8 (COMPILATION CORRECTNESS). Given  $e$ , typed as  $\iota \vdash e \triangleright \mathcal{F}^h(\iota)$ , and a time period  $r$ , we compile its simulation  $\exp(-ir e)$  to quantum circuit, as  $\mathcal{F}^h(\iota) \vdash (e, r) \gg U : \mathcal{F}^u(\iota')$ , for every state  $\psi$ , typed as  $\iota \vdash \psi$ , we transform it to  $\psi'$ , typed as  $\iota' \vdash \psi'$ , let  $\psi_1 = \llbracket \iota \vdash U \triangleright \mathcal{F}^u(\iota) \rrbracket_0(\psi)$ , we transform  $\psi_1$  to  $\psi'_1$ , typed as  $\iota' \vdash \psi'_1$ ; the error is bound by  $\|\psi'_1 - \llbracket \iota' \vdash \exp(-ier) \triangleright \mathcal{F}^u(\iota') \rrbracket_0(\psi')\| < \epsilon$ .

PROOF. Fully mechanized proofs are done by composing the Theorems 5.1, 5.3 and 5.5 to 5.7.  $\square$

The theorem states that the distance of the compiled circuit  $U$  and the semantic definition  $\exp(-ire)$  is less than a threshold  $\epsilon$ , defined as the error bound in Trotterization in Theorem 5.5. The proof combines Theorems 5.1, 5.3 and 5.5 and one of the Theorems 5.6 and 5.7, for compiling the simulation to digital and analog machines, respectively. The compilation correctness theorem, including the perturbative gadget algorithm, is given in Section D.

## 6 Related Work

This section reviews related work most relevant to our approach. While many other contributions exist, we focus on those directly connected to the semantics, type systems, and compilation techniques discussed in this paper.

**Second Quantization.** Second quantization, or occupation number representation, is a mathematical system used to describe and analyze quantum particle systems. The key ideas of the methodology were introduced by Paul Dirac [Dirac 1988] and were later developed by Pascual Jordan [Jordan and Wigner 1928a] and Vladimir Fock [Fock 1932; Reed and Simon 1975]. In this approach, the quantum states are represented in the Fock state basis, which is constructed by filling up each single-site state with a certain number of identical particles [Becchi 2010]. Later, many works were developed for describing second quantization in analyzing different systems, such as fermions in lattice-based systems [Levin and Wen 2003], chemical and biological molecule systems [Gori et al. 2023], nuclear physical systems [Christiansen 2004; Johnson et al. 2013]. Recently, researchers developed algebraic formalisms based on second quantization and Lie algebra [Batista and Ortiz 2004; Schwarz 2021] as a new extension of second quantization, in order to define the transformations from one particle system to another, such as defining a generalization of Jordan-Wigner Transformation [Batista and Ortiz 2001] to transform different particle systems to  $t(2)$  typed particle system, a.k.a., quantum computer systems. Ying [2014] developed a quantum version of recursion and program control flow based on creators and annihilators in second quantization.

The difference between these works and QBLUE is that QBLUE examines the programming aspects of second quantization as we identify its constraint, dynamic, and application semantics, with a certified compiler.

**Quantum Circuit-based Programming Languages.** Quantum circuit-based language development is a central focus in the field. Several industrial quantum circuit languages have been developed, including Q# [Svore et al. 2018], Quilc [Smith et al. 2020], ScaffCC [JavadiAbhari et al. 2015], ProjectQ [Steiger et al. 2018], Cirq [Developers 2023], and Qiskit [Aleksandrowicz et al. 2019]. While these languages lack formal semantics, they are grounded in a standardized denotational semantics for quantum circuits. In contrast, a number of tools focus on formal verification of quantum circuit programs. These include Qwire [Rand 2018], SQIR [Hietala et al. 2021], and QBricks [Chareton et al. 2021], as well as quantum Hoare logic and its extensions [Liu et al. 2019; Ying 2012; Zhou et al. 2023], and Qafny [Li et al. 2024]. These systems have been used to verify a range of quantum algorithms, including Grover’s search and quantum phase estimation. Verification has also been applied to quantum circuit optimizations, such as in voQC [Hietala et al. 2023] and CertiQ [Shi et al. 2019], and to quantum circuit compilation processes, as demonstrated by ReVerC [Amy et al. 2017] and ReQWIRE [Rand et al. 2018].

Several functional languages have been developed to model quantum circuits with formal semantics, including [Altenkirch and Grattage [n. d.]; Díaz-Caro et al. 2019; Fu et al. 2023; Grattage 2011, 2006; Green et al. 2013; Sabry et al. 2018; Selinger and Valiron 2013; van Tonder 2004; Vizzotto et al. 2013; Voichick et al. 2023; Ying 2016]. These languages are typically designed to encode quantum circuits as functional constructs, such as through quantum pattern matching. Silq [Bichsel

et al. 2020] introduces automatic uncomputation within a denotational semantics framework for describing circuit behavior. Finally, the ZX-calculus [Coecke and Duncan 2011; Wang 2023] provides a diagrammatic language for expressing unitary operations without measurement, offering an alternative to algebraic quantum semantics.

**Analog Quantum Computing Languages and Pulse Level Programming.** Several pulse-level and target-machine Hamiltonian programming interfaces treat quantum computers as analog quantum simulators. Notable examples include IBM Qiskit Pulse [Cross et al. 2022], QuEra Bloqade [blo 2023], and Pasqal Pulser [Silvério et al. 2022], all developed by hardware service providers. In parallel, computational quantum physics packages such as QuTiP [Johansson et al. 2012] support Hamiltonian simulation on classical computers. These efforts are inspired by a long history of classical analog compilation techniques [Achour and Rinard 2020; Achour et al. 2016]. SimuQ [Peng et al. 2024] introduces a formal language for analog quantum computing based on the construction of Hamiltonians using Pauli groups. Recent work by Cao et al. [2024] proposes a Trotterization algorithm that improves upon QDrift.

Compared to these approaches, QBLUE provides the first verified compilation framework that transforms user-level Hamiltonian programs, written in second quantization form, into both digital and analog quantum circuits.

**Quantum computational Approaches for Analyzing Particle Systems.** Many quantum computation software and algorithms have been proposed for analyzing particle systems. There are software tools [Bassman Oftelie et al. 2022; Li et al. 2022b; Powers et al. 2021; Schmitz et al. 2024] for performing particle system Hamiltonian simulation, by viewing it as a quantum algorithm and compiling it to quantum circuits. Many other works [Castaldo et al. 2022; Cervera-Lierta 2018; Yamaguchi and Yamamoto 2002; Yang et al. 2020] discuss simulating different particle systems in quantum computers. The variational quantum eigensolver is one of the most well-known algorithms [Cerezo et al. 2022; Tilly et al. 2022a] to analyze particle systems. It is mainly used for performing energy state computation, such as estimating the ground energy state of water molecules [Nam et al. 2020].

## 7 Conclusion and Future Work

We present QBLUE, the first verified compilation framework for second-quantization-based Hamiltonian simulation, aiming to define and analyze lattice-based particle systems. We examine the programmability of the second quantization formalism and identify that second quantization programs are constraints describing a system, and the Hamiltonian simulation is the dynamic semantics of the constraint-based system. We then show the QBLUE syntax, semantics, and type system, a generalization of the qubit-based system, to permit the definition of different particle systems and classical simulation problems. Via the typing and equational properties, we show the verified compilation procedure of compiling the Hamiltonian simulation for QBLUE programs to quantum circuits.

**Future Work.** We intend to certify many different Hamiltonian-level quantum optimization algorithms and develop tools for analyzing Hamiltonian-based programs. Another one is to develop different application semantics, especially for computing ground energy states useful in scientific computation, i.e., we can view the application semantics as computing a ground energy state. One of the previous frameworks, which performs the task and naturally extends from Hamiltonian simulation, is adiabatic quantum computation (AQC). This is a model of quantum computation that solves optimization problems by evolving a quantum system slowly from an initial Hamiltonian  $\hat{H}_m$  with a known ground state to a final Hamiltonian  $\hat{H}_p$  whose ground state encodes the solution. The QBLUE application semantics can be naturally extended to AQC for energy state computation.

## Acknowledgments

This material is based upon work supported by the National Science Foundation under Grant No. OSI-2435255.

## References

2023. Bloqade.jl: Package for the quantum computation and quantum simulation based on the neutral-atom architecture. [https://github.com/QuEraComputing/Bloqade.jl/](https://github.com/QuEraComputing/Bloqade.jl)
- Sara Achour and Martin Rinard. 2020. Noise-Aware Dynamical System Compilation for Analog Devices with Legno. In *Proceedings of the Twenty-Fifth International Conference on Architectural Support for Programming Languages and Operating Systems (Lausanne, Switzerland) (ASPLOS '20)*. Association for Computing Machinery, New York, NY, USA, 149–166. doi:10.1145/3373376.3378449
- Sara Achour, Rahul Sarpeshkar, and Martin C. Rinard. 2016. Configuration synthesis for programmable analog devices with Arco. *SIGPLAN Not.* 51, 6 (jun 2016), 177–193. doi:10.1145/2980983.2908116
- Gadi Aleksandrowicz, Thomas Alexander, Panagiotis Barkoutsos, Luciano Bello, Yael Ben-Haim, David Bucher, Francisco Jose Cabrera-Hernández, Jorge Carballo-Franquis, Adrian Chen, Chun-Fu Chen, Jerry M. Chow, Antonio D. Córcoles-Gonzales, Abigail J. Cross, Andrew Cross, Juan Cruz-Benito, Chris Culver, Salvador De La Puente González, Enrique De La Torre, Delton Ding, Eugene Dumitrescu, Ivan Duran, Pieter Eendebak, Mark Everitt, Ismael Faro Sertage, Albert Frisch, Andreas Fuhrer, Jay Gambetta, Borja Godoy Gago, Juan Gomez-Mosquera, Donny Greenberg, Ikko Hamamura, Vojtech Havlicek, Joe Hellmers, Lukasz Herok, Hiroshi Horii, Shaohan Hu, Takashi Imamichi, Toshinari Itoko, Ali Javadi-Abhari, Naoki Kanazawa, Anton Karazeev, Kevin Krsulich, Peng Liu, Yang Luh, Yunho Maeng, Manoel Marques, Francisco Jose Martin-Fernández, Douglas T. McClure, David McKay, Srujan Meesala, Antonio Mezzacapo, Nikolaj Moll, Diego Moreda Rodriguez, Giacomo Nannicini, Paul Nation, Pauline Ollitrault, Lee James O’Riordan, Hanhee Paik, Jesús Pérez, Anna Phan, Marco Pistoia, Viktor Prutyayov, Max Reuter, Julia Rice, Abdón Rodríguez Davila, Raymond Harry Putra Rudy, Mingi Ryu, Ninad Sathaye, Chris Schnabel, Eddie Schoute, Kanav Setia, Yunong Shi, Adenilton Silva, Yukio Siraichi, Seyon Sivarajah, John A. Smolin, Mathias Soeken, Hitomi Takahashi, Ivano Tavernelli, Charles Taylor, Pete Taylour, Kenso Trabling, Matthew Treinish, Wes Turner, Desiree Vogt-Lee, Christophe Vuillot, Jonathan A. Wildstrom, Jessica Wilson, Erick Winston, Christopher Wood, Stephen Wood, Stefan Wörner, Ismail Yunus Akhalwaya, and Christa Zoufal. 2019. Qiskit: An open-source framework for quantum computing. doi:10.5281/zenodo.2562110
- Thomas Alexander, Naoki Kanazawa, Daniel J Egger, Lauren Capelluto, Christopher J Wood, Ali Javadi-Abhari, and David C McKay. 2020. Qiskit pulse: programming quantum computers through the cloud with pulses. *Quantum Science and Technology* 5, 4 (aug 2020), 044006. doi:10.1088/2058-9565/aba404
- T. Altenkirch and J. Grattage. [n. d.]. A Functional Quantum Programming Language. In *20th Annual IEEE Symposium on Logic in Computer Science (LICS' 05)*. IEEE. doi:10.1109/lics.2005.1
- Matthew Amy, Martin Roetteler, and Krysta M. Svore. 2017. Verified Compilation of Space-Efficient Reversible Circuits. In *Computer Aided Verification*, Rupak Majumdar and Viktor Kunčák (Eds.). Springer International Publishing, Cham, 3–21.
- P.W. Anderson. 1997. *Basic Notions of Condensed Matter Physics*. Westview Press.
- E. Aprà, E. J. Bylaska, W. A. de Jong, N. Govind, K. Kowalski, T. P. Straatsma, M. Valiev, H. J. J. van Dam, Y. Alexeev, J. Anchell, V. Anisimov, F. W. Aquino, R. Atta-Fynn, J. Autschbach, N. P. Bauman, J. C. Becca, D. E. Bernholdt, K. Bhaskaran-Nair, S. Bogatko, P. Borowski, J. Boschen, J. Brabec, A. Bruner, E. Cauët, Y. Chen, G. N. Chuev, C. J. Cramer, J. Daily, M. J. O. Deegan, Jr. Dunning, T. H., M. Dupuis, K. G. Dyall, G. I. Fann, S. A. Fischer, A. Fonari, H. Früchtl, L. Gagliardi, J. Garza, N. Gawande, S. Ghosh, K. Glaesemann, A. W. Götz, J. Hammond, V. Helms, E. D. Hermes, K. Hirao, S. Hirata, M. Jacquelin, L. Jensen, B. G. Johnson, H. Jónsson, R. A. Kendall, M. Klemm, R. Kobayashi, V. Konkov, S. Krishnamoorthy, M. Krishnan, Z. Lin, R. D. Lins, R. J. Littlefield, A. J. Logsdail, K. Lopata, W. Ma, A. V. Marenich, J. Martin del Campo, D. Mejia-Rodriguez, J. E. Moore, J. M. Mullin, T. Nakajima, D. R. Nascimento, J. A. Nichols, P. J. Nichols, J. Nieplocha, A. Otero-de-la Roza, B. Palmer, A. Panyala, T. Pirojsirikul, B. Peng, R. Peverati, J. Pittner, L. Pollack, R. M. Richard, P. Sadayappan, G. C. Schatz, W. A. Shelton, D. W. Silverstein, D. M. A. Smith, T. A. Soares, D. Song, M. Swart, H. L. Taylor, G. S. Thomas, V. Tipparaju, D. G. Truhlar, K. Tsemekhman, T. Van Voorhis, Á. Vázquez-Mayagoitia, P. Verma, O. Villa, A. Vishnu, K. D. Vogiatzis, D. Wang, J. H. Weare, M. J. Williamson, T. L. Windus, K. Woliński, A. T. Wong, Q. Wu, C. Yang, Q. Yu, M. Zacharias, Z. Zhang, Y. Zhao, and R. J. Harrison. 2020. NWChem: Past, present, and future. *The Journal of Chemical Physics* 152, 18 (05 2020), 184102. arXiv:[https://pubs.aip.org/aip/jcp/article-pdf/doi/10.1063/5.0004997/16684361/184102\\_1\\_online.pdf](https://pubs.aip.org/aip/jcp/article-pdf/doi/10.1063/5.0004997/16684361/184102_1_online.pdf) doi:10.1063/5.0004997
- A. Auerbach. 1994. *Interacting Electrons and Quantum Magnetism*. Springer-Verlag, New York.
- Sheldon Axler. 2015. *Linear Algebra Done Right* (third ed.). Springer, Cham. xvii + 340 pages. doi:10.1007/978-3-319-11080-6
- Lindsay Bassman Oflerie, Connor Powers, and Wibe A. De Jong. 2022. ArQTiC: A Full-stack Software Package for Simulating Materials on Quantum Computers. *ACM Transactions on Quantum Computing* 3, 3, Article 17 (jun 2022), 17 pages. doi:10.1145/3511715

- C. D. Batista and G. Ortiz. 2001. Generalized Jordan-Wigner Transformations. *Physical Review Letters* 86, 6 (Feb. 2001), 1082–1085. doi:10.1103/physrevlett.86.1082
- C. D. Batista and G. Ortiz. 2004. Algebraic approach to interacting quantum systems. *Advances in Physics* 53, 1 (Jan. 2004), 1–82. doi:10.1080/00018730310001642086
- Carlo Maria Becchi. 2010. Second quantization. *Scholarpedia* 5, 6 (2010), 7902. doi:10.4249/SCHOLARPEDIA.7902
- Yves Bertot and Pierre Castéran. 2013. *Interactive theorem proving and program development: Coq'Art: the calculus of inductive constructions*. Springer Science & Business Media.
- Benjamin Bichsel, Maximilian Baader, Timon Gehr, and Martin Vechev. 2020. Silq: A High-Level Quantum Language with Safe Uncomputation and Intuitive Semantics. In *Proceedings of the 41st ACM SIGPLAN Conference on Programming Language Design and Implementation* (London, UK) (PLDI 2020). Association for Computing Machinery, New York, NY, USA, 286–300. doi:10.1145/3385412.3386007
- Earl Campbell. 2019. Random Compiler for Fast Hamiltonian Simulation. *Physical Review Letters* 123, 7 (Aug. 2019). doi:10.1103/physrevlett.123.070503
- Xiuqi Cao, Junyu Zhou, Yuhao Liu, Yunong Shi, and Gushu Li. 2024. MarQSim: Reconciling Determinism and Randomness in Compiler Optimization for Quantum Simulation. arXiv:2408.03429 [quant-ph] <https://arxiv.org/abs/2408.03429>
- Yudong Cao, Jonathan Romero, Jonathan P. Olson, Matthias Degroote, Peter D. Johnson, Mária Kieferová, Ian D. Kivlichan, Tim Menke, Borja Peropadre, Nicolas P. D. Sawaya, Sukin Sim, Libor Veis, and Alán Aspuru-Guzik. 2019. Quantum Chemistry in the Age of Quantum Computing. *Chemical Reviews* 119, 19 (09 Oct 2019), 10856–10915. doi:10.1021/acs.chemrev.8b00803
- Davide Castaldo, Soran Jahangiri, Alain Delgado, and Stefano Corni. 2022. Quantum Simulation of Molecules in Solution. *Journal of Chemical Theory and Computation* 18, 12 (2022), 7457–7469. arXiv:<https://doi.org/10.1021/acs.jctc.2c00974> doi:10.1021/acs.jctc.2c00974 PMID: 36351289.
- M. Cerezo, Kunal Sharma, Andrew Arrasmith, and Patrick J. Coles. 2022. Variational quantum state eigensolver. *npj Quantum Information* 8, 1 (21 Sep 2022), 113. doi:10.1038/s41534-022-00611-6
- Alba Cervera-Lierta. 2018. Exact Ising model simulation on a quantum computer. *Quantum* 2 (Dec. 2018), 114. doi:10.22331/q-2018-12-21-114
- Christophe Charetton, Sébastien Bardin, François Bobot, Valentin Perrelle, and Benoît Valiron. 2021. An Automated Deductive Verification Framework for Circuit-building Quantum Programs. In *Programming Languages and Systems - 30th European Symposium on Programming, ESOP 2021, Held as Part of the European Joint Conferences on Theory and Practice of Software, ETAPS 2021, Luxembourg City, Luxembourg, March 27 - April 1, 2021, Proceedings (Lecture Notes in Computer Science, Vol. 12648)*, Nobuko Yoshida (Ed.). Springer, 148–177. doi:10.1007/978-3-030-72019-3\_6
- Andrew M. Childs, Yuan Su, Minh C. Tran, Nathan Wiebe, and Shuchen Zhu. 2021. Theory of Trotter Error with Commutator Scaling. *Phys. Rev. X* 11 (Feb 2021), 011020. Issue 1. doi:10.1103/PhysRevX.11.011020
- Ove Christiansen. 2004. A second quantization formulation of multimode dynamics. *The Journal of Chemical Physics* 120, 5 (02 2004), 2140–2148. arXiv:[https://pubs.aip.org/aip/jcp/article-pdf/120/5/2140/19087082/2140\\_1\\_online.pdf](https://pubs.aip.org/aip/jcp/article-pdf/120/5/2140/19087082/2140_1_online.pdf) doi:10.1063/1.1637578
- Bob Coecke and Ross Duncan. 2011. Interacting quantum observables: categorical algebra and diagrammatics. *New Journal of Physics* 13, 4 (April 2011), 043016. doi:10.1088/1367-2630/13/4/043016
- Andrew Cross, Ali Javadi-Abhari, Thomas Alexander, Niel De Beaudrap, Lev S. Bishop, Steven Heidel, Colm A. Ryan, Prasahnt Sivarajah, John Smolin, Jay M. Gambetta, and Blake R. Johnson. 2022. OpenQASM 3: A Broader and Deeper Quantum Assembly Language. *ACM Transactions on Quantum Computing* 3, 3, Article 12 (sep 2022), 50 pages. doi:10.1145/3505636
- Cirq Developers. 2023. *Cirq*. doi:10.5281/zenodo.10247207
- P. A. M. Dirac. 1939. A new notation for quantum mechanics. *Mathematical Proceedings of the Cambridge Philosophical Society* (1939).
- P. A. M. Dirac. 1988. *The Quantum Theory of the Emission and Absorption of Radiation*. Springer Netherlands, Dordrecht, 157–179. doi:10.1007/978-94-009-3051-3\_9
- Weijie Du and James P. Vary. 2023. Multi-nucleon structure and dynamics via quantum computing. arXiv:2304.04838 [nucl-th]
- Alejandro Diaz-Caro, Gilles Dowek, and Juan Pablo Rinaldi. 2019. Two linearities for quantum computing in the lambda calculus. *Biosystems* 186 (2019), 104012. doi:10.1016/j.biosystems.2019.104012 Selected papers from the International Conference on the Theory and Practice of Natural Computing 2017.
- Prashant S. Emani, Jonathan Warrell, Alan Anticevic, Stefan Bekiranov, Michael Gandal, Michael J. McConnell, Guillermo Sapiro, Alán Aspuru-Guzik, Justin T. Baker, Matteo Bastiani, John D. Murray, Stamatios N. Sotiropoulos, Jacob Taylor, Geetha Senthil, Thomas Lehner, Mark B. Gerstein, and Aram W. Harrow. 2021. Quantum computing at the frontiers of biological sciences. *Nature Methods* 18, 7 (01 Jul 2021), 701–709. doi:10.1038/s41592-020-01004-3
- Francesco A. Evangelista and Victor S. Batista. 2023. Editorial: Quantum Computing for Chemistry. *Journal of Chemical Theory and Computation* 19, 21 (14 Nov 2023), 7435–7436. doi:10.1021/acs.jctc.3c01043

- A. K. Fedorov and M. S. Gelfand. 2021. Towards practical applications in quantum computational biology. *Nature Computational Science* 1, 2 (01 Feb 2021), 114–119. doi:10.1038/s43588-021-00024-z
- Richard P Feynman. 1982. Simulating physics with computers. *International journal of theoretical physics* 21, 6/7 (1982), 467–488.
- V. Fock. 1932. Konfigurationsraum und zweite Quantelung. *Zeitschrift für Physik* 75, 9 (01 Sep 1932), 622–647. doi:10.1007/BF01344458
- Peng Fu, Kohei Kishida, Neil J. Ross, and Peter Selinger. 2023. Proto-Quipper with Dynamic Lifting. *Proc. ACM Program. Lang.* 7, POPL, Article 11 (jan 2023), 26 pages. doi:10.1145/3571204
- Matteo Gori, Philip Kurian, and Alexandre Tkatchenko. 2023. Second quantization of many-body dispersion interactions for chemical and biological systems. *Nature Communications* 14, 1 (12 Dec 2023), 8218. doi:10.1038/s41467-023-43785-z
- Jonathan Grattage. 2011. An Overview of QML With a Concrete Implementation in Haskell, In Proceedings of the Joint 5th International Workshop on Quantum Physics and Logic and 4th Workshop on Developments in Computational Models (QPL/DCM 2008). *Electronic Notes in Theoretical Computer Science* 270, 1, 165–174. arXiv:0806.2735 [quant-ph] doi:10.1016/j.entcs.2011.01.015
- Jonathan James Grattage. 2006. *A functional quantum programming language*. Ph.D. Dissertation. University of Nottingham. <http://eprints.nottingham.ac.uk/10250/>
- Alexander Green, Peter LeFanu Lumsdaine, Neil J. Ross, Peter Selinger, and Benoît Valiron. 2013. Quipper: A scalable quantum programming language. In *Proceedings of the 34th ACM SIGPLAN Conference on Programming Language Design and Implementation (PLDI 2013)*. 333–342. doi:10.1145/2491956.2462177
- Daniel M. Greenberger, Michael A. Horne, and Anton Zeilinger. 1989. *Going beyond Bell's Theorem*. Springer Netherlands, Dordrecht, 69–72. doi:10.1007/978-94-017-0849-4\_10
- Kesha Hietala, Robert Rand, Shih-Han Hung, Liyi Li, and Michael Hicks. 2021. Proving Quantum Programs Correct. In *Proceedings of the Conference on Interactive Theorem Proving (ITP)*.
- Kesha Hietala, Robert Rand, Liyi Li, Shih-Han Hung, Xiaodi Wu, and Michael Hicks. 2023. A Verified Optimizer for Quantum Circuits. *ACM Trans. Program. Lang. Syst.* 45, 3, Article 18 (Sept. 2023), 35 pages. doi:10.1145/3604630
- Ali JavadiAbhari, Shruti Patil, Daniel Kudrow, Jeff Heckey, Alexey Lvov, Frederic T. Chong, and Margaret Martonosi. 2015. ScaffCC: Scalable compilation and analysis of quantum programs. *Parallel Comput.* 45 (June 2015), 2–17. doi:10.1016/j.parco.2014.12.001
- J.R. Johansson, P.D. Nation, and Franco Nori. 2012. QuTiP: An open-source Python framework for the dynamics of open quantum systems. *Computer Physics Communications* 183, 8 (2012), 1760–1772. doi:10.1016/j.cpc.2012.02.021
- Calvin W. Johnson, W. Erich Ormand, and Plamen G. Krastev. 2013. Factorization in large-scale many-body calculations. *Computer Physics Communications* 184, 12 (Dec. 2013), 2761–2774. doi:10.1016/j.cpc.2013.07.022
- P. Jordan and E. Wigner. 1928a. Über das Paulische Äquivalenzverbot. *Zeitschrift für Physik* 47, 9 (01 Sep 1928), 631–651. doi:10.1007/BF01331938
- Pascal Jordan and Eugene P. Wigner. 1928b. About the Pauli exclusion principle. *Z. Phys.* 47 (1928), 631–651. doi:10.1007/BF01331938
- Stephen P. Jordan and Edward Farhi. 2008. Perturbative Gadgets at Arbitrary Orders. *Phys. Rev. A* 77 (Jun 2008), 062329. Issue 6. doi:10.1103/PhysRevA.77.062329
- Michael Kreshchuk, Shaoyang Jia, William Kirby, Gary Goldstein, James Vary, and Peter Love. 2021. Light-Front Field Theory on Current Quantum Computers. *Entropy* 23, 5 (5 2021). doi:10.3390/e23050597
- Antonis Kyrianiadis, A J Rasmusson, and Philip Richerme. 2024. Interaction graph engineering in trapped-ion quantum simulators with global drives. *New Journal of Physics* 26, 2 (Feb. 2024), 023033. doi:10.1088/1367-2630/ad264d
- B. P. Lanyon, J. D. Whitfield, G. G. Gillett, M. E. Goggin, M. P. Almeida, I. Kassal, J. D. Biamonte, M. Mohseni, B. J. Powell, M. Barbieri, A. Aspuru-Guzik, and A. G. White. 2010. Towards quantum chemistry on a quantum computer. *Nature Chemistry* 2, 2 (01 Feb 2010), 106–111. doi:10.1038/nchem.483
- Lingling Lao and Dan E. Browne. 2022. 2QAN: a quantum compiler for 2-local qubit hamiltonian simulation algorithms. In *Proceedings of the 49th Annual International Symposium on Computer Architecture (New York, New York) (ISCA '22)*. Association for Computing Machinery, New York, NY, USA, 351–365. doi:10.1145/3470496.3527394
- Seunghoon Lee, Joonho Lee, Huanchen Zhai, Yu Tong, Alexander M. Dalzell, Ashutosh Kumar, Phillip Helms, Johnnie Gray, Zhi-Hao Cui, Wenyuan Liu, Michael Kastoryano, Ryan Babbush, John Preskill, David R. Reichman, Earl T. Campbell, Edward F. Valeev, Lin Lin, and Garnet Kin-Lic Chan. 2023. Evaluating the evidence for exponential quantum advantage in ground-state quantum chemistry. *Nature Communications* 14, 1 (07 Apr 2023), 1952. doi:10.1038/s41467-023-37587-6
- Michael Levin and Xiao-Gang Wen. 2003. Fermions, strings, and gauge fields in lattice spin models. *Phys. Rev. B* 67 (2003), 245316. arXiv:cond-mat/0302460 doi:10.1103/PhysRevB.67.245316
- Boxi Li, Shah Nawaz Ahmed, Sidhant Saraogi, Neill Lambert, Franco Nori, Alexander Pitchford, and Nathan Shammah. 2022a. Pulse-level noisy quantum circuits with QuTiP. *Quantum* 6 (Jan. 2022), 630. doi:10.22331/q-2022-01-24-630

- Gushu Li, Anbang Wu, Yunong Shi, Ali Javadi-Abhari, Yufei Ding, and Yuan Xie. 2022b. Paulihedral: a generalized block-wise compiler optimization framework for Quantum simulation kernels. In *Proceedings of the 27th ACM International Conference on Architectural Support for Programming Languages and Operating Systems (Lausanne, Switzerland) (ASPLOS '22)*. Association for Computing Machinery, New York, NY, USA, 554–569. doi:10.1145/3503222.3507715
- Liyi Li, Mingwei Zhu, Rance Cleaveland, Alexander Nicoletti, Yi Lee, Le Chang, and Xiaodi Wu. 2024. Qafny: A Quantum-Program Verifier. In *ECOOP 2024*.
- Sophus Lie. 1880. Theorie der Transformationsgruppen I. *Math. Ann.* 16, 4 (01 Dec 1880), 441–528. doi:10.1007/BF01446218
- Junyi Liu, Bohua Zhan, Shuling Wang, Shenggang Ying, Tao Liu, Yangjia Li, Mingsheng Ying, and Naijun Zhan. 2019. Formal Verification of Quantum Algorithms Using Quantum Hoare Logic. In *Computer Aided Verification*, Isil Dillig and Serdar Tasiran (Eds.). Springer International Publishing, Cham, 187–207.
- Seth Lloyd. 1996. Universal Quantum Simulators. *Science* 273, 5278 (1996), 1073–1078. arXiv:<https://www.science.org/doi/pdf/10.1126/science.273.5278.1073> doi:10.1126/science.273.5278.1073
- Sam McArdle, Suguru Endo, Alan Aspuru-Guzik, Simon C. Benjamin, and Xiao Yuan. 2020. Quantum computational chemistry. *Rev. Mod. Phys.* 92 (Mar 2020), 015003. Issue 1. doi:10.1103/RevModPhys.92.015003
- Filipe V. Melo, Alexandre M. Souza, Ivan S. Oliveira, and Roberto S. Sarthour. 2021. Quantum simulation of the two-site Hubbard Hamiltonian. *Physics Open* 6 (2021), 100053. doi:10.1016/j.physo.2020.100053
- Yunseong Nam, Jwo-Sy Chen, Neal C. Pseni, Kenneth Wright, Conor Delaney, Dmitri Maslov, Kenneth R. Brown, Stewart Allen, Jason M. Amini, Joel Apisdorf, Kristin M. Beck, Aleksey Blinov, Vandiver Chaplin, Mika Chmielewski, Coleman Collins, Shantanu Debnath, Kai M. Hudek, Andrew M. Ducore, Matthew Keesan, Sarah M. Kreikemeier, Jonathan Mizrahi, Phil Solomon, Mike Williams, Jaime David Wong-Campos, David Moehring, Christopher Monroe, and Jungsang Kim. 2020. Ground-state energy estimation of the water molecule on a trapped-ion quantum computer. *npj Quantum Information* 6, 1 (03 Apr 2020), 33. doi:10.1038/s41534-020-0259-3
- Michael A. Nielsen and Isaac L. Chuang. 2011. *Quantum Computation and Quantum Information* (10th anniversary ed.). Cambridge University Press, USA.
- Carlos Outeiral, Martin Strahm, Jiye Shi, Garrett M. Morris, Simon C. Benjamin, and Charlotte M. Deane. 2021. The prospects of quantum computing in computational molecular biology. *WIREs Computational Molecular Science* 11, 1 (2021), e1481. arXiv:<https://wires.onlinelibrary.wiley.com/doi/pdf/10.1002/wcms.1481> doi:10.1002/wcms.1481
- Yuxiang Peng, Jacob Young, Pengyu Liu, and Xiaodi Wu. 2024. SimuQ: A Framework for Programming Quantum Hamiltonian Simulation with Analog Compilation. *Proc. ACM Program. Lang.* 8, POPL, Article 81 (Jan 2024), 31 pages. doi:10.1145/3632923
- Connor Powers, Lindsay Bassman, Thomas M. Linker, Ken ichi Nomura, Sahil Gulania, Rajiv K. Kalia, Aiichiro Nakano, and Priya Vashishta. 2021. MISTIQS: An open-source software for performing quantum dynamics simulations on quantum computers. *SoftwareX* 14 (2021), 100696. doi:10.1016/j.softx.2021.100696
- QuEra. 2024. *QuEra Computing Inc.* <https://github.com/QuEraComputing/>
- Robert Rand. 2018. *Formally verified quantum programming*. Ph.D. Dissertation. University of Pennsylvania.
- Robert Rand, Jennifer Paykin, Dong-Ho Lee, and S. Zdancewic. 2018. ReQWIRE: Reasoning about Reversible Quantum Circuits. In *QPL*.
- M. Reed and B. Simon. 1975. *Methods of Modern Mathematical Physics. 2. Fourier Analysis, Self-adjointness*.
- Philip Richerme. 2025. Multi-Mode Global Driving of Trapped Ions for Quantum Circuit Synthesis. arXiv:2502.13302 [quant-ph] <https://arxiv.org/abs/2502.13302>
- Amr Sabry, Benoît Valiron, and Juliana Kaizer Vizzotto. 2018. From Symmetric Pattern-Matching to Quantum Control. In *Foundations of Software Science and Computation Structures*, Christel Baier and Ugo Dal Lago (Eds.). Springer International Publishing, Cham, 348–364.
- S. Sachdev. 2011. *Quantum Phase Transitions* (2nd ed.). Cambridge University Press.
- Michael W. Schmidt, Kim K. Baldridge, Jerry A. Boatz, Steven T. Elbert, Mark S. Gordon, Jan H. Jensen, Shiro Koseki, Nikita Matsunaga, Kiet A. Nguyen, Shujun Su, Theresa L. Windus, Michel Dupuis, and John A. Montgomery Jr. 1993. General atomic and molecular electronic structure system. *Journal of Computational Chemistry* 14, 11 (1993), 1347–1363. arXiv:<https://onlinelibrary.wiley.com/doi/pdf/10.1002/jcc.540141112> doi:10.1002/jcc.540141112
- Albert T. Schmitz, Nicolas P. D. Sawaya, Sonika Johri, and A. Y. Matsuura. 2024. Graph optimization perspective for low-depth Trotter-Suzuki decomposition. *Phys. Rev. A* 109 (Apr 2024), 042418. Issue 4. doi:10.1103/PhysRevA.109.042418
- A. Schwarz. 2021. Geometric and algebraic approaches to quantum theory. *Nuclear Physics B* 973 (2021), 115601. doi:10.1016/j.nuclphysb.2021.115601
- Peter Selinger and Benoit Valiron. 2013. Quantum Lambda Calculus. *Semantic Techniques in Quantum Computation* (01 2013). doi:10.1017/CBO9781139193313.005
- Yunong Shi, Xupeng Li, Runzhou Tao, Ali Javadi-Abhari, Andrew W. Cross, Frederic T. Chong, and Ronghui Gu. 2019. Contract-based verification of a realistic quantum compiler. *arXiv e-prints* (Aug 2019). arXiv:1908.08963 [quant-ph]

- Henrique Silvério, Sebastián Grijalva, Constantin Dalyac, Lucas Leclerc, Peter J. Karalekas, Nathan Shammah, Mourad Beji, Louis-Paul Henry, and Loïc Henriët. 2022. Pulser: An open-source package for the design of pulse sequences in programmable neutral-atom arrays. *Quantum* 6 (Jan. 2022), 629. doi:10.22331/q-2022-01-24-629
- Robert S. Smith, Eric C. Peterson, Mark G. Skilbeck, and Erik J. Davis. 2020. An Open-Source, Industrial-Strength Optimizing Compiler for Quantum Programs. arXiv:2003.13961 [quant-ph]
- Damian S. Steiger, Thomas Häner, and Matthias Troyer. 2018. ProjectQ: an open source software framework for quantum computing. *Quantum* 2 (Jan. 2018), 49. doi:10.22331/q-2018-01-31-49
- Masuo Suzuki. 1991. General theory of fractal path integrals with applications to many-body theories and statistical physics. *J. Math. Phys.* 32, 2 (02 1991), 400–407. arXiv:https://pubs.aip.org/aip/jmp/article-pdf/32/2/400/19166143/400\_1\_online.pdf doi:10.1063/1.529425
- Krysta Svore, Alan Geller, Matthias Troyer, John Azariah, Christopher Granade, Bettina Heim, Vadym Kliuchnikov, Mariia Mykhailova, Andres Paz, and Martin Roetteler. 2018. Q#: Enabling Scalable Quantum Computing and Development with a High-level DSL. In *Proceedings of the Real World Domain Specific Languages Workshop 2018 (RWDSL2018)*. ACM. doi:10.1145/3183895.3183901
- Francesco Tacchino, Alessandro Chiesa, Stefano Carretta, and Dario Gerace. 2019. Quantum Computers as Universal Quantum Simulators: State-of-the-Art and Perspectives. *Advanced Quantum Technologies* 3, 3 (Dec. 2019). doi:10.1002/qute.201900052
- Jules Tilly, Hongxiang Chen, Shuxiang Cao, Dario Picozzi, Kanav Setia, Ying Li, Edward Grant, Leonard Wossnig, Ivan Rungger, George H. Booth, and Jonathan Tennyson. 2022a. The Variational Quantum Eigensolver: A review of methods and best practices. *Physics Reports* 986 (Nov. 2022), 1–128. doi:10.1016/j.physrep.2022.08.003
- Jules Tilly, Hongxiang Chen, Shuxiang Cao, Dario Picozzi, Kanav Setia, Ying Li, Edward Grant, Leonard Wossnig, Ivan Rungger, George H. Booth, and Jonathan Tennyson. 2022b. The Variational Quantum Eigensolver: A review of methods and best practices. *Physics Reports* 986 (2022), 1–128. doi:10.1016/j.physrep.2022.08.003 The Variational Quantum Eigensolver: a review of methods and best practices.
- André van Tonder. 2004. A Lambda Calculus for Quantum Computation. *SIAM J. Comput.* 33, 5 (Jan. 2004), 1109–1135. doi:10.1137/s0097539703432165
- Libor Veis, Jakub Višňák, Hiroaki Nishizawa, Hiromi Nakai, and Jiří Pittner. 2016. Quantum chemistry beyond Born–Oppenheimer approximation on a quantum computer: A simulated phase estimation study. *International Journal of Quantum Chemistry* 116, 18 (2016), 1328–1336. arXiv:https://onlinelibrary.wiley.com/doi/pdf/10.1002/qua.25176 doi:10.1002/qua.25176
- Juliana Kaizer Vizzotto, Bruno Crestani Calegari, and Eduardo Kessler Piveta. 2013. A Double Effect  $\lambda$ -calculus for Quantum Computation. In *Programming Languages*, André Rauber Du Bois and Phil Trinder (Eds.). Springer Berlin Heidelberg, Berlin, Heidelberg, 61–74.
- Finn Voichick, Liyi Li, Robert Rand, and Michael Hicks. 2023. Qunity: A Unified Language for Quantum and Classical Computing. *Proceedings of the ACM on Programming Languages* 7, POPL (Jan. 2023), 921–951. doi:10.1145/3571225
- Quanlong Wang. 2023. Completeness of the ZX-calculus. arXiv:2209.14894 [quant-ph]
- James D. Whitfield, Jacob Biamonte, and Alán Aspuru-Guzik. 2011. Simulation of electronic structure Hamiltonians using quantum computers. *Molecular Physics* 109, 5 (March 2011), 735–750. doi:10.1080/00268976.2011.552441
- Mingquan Xu, Zikun Li, Oded Padon, Sina Lin, Jessica Pointing, Auguste Hirth, Henry Ma, Jens Palsberg, Alex Aiken, Umut A. Acar, and Zhihao Jia. 2022. Quartz: superoptimization of Quantum circuits. In *Proceedings of the 43rd ACM SIGPLAN International Conference on Programming Language Design and Implementation (San Diego, CA, USA) (PLDI 2022)*. Association for Computing Machinery, New York, NY, USA, 625–640. doi:10.1145/3519939.3523433
- Fumiko Yamaguchi and Yoshihisa Yamamoto. 2002. Quantum simulation of the t–J model. *Superlattices and Microstructures* 32, 4 (2002), 343–345. doi:10.1016/S0749-6036(03)00039-9 Papers from the 8th International Symposium of Advanced Physical Fields on Advanced Materials for Quantum Computing.
- Bing Yang, Hui Sun, Robert Ott, Han-Yi Wang, Torsten V. Zache, Jad C. Halimeh, Zhen-Sheng Yuan, Philipp Hauke, and Jian-Wei Pan. 2020. Observation of gauge invariance in a 71-site Bose–Hubbard quantum simulator. *Nature* 587, 7834 (Nov. 2020), 392–396. doi:10.1038/s41586-020-2910-8
- Mingsheng Ying. 2012. Floyd–Hoare Logic for Quantum Programs. *ACM Trans. Program. Lang. Syst.* 33, 6, Article 19 (Jan. 2012), 49 pages. doi:10.1145/2049706.2049708
- Mingsheng Ying. 2014. Quantum Recursion and Second Quantisation. arXiv:1405.4443 [quant-ph]
- Mingsheng Ying. 2016. *Foundations of Quantum Programming*. Elsevier Science, Cambridge, MA. xii + 357 pages.
- Federico Zahariev, Peng Xu, Bryce M. Westheimer, Simon Webb, Jorge Galvez Vallejo, Ananta Tiwari, Vaibhav Sundriyal, Masha Sosonkina, Jun Shen, George Schoendorff, Megan Schlinsog, Tosaporn Sattasathuchana, Klaus Ruedenberg, Luke B. Roskop, Alistair P. Rendell, David Poole, Piotr Piecuch, Buu Q. Pham, Vladimir Mironov, Joani Mato, Sam Leonard, Sarom S. Leang, Joe Ivanić, Jackson Hayes, Taylor Harville, Karthik Gururangan, Emilie Guidez, Igor S. Gerasimov, Christian Friedl, Katherine N. Ferreras, George Elliott, Dipayan Datta, Daniel Del Angel Cruz, Laura Carrington, Colleen

- Bertoni, Giuseppe M. J. Barca, Melisa Alkan, and Mark S. Gordon. 2023. The General Atomic and Molecular Electronic Structure System (GAMESS): Novel Methods on Novel Architectures. *Journal of Chemical Theory and Computation* 19, 20 (24 Oct 2023), 7031–7055. doi:10.1021/acs.jctc.3c00379
- Dan-Bo Zhang, Hongxi Xing, Hui Yan, Enke Wang, and Shi-Liang Zhu. 2021. Selected topics of quantum computing for nuclear physics\*. *Chinese Physics B* 30, 2 (feb 2021), 020306. doi:10.1088/1674-1056/abd761
- Li Zhou, Gilles Barthe, Pierre-Yves Strub, Junyi Liu, and Mingsheng Ying. 2023. CoQ: Foundational Verification of Quantum Programs. *Proc. ACM Program. Lang.* 7, POPL, Article 29 (jan 2023), 33 pages. doi:10.1145/3571222

## A In Depth Background

This section provides additional background information.

### A.1 Quantum Hardware Circuit Operations

Computation on a quantum value consists of a series of *quantum operations*, each acting on a subset of qubits in the quantum value. In the standard form, quantum computations are expressed as *circuits*, as in Figure 13, which depicts a circuit that prepares the Greenberger-Horne-Zeilinger (GHZ) state [Greenberger et al. 1989] – an  $n$ -qubit entangled value of the form:  $|\text{GHZ}^n\rangle = \frac{1}{\sqrt{2}}(|0\rangle^{\otimes n} + |1\rangle^{\otimes n})$ , where  $|d\rangle^{\otimes n} = \bigotimes_{d=0}^{n-1} |d\rangle$ .

In these circuits, each horizontal wire represents a qubit, and boxes on these wires indicate quantum operations, or *gates*. The circuit in Figure 13 uses  $n$  qubits and applies  $n$  gates: a *Hadamard* (H) gate and  $n - 1$  *controlled-not* (CNOT) gates. Applying a gate to a quantum value *evolves* it. Its traditional semantics is expressed by multiplying the value’s vector form by the gate’s corresponding matrix representation:  $n$ -qubit gates are  $2^n$ -by- $2^n$  matrices. Except for measurement gates, a gate’s matrix must be *unitary* and thus preserve appropriate invariants of quantum values’ amplitudes.

A *measurement* operation extracts classical information from a quantum value. It collapses the value to a basis state with a probability related to the value’s amplitudes (*measurement probability*), e.g., measuring  $\frac{1}{\sqrt{2}}(|0\rangle + |1\rangle)$  collapses the value to  $|0\rangle$  with probability  $\frac{1}{2}$ , and likewise for  $|1\rangle$ , returning classical value 0 or 1, respectively. A more general form of quantum measurement is *partial measurement*, which measures a subset of qubits in a qubit array; such operations often have simultaneity effects due to entanglement, *i.e.*, in a Bell pair  $\frac{1}{\sqrt{2}}(|00\rangle + |11\rangle)$ , measuring one qubit guarantees the same outcome for the other – if the first bit is measured as 0, the second bit is too.

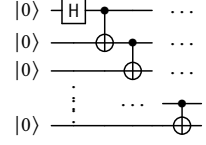


Fig. 13. GHZ Circuit

### A.2 Connecting Pauli Strings and Second Quantization

There are many interpretations of creators and annihilators in second quantization based on different particle types, which QBLUE classifies them in our type system. The basic form is the creators and annihilators in a *two-dimensional boson-like particle system* with  $t(2)$  typed sites: the lowering  $a$  and raising  $a^\dagger$  operations in ladder algebra, with the semantic rules below. In this system, as shown above, applying a single creator  $a^\dagger$  (having the matrix representation  $\begin{pmatrix} 0 & 0 \\ 1 & 0 \end{pmatrix}$ ) turning  $|0\rangle$  to  $|1\rangle$ , but it eliminates  $|1\rangle$  to be  $O$ , while applying a single annihilator  $a$  (having the matrix representation  $\begin{pmatrix} 0 & 1 \\ 0 & 0 \end{pmatrix}$ ) turning  $|1\rangle$  to  $|0\rangle$ , but it eliminates  $|0\rangle$  to be  $O$ .

$$\begin{aligned} a^\dagger |0\rangle &= |1\rangle & a^\dagger |1\rangle &= O & a |1\rangle &= |0\rangle & a |0\rangle &= O \\ a^\dagger \circ a |1\rangle &= |1\rangle & a^\dagger \circ a |0\rangle &= O & a \circ a^\dagger |0\rangle &= |0\rangle & a \circ a^\dagger |1\rangle &= O \\ a^\dagger \circ a \otimes a \circ a^\dagger |1\rangle |0\rangle &= |1\rangle |0\rangle & a^\dagger \circ a \otimes a \circ a^\dagger |b_1\rangle |b_2\rangle &= O & \text{if } b_1 \neq 1 \vee b_2 \neq 0 \end{aligned}$$

We define the  $\mathbb{0}$  and  $\mathbb{1}$  operations in Section 1 by composing creators and annihilators, *i.e.*,  $a^\dagger \circ a$ , defining  $\mathbb{1}$ , preserves  $|1\rangle$ , and  $a \circ a^\dagger$ , defining  $\mathbb{0}$ , preserves  $|0\rangle$ , as shown in the second line above. As an instance in a two qubit system,  $\frac{1}{\sqrt{2}}(|0\rangle |1\rangle + |1\rangle |0\rangle)$ , applying  $\mathbb{1}$  to the second site results the state  $\frac{1}{\sqrt{2}} |0\rangle |1\rangle$ <sup>10</sup>, by preserving  $|1\rangle$  in the second site. The composition effect can also deal with a composed state of multiple qubits, such as the third line above, with transitions below.

$$a^\dagger \circ a \otimes a \circ a^\dagger |1\rangle |0\rangle = a^\dagger \circ a \otimes a \circ a^\dagger (|1\rangle \otimes |0\rangle) = a^\dagger \circ a |1\rangle \otimes a \circ a^\dagger |0\rangle = |1\rangle |0\rangle$$

<sup>10</sup>This is the constraint semantics not the quantum dynamic unitary semantics, so operations are not necessarily unitary.

We can see that Pauli strings are a special case of tensor strings, as they can be constructed by performing the above two-dimensional lowering and raising operations. The identity operation  $I$  below is assumed to be two-dimensional.

$$\begin{array}{llll}
 I \triangleq \begin{bmatrix} 1 & 0 \\ 0 & 1 \end{bmatrix} & X \triangleq \begin{bmatrix} 0 & 1 \\ 1 & 0 \end{bmatrix} & Y \triangleq \begin{bmatrix} 0 & -i \\ i & 0 \end{bmatrix} & Z \triangleq \begin{bmatrix} 1 & 0 \\ 0 & -1 \end{bmatrix} \\
 I = a \circ a^\dagger + a^\dagger \circ a = \mathbb{0} + \mathbb{1} & X = a^\dagger + a & Y = ia - ia^\dagger & Z = a \circ a^\dagger - a^\dagger \circ a = \mathbb{0} - \mathbb{1}
 \end{array}$$

The second line above defines Pauli operations based on the two-dimensional lowering and raising operations above, with the matrix forms of the Pauli operations listed as the first line above. Here,  $i$  is a complex amplitude value, and  $ia - ia^\dagger$  is an abbreviation of  $ia + ((-i) a^\dagger)$ . Note that the meaning of Pauli groups in terms of second quantization differs from the gates in a quantum circuit, which provides a way of defining particle constraints by describing particle movements as spin rotations across  $X$ ,  $Y$ , and  $Z$  bases.

### A.3 Linear Sums and Quantum Choices

A linear sum in a state connects kets in Figure 2 represents superposition state; the sum operation  $e_1 + e_2$  is reinterpreted a *quantum choice* operation, in the sense that one can perform either  $e_1$  or  $e_2$  to the state  $\psi$  at the same time, e.g., it might produce a superposition if  $\psi$  is a state just initialized as a ket.

When second-quantization users employ quantum choices to constrain a lattice-based molecular system, they typically have two intentions. The *first intention* is to "create" a state going in two different directions simultaneously in a possible superposition. For example, applying a quantum choice operation  $a + a^\dagger$  on a  $t(4)$  particle state  $|1\rangle$ , with state *normalization*, results in the following:

$$\frac{1}{\sqrt{2}} |0\rangle + \frac{1}{\sqrt{2}} |2\rangle$$

In the Hubbard system  $\hat{H}$ , for each  $j$ -th site, the sum of the two terms,  $a^\dagger(j) \circ a(j+1)$  and  $a^\dagger(j+1) \circ a(j)$ , model all the possibilities of electrons, being relocated to adjacent particle site. Normalization means that the norm of the amplitudes in different kets must be summed to 1, referring to the total probabilities of different parts. State normalization permits Hamiltonian simulation and quantum computing, while the non-normalized state plays a role in computing expectation values. In the extended version of QBLUE, we permit a *nor* operation to normalize a state. Quantum simulation is essentially defined as  $\exp(-ir\hat{H})\psi(0)$  for arbitrary state  $\psi(0)$ , applying  $\exp(-ir\hat{H})$  to a normalized state  $\psi(0)$ . We show a theorem in Section 4.6 to link simulations on normalized and non-normalized states.

The *second intention* is to add repulsion, i.e., we view a quantum choice term as some extra force applied to the system to increase or decrease the probability of observing a basis vector state. Recall that the normalization procedure ensures that a system's total probability is 1. Conceptually, adding a quantum choice term for certain basis vectors with a positive or negative amplitude increases or reduces the choice of observing the basis vectors, respectively. For example, the term  $z_u \sum_j \mathbb{1}(j) \circ \mathbb{1}(j+1)$ , in the Hubbard system (Section F), usually refers to the repulsion force, reducing the likelihood of the happening of some basis vectors. Let's name the above term as  $\hat{H}_u$  and the term  $-z_t \sum_j (a^\dagger(j) \circ a(j+2) + a^\dagger(j+2) \circ a(j))$  as  $\hat{H}_t$ . Notice that the complex amplitudes  $-z_t$  and  $z_u$  have opposite signs. Applying the whole Hamiltonian to a quantum state  $\psi$  results in a quantum state of two pieces:  $(\hat{H}_t\psi) + (\hat{H}_u\psi)$ , connected by  $+$ . A non-zero ket in the state  $\hat{H}_t\psi$  has an amplitude with an opposite sign as the same basis-vector amplitude in  $\hat{H}_u\psi$ , which means that the sum of their amplitudes is reduced; thus, the quantum choice term  $\hat{H}_u$  acts as a penalty for a

specific group of ket states. To see how this happens, realize that the Hubbard system describes  $t(2)$  typed particles, so there are four cases of the basis vectors of two adjacent particles:

$$|0\rangle_0 |0\rangle_1 \quad |0\rangle_0 |1\rangle_1 \quad |1\rangle_0 |0\rangle_1 \quad |1\rangle_0 |1\rangle_1$$

Assuming that we are dealing with a single particle site, the  $\hat{H}_u$  term turns all basis vectors, except  $|1\rangle_0 |1\rangle_1$ , to 0, where  $|1\rangle_0 |1\rangle_1$  actually represents two electrons in opposite spins. Assume that a single  $t(2, 2)$  typed particle state  $\varphi$  contains the ket  $z |1\rangle_0 |1\rangle_1$ , applying  $\hat{H}_u$  to a state  $\varphi$  results in a ket  $z_u * z |1\rangle_0 |1\rangle_1$ . When applying  $\hat{H}_t$  to  $\varphi$ , we expect to have another ket  $-z_t * z |1\rangle_0 |1\rangle_1$ , with the same basis vector as above. The sum of the two sub-parts turns the amplitude of the basis vector  $|1\rangle_0 |1\rangle_1$  to become  $z * (z_u - z_t)$ , with  $|z * (z_u - z_t)| \leq |z|$ . This is why the additional repulsion term acts as a penalty on the ket  $|1\rangle_0 |1\rangle_1$  to reduce its probability of happening.

#### A.4 Energy Expectation Value Calculation.

Other than Hamiltonian simulation, another key application is the energy state computation based on expectation value calculation, described above. One of the central pieces in energy state computation is to find the exact ground state energy expectation value  $E_0$  and the state  $\psi$  holding the energy value. Based on the variational principle, the expectation value of the Hamiltonian over all possible states  $\psi$  is minimized:

$$E_0 = \min_{\psi} \psi^\dagger (\hat{H} \psi)$$

The exact ground state can be obtained by minimizing this expectation value over all possible normalized states. In QBLUE, we compile the computation to HPC software through classical optimization techniques, such as gradient descent methods, to “guess” the minimal expectation value and its associated state of a given Hamiltonian. Many HPC particle computation platforms use other sophisticated techniques based on the guessing-out strategy. For example, Gamess [Schmidt et al. 1993; Zahariev et al. 2023] and NWChem [Aprà et al. 2020] are HPC software to compute energy states of chemical molecule structures, and users can define the structures in second quantization in the software. The quantum supremacy of the energy state calculation problems is murky, as some researchers [Lee et al. 2023] do not believe in the existence of such supremacy. Nevertheless, the typical way to calculate in quantum computers is through the variational quantum eigensolver concept [Tilly et al. 2022b], having similar procedures as the HPC counterpart.

#### A.5 Direct Sum and Quantum State and Hilbert spaces

Section 4.1 provides a Hilbert space state representation for QBLUE, this section expands the background of constructing high dimensional Hilbert spaces based on the direct sum concept.

Assuming that readers are familiar with *inner product spaces*, vector spaces equipped with an inner product [Axler 2015, p. 167]. A finite-dimensional *Hilbert space* is simply a finite-dimensional inner product space [Nielsen and Chuang 2011, p. 66]. The definition of Hilbert space is restricted in the infinite-dimensional case, but we are only concerned with finite dimensions in this work. All of our Hilbert spaces will be denoted with the letter  $\mathcal{H}$  and will be over the field  $\mathbb{C}$  of complex numbers.

Dirac Bra-ket notation is a convenient notation for describing vectors and operators in Hilbert spaces. A vector is written using ket notation, writing “ $|Q\rangle$ ” rather than “ $\vec{x}_Q$ ” used in other areas of mathematics. The inner product of any vectors  $|\phi\rangle$  and  $|\psi\rangle$  is written  $\langle\phi|\psi\rangle$ , and is linear in the second argument  $|\psi\rangle$ . The outer product, written  $|\phi\rangle\langle\psi|$ , is the linear operator defined such that  $|\phi\rangle\langle\psi|\psi'\rangle = \langle\psi|\psi'\rangle \cdot |\phi\rangle$ , where “ $\cdot$ ” denotes scalar multiplication. It is often useful to treat a “ket”  $|\psi\rangle$  as a *column vector* and a “bra”  $\langle\psi| = |\psi\rangle^\dagger$  as a *row vector* (where “ $\dagger$ ” denotes the conjugate transpose), and then both the inner and outer product are simply matrix multiplication.

$$\begin{aligned}
|\phi\rangle &\triangleq \begin{bmatrix} a \\ b \end{bmatrix} & |\psi\rangle &\triangleq \begin{bmatrix} c \\ d \\ e \end{bmatrix} \\
|\phi\rangle \oplus |\psi\rangle &= \begin{bmatrix} a \\ b \\ c \\ d \\ e \end{bmatrix} & |\phi\rangle \otimes |\psi\rangle &= \begin{bmatrix} ac \\ ad \\ ae \\ bc \\ bd \\ be \end{bmatrix} \\
E_A &\triangleq \begin{bmatrix} f & g & h & i \\ j & k & l & m \\ n & o & p & q \end{bmatrix} & E_A \oplus E_B &= \begin{bmatrix} f & g & h & i & 0 & 0 \\ j & k & l & m & 0 & 0 \\ n & o & p & q & 0 & 0 \\ 0 & 0 & 0 & 0 & r & s \\ 0 & 0 & 0 & 0 & t & u \\ 0 & 0 & 0 & 0 & v & w \end{bmatrix} \\
E_B &\triangleq \begin{bmatrix} r & s \\ t & u \\ v & w \end{bmatrix} \\
E_A \otimes E_B &= \begin{bmatrix} fr & fs & gr & gs & hr & hs & ir & is \\ ft & fu & gt & gu & ht & hu & it & iu \\ fv & fw & gv & gw & hv & hw & iv & iw \\ jr & js & kr & ks & lr & ls & mr & ms \\ jt & ju & kt & ku & lt & lu & mt & mu \\ jv & jw & kv & kw & lv & lw & mv & mw \\ nr & ns & or & os & pr & ps & qr & qs \\ nt & nu & ot & ou & pt & pu & qt & qu \\ nv & nw & ov & ow & pv & pw & qv & qw \end{bmatrix}
\end{aligned}$$

Fig. 14. Matrix examples for direct sums and tensor products

To distinguish a quantum state with computational basis-vector, QBLUE write quantum states  $|\psi\rangle$  and  $|\phi\rangle$  as  $\psi$  and  $\phi$ , we denote row vectors as  $\phi^\dagger$  and  $\psi^\dagger$ . The inner product is written as  $\phi \psi^\dagger$ .

Our algebraic data types in this paper rely on two ways of composing Hilbert spaces: (external) direct sums  $\oplus$  and tensor products  $\otimes$ . Given two Hilbert spaces  $\mathcal{H}_M$  and  $\mathcal{H}_N$  with  $\dim(\mathcal{H}_M) = M$  and  $\dim(\mathcal{H}_N) = N$ , the direct sum and tensor product are defined so that  $\dim(\mathcal{H}_M \oplus \mathcal{H}_N) = M + N$  and  $\dim(\mathcal{H}_M \otimes \mathcal{H}_N) = M \cdot N$ . These operators apply to Hilbert spaces, as well as vectors and operators within these spaces. For example, if  $|\phi\rangle \in \mathcal{H}_M$  and  $|\psi\rangle \in \mathcal{H}_N$ , then  $|\phi\rangle \oplus |\psi\rangle \in \mathcal{H}_M \oplus \mathcal{H}_N$  and  $|\phi\rangle \otimes |\psi\rangle \in \mathcal{H}_M \otimes \mathcal{H}_N$ , and if  $E_M : \mathcal{H}_{M,1} \rightarrow \mathcal{H}_{M,2}$  and  $E_N : \mathcal{H}_{N,1} \rightarrow \mathcal{H}_{N,2}$  are linear operators, then  $E_M \oplus E_N : \mathcal{H}_{M,1} \oplus \mathcal{H}_{N,1} \rightarrow \mathcal{H}_{M,2} \oplus \mathcal{H}_{N,2}$  is also a linear operator, as well as  $E_M \otimes E_N : \mathcal{H}_{M,1} \otimes \mathcal{H}_{N,1} \rightarrow \mathcal{H}_{M,2} \otimes \mathcal{H}_{N,2}$ .

The tensor product will be familiar to anyone with a basic understanding of quantum computing. It is used to describe *joint states*. If a qubit inhabits a two-dimensional Hilbert space  $\mathcal{H}_2$ , and a qutrit inhabits a three-dimensional Hilbert space  $\mathcal{H}_3$ , then the six-dimensional Hilbert space  $\mathcal{H}_2 \otimes \mathcal{H}_3$  describes a physical system containing a qubit and a qutrit, possibly entangled. In the context of programming languages, tensor products correspond nicely to *product types*.

Qubit arrays serve as a sufficient physical model for most of the interesting results in quantum computing. An  $n$ -qubit system is described by a  $2^n$ -dimensional Hilbert space, which is what allows quantum computing to achieve its famed exponential advantages. For a programmer, however, this

can be fairly limiting for expressiveness, effectively restricting one's data types to those whose cardinality is a power of two. To allow for arbitrary finite data types, the direct sum is useful, serving as an "OR" where the tensor product serves as "AND." The five-dimensional Hilbert space  $\mathcal{H}_2 \oplus \mathcal{H}_3$  describes quantum states that are *either* a qubit *or* a qutrit, or a superposition of the two.

These constructions may be more intuitive given matrix representations. The direct sum of two vectors is their concatenation, while the direct sum of two matrices is their block diagonalization, as shown by the examples in Figure 14.

Suppose Hilbert space  $\mathcal{H}_M$  is spanned by an orthonormal basis  $B_M$ , and Hilbert space  $\mathcal{H}_N$  is spanned by an orthonormal basis  $B_N$ . Then  $\mathcal{H}_M \oplus \mathcal{H}_N$  is spanned by an orthonormal basis  $\{|u\rangle \oplus 0 : |u\rangle \in B_M\} \cup \{0 \oplus |v\rangle : |v\rangle \in B_N\}$ , and  $\mathcal{H}_M \otimes \mathcal{H}_N$  is spanned by an orthonormal basis  $\{|u\rangle \otimes |v\rangle : |u\rangle \in B_M, |v\rangle \in B_N\}$ . The following identities may be useful for understanding operations on these spaces.

$$\begin{aligned}
(|\phi_0\rangle \oplus |\psi_0\rangle) + (|\phi_1\rangle \oplus |\psi_1\rangle) &= (|\phi_0\rangle + |\phi_1\rangle) \oplus (|\psi_0\rangle + |\psi_1\rangle) \\
z (|\phi\rangle \oplus |\psi\rangle) &= z |\phi\rangle \oplus z |\psi\rangle \\
(|\phi\rangle \oplus |\psi\rangle)^\dagger &= \langle\phi| \oplus \langle\psi| \\
(\langle\phi_0| \oplus \langle\psi_0|) (|\phi_1\rangle \oplus |\psi_1\rangle) &= \langle\phi_0|\phi_1\rangle + \langle\psi_0|\psi_1\rangle \\
(E_M \oplus E_N) (|\phi\rangle \oplus |\psi\rangle) &= E_M |\phi\rangle \oplus E_N |\psi\rangle \\
z |\phi\rangle \otimes |\psi\rangle &= |\phi\rangle \otimes z |\psi\rangle \\
&= z (|\phi\rangle \otimes |\psi\rangle) \\
(|\phi\rangle \otimes |\psi\rangle)^\dagger &= \langle\phi| \otimes \langle\psi| \\
(\langle\phi_0| \otimes \langle\psi_0|) (|\phi_1\rangle \otimes |\psi_1\rangle) &= \langle\phi_0|\phi_1\rangle \cdot \langle\psi_0|\psi_1\rangle \\
(E_M \otimes E_N) (|\phi\rangle \otimes |\psi\rangle) &= E_M |\phi\rangle \otimes E_N |\psi\rangle
\end{aligned}$$

## B Error Bound Lemmas for Trotterization

The Coq proof of the standard Trotterization relies on a key error bound lemma below.

LEMMA B.1 (ERROR BOUND FOR TROTTERIZATION). Given  $\hat{H} = \sum_{i=1}^N \hat{H}_i$  and time  $r$ , we have error bound as below:

$$\|\Pi_{i=1}^N \exp(-ir\hat{H}_i) - \exp(-ir\hat{H})\| \leq \frac{r^2}{2} \sum_{k=1}^N \left\| \left( \sum_{j=k+1}^N \hat{H}_j \right) \circ \hat{H}_k - \hat{H}_k \circ \left( \sum_{j=k+1}^N \hat{H}_j \right) \right\|.$$

Here  $\|\cdot\|$  denotes the operator norm.

The Coq proof scratch of Theorem B.1 is listed below.

PROOF.

$$\begin{aligned}
& \Pi_{i=1}^N \exp(-ir\hat{H}_i) - \exp(-ir\hat{H}) \\
&= \Pi_{i=1}^N \exp(-ir\hat{H}_i) - \exp(-ir \sum_{j=N}^N H_j) \cdot \Pi_{i=1}^{N-1} \exp(-ir\hat{H}_i) \\
& \quad + \exp(-ir \sum_{j=N}^N H_j) \cdot \Pi_{i=1}^{N-1} \exp(-ir\hat{H}_i) - \exp(-ir \sum_{j=N-1}^N H_j) \cdot \Pi_{i=1}^{N-2} \exp(-ir\hat{H}_i) \\
& \quad + \dots \\
& \quad + \exp(-ir \sum_{j=2}^N H_j) \cdot \Pi_{i=1}^1 \exp(-ir\hat{H}_i) - \exp(-ir\hat{H})
\end{aligned}$$

Using the triangle inequality of operator norm, we get

$$\|\Pi_{i=1}^N \exp(-ir\hat{H}_i) - \exp(-ir\hat{H})\| \quad (1)$$

$$\leq \sum_{k=1}^N \|\exp(-ir \sum_{j=k+1}^N \hat{H}_j) \cdot \Pi_{i=1}^k \exp(-ir\hat{H}_i) - \exp(-ir \sum_{j=k}^N \hat{H}_j) \cdot \Pi_{i=1}^{k-1} \exp(-ir\hat{H}_i)\| \quad (2)$$

$$\leq \sum_{k=1}^N \|\exp(-ir \sum_{j=k+1}^N \hat{H}_j) \cdot \exp(-ir\hat{H}_k) - \exp(-ir \sum_{j=k}^N \hat{H}_j)\| \quad (3)$$

$$\leq \frac{r^2}{2} \sum_{k=1}^N \|(\sum_{j=k+1}^N \hat{H}_j) \circ \hat{H}_k - \hat{H}_k \circ (\sum_{j=k+1}^N \hat{H}_j)\|. \quad (4)$$

Step (2) is from the triangle inequality of operator norm; step (3) is because the norm of a unitary matrix is 1; step (4) can be proved by an inductive proof, which shows

$$\|\exp(-irB) \circ \exp(-irA) - \exp(-ir(A+B))\| \leq \frac{r^2}{2} \|B \circ A - A \circ B\|. \quad (5)$$

□

The Coq proof for QDrift relies on a key error bound lemma below. Here, we rely on the concept of a superoperator of a quantum state. Quantum physicists have two main ways to mathematically represent a quantum state: a *pure* state is represented by a state *vector* as in Figure 2, while a *mixed* state is represented by a density *operator* (or density *matrix*). A computation on a pure state is described by a linear operator from the input Hilbert space to the output Hilbert space, while a computation on mixed states is described by a *superoperator*, a sort of higher-order function that acts as a linear operator from density operators to density operators.

LEMMA B.2 (ERROR BOUND FOR QDRIFT). Given  $\hat{H} = \sum_{i=0}^{d-1} \theta_i \hat{H}_i$  and time  $r$ , where  $\theta_i$  is positive and is decided by normalizing the terms such that  $\max_i \|H_i\| = 1$ . Let  $\lambda = \sum_i \theta_i$ . We randomly sample  $N$  times among the terms following the probability distribution that the frequency of  $H_i$  in the sampled list is  $\theta_i/\lambda$ . Let  $\vec{j} = \{j_1, j_2, \dots, j_N\}$  denote the order of the sampling where  $j_k \in [1, d]$ , and create superoperator  $L$  and  $L_i$  for the Hamiltonian which satisfies that for any quantum state  $\psi$ , with its density operator  $\rho = \psi \psi^\dagger$ ,  $L(\rho) = -i(\hat{H}\rho - \rho\hat{H})$  and  $L_i(\rho) = -i(\hat{H}_i\rho - \rho\hat{H}_i)$ . Then we can get the following error bound:

$$\|\Pi_{k=1}^N \exp(-i\frac{\lambda r}{N} L_{j_k}) - \Pi^N \exp(-i\frac{r}{N} L)\|_\diamond \leq \frac{2\lambda^2 r^2}{N}.$$

Here  $\|\cdot\|_\diamond$  denotes the diamond norm.

The Coq proof scratch of Theorem B.2 is listed below.

PROOF. Based on the definition of superoperators  $L\rho = i(\hat{H}\rho - \rho\hat{H})$ , triangle inequality of diamond norm, and  $\|\rho\|_\diamond = 1$ , we can get  $\|L\|_\diamond \leq \|H\| \leq 2\lambda$ .

Similarly, as  $\max_i \|H_i\| = 1$ , we have  $\|L_i\|_\diamond \leq \|H_i\| \leq 2$ .

In each step of QDrift, a randomly chosen gate is  $\varepsilon = \sum_i \frac{\theta_i}{\lambda} \exp(-i\frac{\lambda r}{N} L_i)$ .

It is compared to  $\mu = \exp(-irL/N)$ .

Using the expansion of  $\exp(-irA) = \sum_{n=0}^{\infty} \frac{(ir)^n A^n}{n!}$ , we can get  $d = \|\mu - \varepsilon\|_\diamond \leq 2 \sum_{n=2}^{\infty} \frac{1}{n!} (\frac{2\lambda r}{N})^n$ .

Using  $\sum_{n=2}^{\infty} \frac{x^n}{n!} \leq \frac{x^2}{2} e^x$ , we get  $d \leq \frac{2\lambda^2 r^2}{N^2} e^{2\lambda r/N} \simeq \frac{2\lambda^2 r^2}{N^2}$ .

Thus, the total error of the  $N$  random sampling satisfies  $D \leq Nd \leq \frac{2\lambda^2 r^2}{N} e^{2\lambda r/N} \simeq \frac{2\lambda^2 r^2}{N}$ . So we get the claimed error bound.  $\square$

### C Gate Syntheses in Analog Quantum Machines

At the quantum computer machine level, every gate is implemented as the simulation of a gate Hamiltonian over a certain time period. To define a unitary gate  $U$ , theoretically, we need to find its snapshot Hamiltonian by taking the logarithm  $-i\log(U)$ . Since  $U$  is usually small, we typically perform reverse engineering by computing the eigendecomposition of  $U$  and forming a  $t(2)$ -typed Hamiltonian  $\hat{H}_U$  based on the eigenstates found through eigendecomposition, and simulates the gate based on  $\exp(-ir\hat{H}_U)$  with respect to time  $r$ . We show below the simulation of a Hadamard (H) and controlled-not (CX) gate, with respect to time period  $\pi$ .

$$\hat{H}_H = \frac{1}{2\sqrt{2}} \cdot (X + Z) \quad H = \exp(-i\pi\hat{H}_H)$$

$$\hat{H}_H = \left(\frac{1}{2} - \frac{\sqrt{2}}{4}\right) \cdot \mathbb{0} + \left(\frac{1}{2} - \frac{\sqrt{2}}{4}\right) \cdot \mathbb{1} + \left(-\frac{\sqrt{2}}{4}\right) \cdot X \quad H = \exp(-i\pi\hat{H}_H)$$

The above formula is the one-particle Hamiltonian for simulating a Hadamard gate (H). To reverse engineer the Hamiltonian, we perform an eigendecomposition on Hadamard gates (H), find an eigenstate  $\psi = -\sin(\frac{\pi}{8})|0\rangle + \cos(\frac{\pi}{8})|1\rangle$ . We can then construct Hadamard Hamiltonians by the matrix multiplication  $\psi \circ \psi^\dagger$ , which is the QBLUE Hamiltonian  $\hat{H}_H$  above. The Hadamard gate (H) can then be defined as a simulation of the Hamiltonian, as  $H = \exp(-i\pi\hat{H}_H)$ , with the time period  $\pi$ . Similarly, we can find the two-particle Hamiltonian for a controlled-not gate (CX) through eigendecomposition and implement it in QBLUE, as shown below. The gate can then be defined as a simulation of the Hamiltonian as  $CX = \exp(-i\pi\hat{H}_{CX})$ , with the time period  $\pi$ .

$$\hat{H}_{CX} = \mathbb{1} \otimes \left(-\frac{1}{2} \cdot X + \frac{1}{2} \cdot I\right) \quad CX = \exp(-i\pi\hat{H}_{CX})$$

In short, matrix exponential operations turn a Hamiltonian snapshot into a quantum system simulation, while a matrix logarithm operation, modeled in QBLUE, reverses a simulation to a Hamiltonian snapshot. For example, by applying a matrix logarithm on the H and CX gates, we might find a set of results, and  $\hat{H}_H$  and  $\hat{H}_{CX}$  are in the set <sup>11</sup>.

**Hamiltonian for Better Compilation.** Finding the right target machine Hamiltonian to simulate a gate, i.e., gate synthesis, is usually referred to as control pulse level quantum programming [Li et al. 2022a; Tacchino et al. 2019] as control pulses can theoretically be described as *target machine Hamiltonians*, and previous work [Peng et al. 2024] has discovered the advantage of compiling

<sup>11</sup>Matrix logarithms are not unique. QBLUE fixes the uniqueness by choosing one implementation. However, the QBLUE type system and equivalence relations are general enough without relying on the specific implementation.

system Hamiltonians directly to target machine Hamiltonians by bypassing the series of simulations of individual gates. To see how this bypassing works, we simulate a simple 1D Ising model system, describing phase transition and quantum magnetism behaviors in insulating magnetic systems.

$$\hat{H}_{I_2} = \sum_j Z(j) \circ Z(j+1) + z_h \sum_j X(j) \quad (3.3.2)$$

The  $\hat{H}_{I_2}$  equation is a special 1D Ising model with uniformed interaction strength, where the first terms in the quantum choice represent the particle interactions, while the second terms represent effects from the external transverse magnetic field, with  $z_h$  being the external transverse magnetic field strength. Simulating the system with respect to a time period  $r$  is equivalent to compiling the exponent  $\exp(-ir\hat{H}_{I_2})$  to quantum computers. The main step involves the Trotterization procedure, a technique that splits  $\hat{H}_{I_2}$  into small Hamiltonians, executed in sequence, each of which is implementable in a target machine Hamiltonian. One small target machine Hamiltonian is  $Z(j) \circ Z(j+1)$ , applying on  $j$ -th and  $j+1$ -th qubits, with respect to a very small time period  $\frac{r}{n}$ , i.e., Trotterization tries to find a large number  $n$  so the simulation of many small time periods  $\frac{r}{n}$  can correctly approximate the simulation of the original system Hamiltonian. The result of gate synthesizing on the machine Hamiltonian, as to find gates representing  $\exp(-i\frac{r}{n}Z(j) \circ Z(j+1))$ , is shown as the left-hand side circuit in Figure 11, performing the circuit program, performing two controlled-not gates and an  $Rz(2\frac{r}{n})$  gate in the middle for the  $j$ -th and  $j+1$ -th qubits, i.e.,  $Rz(\theta)$  is an  $z$ -axis phase rotation gate. As we mentioned above, these quantum gates are eventually simulated as Hamiltonians in pulse-level programming.

On the other hand, instead of performing the sequence of the three gate simulations above, one can directly implement the small Hamiltonian in an IBM machine, which supports direct pulse level programming and provides the  $ZZ$  interaction gate shown as the right in Figure 11; the special gate essentially simulates the target machine Hamiltonian  $Z(j) \circ Z(j+1)$  in a much more effective way than the above gate synthesis step. The bypass demonstrates the potential for improving compilation effectiveness. In many cases, even if one is willing to implement system Hamiltonians as circuit gates, it is still valuable for them to notice the potential optimization done through the above procedure, definable in QBLUE, as many optimization frameworks [Hietala et al. 2023; Xu et al. 2022] decompose a  $ZZ$  gate as the three gates above, which is counterproductive.

## D Perturbative Gadget

Below, we show the perturbative gadget algorithm.

*Definition D.1 (Perturbative Gadget).* Let  $\hat{H}^{\text{target}}$  be a  $k$ -local Hamiltonian acting on  $n$  qubits, expressed as

$$\hat{H}^{\text{target}} = \sum_{j=1}^N r_j \hat{P}_j,$$

where each  $\hat{P}_j$  is a tensor product of  $k$  single-qubit Pauli operators acting on a subset of the  $n$  computational qubits:

$$\hat{P}_j = \mathcal{P}_{j,1} \otimes \mathcal{P}_{j,2} \otimes \cdots \otimes \mathcal{P}_{j,k}.$$

To simulate  $\hat{H}^{\text{target}}$  using only two-local interactions, we construct a *gadget Hamiltonian*  $\hat{H}^{\text{gad}}$ , acting on the original  $n$  computational qubits together with  $Nk$  ancilla qubits. The gadget Hamiltonian is defined as:

$$\hat{H}_{\text{gad}} = \sum_{j=1}^N \hat{H}_j^{\text{anc}} + \lambda \sum_{j=1}^N \hat{H}_j^{\text{y}},$$

where

$$\hat{H}_j^{\text{anc}} = \frac{1}{2} \sum_{1 \leq m < n \leq k} (I - Z(m(j)) \circ Z(n(j))),$$

and

$$\hat{H}_j^{\text{y}} = \sum_{n=1}^N r_{j,n} \mathcal{P}_{j,n}(n) \circ X(n(j)), \quad \text{with} \quad r_{j,n} = \begin{cases} r_j, & \text{if } n = 1, \\ 1, & \text{otherwise.} \end{cases}$$

Here,  $X(n(j))$  and  $Z(n(j))$  are Pauli operators acting on the  $n$ -th ancilla qubit associated with the  $j$ -th term. This construction ensures that all terms in  $\hat{H}^{\text{gad}}$  involve only two-qubit interactions.

We show below the two lemmas for perturbative gadget, which are mechanized in Rocq.

LEMMA D.2 (EFF HAMILTONIAN EXISTANCE). Let  $\hat{H}^{\text{target}}$  and  $\hat{H}^{\text{gad}}$  be defined as in Theorem D.1, and suppose the perturbation strength satisfies  $\lambda \leq \lambda_{\text{max}}$ , where

$$\lambda_{\text{max}} = \frac{k-1}{4} \left( \sum_{j=1}^N |r_j| + N(k-1) \right)^{-1}.$$

Then, there exists a function  $f(\lambda) = O(\text{poly}(\lambda))$  and a constant  $\Xi = O(\text{poly}(k))$  such that the effective Hamiltonian satisfies

$$\hat{H}^{\text{eff}}(\hat{H}^{\text{gad}}, 2n) = \frac{\lambda^k}{\Xi} \hat{H}^{\text{target}} \otimes |0\rangle\langle 0|^{\otimes rk} + f(\lambda) \Pi + O(\lambda^{k+1}),$$

where  $\Pi$  is the projector onto the support of  $\hat{H}^{\text{eff}}(\hat{H}^{\text{gad}}, 2n)$ .

LEMMA D.3 (PERTURBATIVE GADGET CORRECTNESS). Let  $\hat{H}^{\text{target}}$  and  $\hat{H}^{\text{gad}}$  be as in Theorem D.2. Then there exists a perturbation threshold  $\lambda^*$ , with

$$\lambda^* \ll \lambda_{\text{max}} \quad \text{and} \quad \lambda^* \ll \frac{E_1^{\text{target}} - E_0^{\text{target}}}{\Xi \|O_{\text{err}}\|},$$

such that for all  $\lambda \leq \lambda^*$ , the ground states  $\psi_0 = |\psi_0\rangle\langle\psi_0|$  of  $\hat{H}^{\text{target}}$  and  $\phi_0 = |\phi_0\rangle\langle\phi_0|$  of  $\hat{H}^{\text{gad}}$  satisfy:

$$\|\psi_0 - \text{Tr}_{\text{aux}}[\phi_0]\|_2 = O(\lambda),$$

where  $\text{Tr}_{\text{aux}}[\cdot]$  denotes the partial trace over all ancilla qubits.

We can now demonstrate the entire pipeline's compilation correctness, including the error introduced by the perturbative gadget algorithm.

THEOREM D.4 (COMPILATION CORRECTNESS INCLUDING PERTURBATIVE GADGET). Given  $e$ , typed as  $\iota \vdash e \triangleright \mathcal{F}^h(\iota)$ , and a time period  $r$ , we compile the simulation  $\exp(-ir e)$  to quantum circuit, via the compilation pipeline  $\mathcal{F}^h(\iota) \vdash (e, r) \gg U : \mathcal{F}^u(\iota')$ , for every state  $\psi$ , typed as  $\iota \vdash \psi$ , we transform it to  $\psi'$ , typed as  $\iota' \vdash \psi'$ , let  $\psi_1 = \llbracket \iota \vdash U \triangleright \mathcal{F}^u(\iota) \rrbracket_0(\psi)$ , we transform  $\psi_1$  to  $\psi'_1$ , typed as  $\iota' \vdash \psi'_1$ ; thus,  $\|\psi'_1 - \llbracket \iota' \vdash \exp(-ier) \triangleright \mathcal{F}^u(\iota') \rrbracket_0(\psi')\| < \epsilon + O(\lambda)$ .

## E Other Particle Transformation Methods

Section 5.1 provides a simple particle transformation method. We introduce another transformation method, the Bravyi-Kitaev transformation, which might result in more effective compilation.

The Bravyi-Kitaev mapping stores the parity of fermionic modes in a nonlocal Fenwick tree data structure. A Fenwick tree is a partial ordering of binary representations where each node is a copy of its parent with one of the ones changed to zero. This structure allows encoding fermionic operators with Pauli weight scaling as  $O(\log m)$  for  $m$  fermionic modes.

Each fermionic mode corresponds to a qubit associated with a node in the Fenwick tree. Each qubit stores the total parity of the fermionic modes below it in the tree. Fermionic creation and annihilation operators can be constructed using three key subsets of the Fenwick tree: the update set  $U(\alpha)$ , parity set  $P(\alpha)$ , and flip set  $F(\alpha)$ . They act as follows:

$$a_i \mapsto \frac{1}{2} \left( \bigotimes_{j \in U(i)} X_j \otimes X_i \otimes \bigotimes_{j \in P(i)} Z_j + i \bigotimes_{j \in U(i)} X_j \otimes Y_i \otimes \bigotimes_{j \in P(i) \setminus F(i)} Z_j \right),$$

$$a_i^\dagger \mapsto \frac{1}{2} \left( \bigotimes_{j \in U(i)} X_j \otimes X_i \otimes \bigotimes_{j \in P(i)} Z_j - i \bigotimes_{j \in U(i)} X_j \otimes Y_i \otimes \bigotimes_{j \in P(i) \setminus F(i)} Z_j \right).$$

*Definition E.1 (Update Set  $U(\alpha)$ ).* Let the update set  $U(\alpha)$  be such that  $\beta \in U(\alpha)$  if and only if there exists an index  $i_0$  such that  $\alpha_{i_0} = 0$ , and for all  $i > i_0$ ,  $\alpha_i = \beta_i$ , and for all  $i < i_0$ ,  $\beta_i = 1$ . Equivalently,  $\beta \in U(\alpha)$  if and only if  $\alpha \prec \beta$  in the Fenwick tree partial order.

*Definition E.2 (Parity Set  $P(\alpha)$ ).* The parity set  $P(\alpha)$  contains elements  $\beta \in P(\alpha)$  if and only if there exists an index  $i_0$  such that  $\alpha_{i_0} = 1$ ,  $\beta_{i_0} = 0$ , for all  $i > i_0$ ,  $\beta_i = \alpha_i$ , and for all  $i < i_0$ ,  $\beta_i = 1$ . This implies

$$\prod_{j \in P(i)} q_j = \prod_{j < i} f_j.$$

*Definition E.3 (Flip Set  $F(\alpha)$ ).* The flip set  $F(\alpha)$  contains elements  $\beta \in F(\alpha)$  if and only if there exists an index  $i_0$  such that  $\beta_{i_0} = 0$ ,  $\beta_i = \alpha_i$  for all  $i \neq i_0$ , and for all  $i < i_0$ ,  $\alpha_i = 1$ . This implies

$$\prod_{j \in F(i)} q_j = \prod_{j < i} f_j.$$

We show an example of transforming the T-J model via the BK-transformation in Section G.4.

## F A Hubbard Model for Hydrogen Chains

The Hubbard model (system) describes the interactions between elementary particles, specifically focusing on the electrons having fermionic behavior. Here, we focus on the one-dimensional Hydrogen chain, one of the most quintessential systems described using the Hubbard system, which consists of many sites of  $t^{\mathbb{N}}(2)$  typed Hydrogen atoms (fermions). Section 2 describes a two-site version for this system, as we list the simplified version below.

$$\hat{H}_T = -z_t \sum_j \left( a^\dagger(j) : t^{\mathbb{N}}(2) \circ a(j+1) : t^{\mathbb{N}}(2) + a^\dagger(j+1) : t^{\mathbb{N}}(2) \circ a(j) : t^{\mathbb{N}}(2) \right) + z_u \sum_j \mathbb{1}(j) : t^{\mathbb{N}}(2) \circ \mathbb{1}(j+1) : t^{\mathbb{N}}(2)$$

We explain the physical constraints of the two terms in the Hamiltonian. The first accounts for the energy due to the movement (hopping) of electrons, whereas the second term accumulates the energy due to electron repulsion. As the atoms are arranged in a one-dimensional array, the

---

**Algorithm 4** Generate Update Set  $U(\alpha)$ 

---

```

1: Input: Fermionic index  $\alpha$ , number of modes  $n$ 
2: Output: Update set  $U(\alpha)$ 
3: updateSet  $\leftarrow \emptyset$ 
4:  $l \leftarrow$  bit-length of  $\alpha$ 
5: for  $i = 0$  to  $l - 1$  do
6:   if bit  $i$  of  $\alpha$  is 0 then
7:     Create  $\beta$  by setting bit  $i$  of  $\alpha$  to 1 and bits  $< i$  to 0
8:     if  $\beta < n$  then
9:       Add  $\beta$  to updateSet
10:    end if
11:  end if
12: end for
13: Return updateSet

```

---



---

**Algorithm 5** Generate Parity Set  $P(\alpha)$ 

---

```

1: Input: Fermionic index  $\alpha$ 
2: Output: Parity set  $P(\alpha)$ 
3: paritySet  $\leftarrow \emptyset$ 
4:  $l \leftarrow$  bit-length of  $\alpha$ 
5: for  $i = l - 1$  down to 0 do
6:   if bit  $i$  of  $\alpha$  is 1 then
7:     Create  $\beta$  by setting bit  $i$  to 0 and bits  $< i$  to 1
8:     Add  $\beta$  to paritySet
9:   end if
10: end for
11: Return paritySet

```

---



---

**Algorithm 6** Generate Flip Set  $F(\alpha)$ 

---

```

1: Input: Fermionic index  $\alpha$ 
2: Output: Flip set  $F(\alpha)$ 
3: flipSet  $\leftarrow \emptyset$ 
4:  $i \leftarrow 0$ 
5: while bit  $i$  of  $\alpha$  is 1 do
6:   Create  $\beta$  by setting bit  $i$  to 0
7:   Add  $\beta$  to flipSet
8:    $i \leftarrow i + 1$ 
9: end while
10: Return flipSet

```

---

electrons can only move (hop) to the neighboring adjacent atoms, such as moving from  $j$ -th to  $j+1$ -th site, in this system.

When simulating the Hubbard system, users typically attempt to manipulate different  $z_t$  and  $z_u$  values to utilize the Hubbard system for analyzing various particle behaviors. In simulating the Hydrogen chain [Melo et al. 2021], we assign a constant to  $z_t$  and make  $z_u$  dependent on the time

periods. For a period of  $T$ ,  $z_u$  will transit from the initial value  $z_{u0}$  at time  $t = 0$  to the final value  $z_{uf}$  at time  $t = T$ , and the equation looks like  $z_u(t) = (1 - \frac{t}{T})z_{u0} + \frac{t}{T}z_{uf}$ .

**Determining the Parameters  $z_t$  and  $z_u$  in Hubbard System.** The parameters  $z_t$  and  $z_u$  in the Hubbard system are crucial for accurately describing the physical system. For a 1D chain of hydrogen atoms, these parameters can be determined as follows:

1. **Hopping Integral  $z_t$ :** The hopping integral  $z_t$  represents the kinetic energy associated with an electron hopping from one site to another. It can be estimated using the overlap integral of the atomic orbitals on neighboring sites. For hydrogen atoms, the 1s orbitals are used. The hopping integral can be calculated as:

$$z_t = \int \psi_{1s}^*(r - R_i) \hat{H} \psi_{1s}(r - R_j) dr$$

where  $\psi_{1s}(r)$  is the 1s orbital wave function,  $\hat{H}$  is the Hamiltonian of the system, and  $R_i$  and  $R_j$  are the positions of the neighboring atoms. In practice, this integral is often approximated using empirical or computational methods, such as density functional theory (DFT).

2. **On-Site Interaction  $z_u$ :** The on-site interaction  $z_u$  represents the Coulomb repulsion between two electrons occupying the same site. For hydrogen atoms, this can be approximated using the Coulomb integral:

$$z_u = \int \psi_{1s}^*(r_1) \psi_{1s}^*(r_2) \frac{e^2}{|r_1 - r_2|} \psi_{1s}(r_1) \psi_{1s}(r_2) dr_1 dr_2$$

where  $e$  is the electron charge, and  $\psi_{1s}(r)$  is the 1s orbital wave function. This integral can also be evaluated using computational techniques, providing an estimate of the electron repulsion energy at each site.

$$\mathfrak{N} ::= \uparrow \mid \downarrow$$

$$\begin{aligned} & \text{S-TEN} \\ & \llbracket \frac{\iota \vdash e \triangleright \mathcal{F}^\zeta(\iota) \quad \iota' \vdash e' \triangleright \mathcal{F}^\zeta(\iota')}{\iota \otimes \iota' \vdash e \otimes e' \triangleright \mathcal{F}^\zeta(\iota \otimes \iota')} \rrbracket_g (w_1 \otimes w_2) := \llbracket \iota \vdash e \triangleright \mathcal{F}^\zeta(\iota) \rrbracket_g w_1 \otimes \llbracket \iota' \vdash e' \triangleright \mathcal{F}^\zeta(\iota') \rrbracket_{S(\iota)(w_1)(g)} w_2 \\ & S(t^\uparrow(m))(l_j)(g_1, g_2) = (g_1 + j, g_2) \quad S(t^\downarrow(m))(l_j)(g_1, g_2) = (g_1, g + j) \\ & S(t(m))(l_j)(g_1, g_2) = (g_1, g_2) \quad S(\iota \otimes \iota')(\eta \otimes \eta')(g) = S(\iota')(\eta') (S(\iota)(\eta)(g)) \end{aligned}$$

Fig. 15. Extended QBLUE to spinning fermions.

**Including Spin Terms.** In the traditional Hubbard model, there are two types of fermions, spin-up ( $\uparrow$ ) and spin-down ( $\downarrow$ ) fermions. In constraining the system, we can think of the two kinds of fermions as two different particles and split the fermion type flag  $\mathfrak{N}$  in the QBLUE, into two different type flags  $\uparrow$  and  $\downarrow$ . We then rewrite the semantic rule for S-TEN to be the one in Figure 15. The main difference is to modify the context  $g$  to become a pair of real numbers, one for recording the effects of each type of the two fermions. We can then rewrite the Hubbard model equation above to the one below.

$$\hat{H}_T = -z_t \sum_j \left( a^\dagger(j) \circ a(j+2) + a^\dagger(j+2) \circ a(j) \right) + z_u \sum_{\text{even}(j)} \mathbb{1}(j) \circ \mathbb{1}(j+1)$$

In the new Hamiltonian, we model the  $\uparrow$  and  $\downarrow$  fermions to appear alternatively; that is, odd-indexed sites store the  $\uparrow$  fermion, and even-indexed sites store the  $\downarrow$  fermion. The first term in the Hamiltonian restricts that fermions can only reach same kind fermion sites, e.g.,  $a^\dagger(j) \circ a(j+2)$

means that the disappearing of a fermion in the  $j+2$  site results in the fermion appearing in the  $j$ -th site. The second term above is a constraint that we restrict the appearing of opposite kind fermions in the adjacent sites, e.g.,  $\mathbb{1}(j) \circ \mathbb{1}(j+1)$  means that  $j$ -th and  $j+1$ -th sites are not likely to have fermions occupied at the same time. Since the term is a sum over  $\text{even}(j)$ , the above restriction only constrains the same kind of fermions.

## G Other Physical Models Definable in QBLUE

Here, we show many other systems that are definable in QBLUE.

### G.1 Ising Model

The Ising model is one of the simplest quantum spin lattice models. It considers spins that can be in one of two states (up or down) interacting with their nearest neighbors. The Hamiltonian for the quantum Ising model in a transverse field is given by:

$$H = -J \sum_{\langle i,j \rangle} Z(i) \circ Z(j) - h \sum_i X(i) \quad (6)$$

where  $J$  represents the interaction strength between neighboring spins,  $h$  is the external magnetic field (which is a constant), and the sum  $\langle i, j \rangle$  runs over all pairs of nearest neighbors.

### G.2 Heisenberg Model

The Heisenberg model includes interaction in all three spin components. Its Hamiltonian is expressed as:

$$H = -J \sum_{\langle i,j \rangle} (X(i) \circ X(j) + Y(i) \circ Y(j) + Z(i) \circ Z(j)) \quad (7)$$

In this model,  $J$  represents the interaction strength, and the  $S$  terms are spin- $\frac{1}{2}$  operators, allowing for complex spin interactions.

### G.3 XY Model

The XY model restricts interactions to the X and Y axis components. Its Hamiltonian is:

$$H = -J \sum_{\langle i,j \rangle} (X(i) \circ X(j) + Y(i) \circ Y(j)) \quad (8)$$

The quantum spin lattice models are fundamental for understanding quantum phase transitions, magnetic properties, and many-body quantum phenomena. They provide a rich framework for exploring quantum correlations, entanglement, and the effects of quantum fluctuations on macroscopic systems.

### G.4 t-J Model

The t-J model is a pivotal framework in condensed matter physics for exploring high-temperature superconductivity in cuprate materials. Originating from the Hubbard model in the limit of strong on-site Coulomb repulsion, it prohibits double occupancy of lattice sites, thereby allowing for a focused analysis of electron hopping and spin interactions. This approach is key to understanding superconductivity and magnetism in strongly correlated electron systems.

**Hilbert Space.** The Hilbert space  $\mathcal{H}$  excludes states with double occupancy. Basis states  $|s_1, s_2, \dots, s_N\rangle$  represent each site as empty (0), occupied by an electron with spin up ( $\uparrow$ ), or spin down ( $\downarrow$ ). This space is formally defined as:

$$\mathcal{H} = \{|s_1, s_2, \dots, s_N\rangle : s_i \in \{0, \uparrow, \downarrow\} \forall i\}$$

**Hamiltonian.** The Hamiltonian  $H$  includes terms for electron mobility and spin interactions:

$$H = -t \sum_{\langle ij \rangle, \sigma} (a^\dagger(i, \sigma) \circ a(j, \sigma) + a^\dagger(j, \sigma) \circ a(i, \sigma)) + J \sum_{\langle ij \rangle} (\mathbf{S}(i) \cdot \mathbf{S}(j) - \frac{1}{4} \mathbb{1}(i) \circ \mathbb{1}(j))$$

**Hopping Term** ( $-t$ ). Allows electrons to move between adjacent sites, governed by:

$$-t \sum_{\langle ij \rangle, \sigma} (a^\dagger(i, \sigma) \circ a(j, \sigma) + a^\dagger(j, \sigma) \circ a(i, \sigma))$$

**Spin-Spin Interaction Term** ( $J$ ). Models antiferromagnetic interactions:

$$J \sum_{\langle ij \rangle} (\mathbf{S}(i) \cdot \mathbf{S}(j) - \frac{1}{4} \mathbb{1}(i) \circ \mathbb{1}(j))$$

**Spin Operators and Pauli Matrices.**

$$S^x(i) = \frac{\hbar}{2} X, \quad S^y(i) = \frac{\hbar}{2} Y, \quad S^z(i) = \frac{\hbar}{2} Z$$

For further details, see [Anderson 1997; Auerbach 1994; Sachdev 2011].

**Transformed t-J Model.** The Jordan-Wigner transformation allows us to map the fermionic operators in the t-J model into spin operators. Below is the transformed t-J model for a one-dimensional lattice system.

**Hopping Term.** The fermionic hopping terms in the t-J model are transformed as follows:

$$-t \sum_{\langle i, j \rangle} \left( \exp \left( i\pi \sum_{l=i}^{j-1} n_l \right) S_i^+ \circ S_j^- + \text{h.c.} \right), \quad (9)$$

where  $S_i^+$  and  $S_j^-$  are spin raising and lowering operators at sites  $i$  and  $j$ , respectively. The term  $n_l = \frac{1}{2}(I - Z)$  corresponds to the number operator after transformation, and the exponential term arises due to the non-local string of  $Z$  operators, ensuring the preservation of fermionic anticommutation relations.

**Spin-Spin Interaction Term.** The exchange interaction term, crucial in the t-J model, transforms into:

$$J \sum_{\langle i, j \rangle} \left( \frac{1}{2} (S_i^+ \circ S_j^- + S_i^- \circ S_j^+) + S_i^z \circ S_j^z \right), \quad (10)$$

where the terms now involve combinations of the spin raising, lowering, and z-component operators, indicative of the transformed spin interactions.

**Transformed t-J Model via BK transformation.** In the context of the t-J model, the Bravyi-Kitaev transformation enables the efficient simulation of electron dynamics and spin interactions on a quantum computer. The transformed Hamiltonian in the Bravyi-Kitaev framework for the t-J model takes the form:

$$\hat{H}_{t-J}^{\text{BK}} = -t \sum_{\langle m, j \rangle, \sigma} \left( \frac{1}{2} (\hat{Q}(m) \circ \hat{X}(m) - i\hat{Q}(m) \circ \hat{Y}(n)) \frac{1}{2} (\hat{Q}(j) \circ \hat{X}(j) + i\hat{Q}(j) \circ \hat{Y}(j)) + \text{h.c.} \right) + J \sum_{\langle m, j \rangle} (\mathbf{S}(m) \cdot \mathbf{S}(j) - \frac{1}{4} \mathbb{1}(m) \circ \mathbb{1}(j))$$

where  $S(m)$  and  $\mathbb{1}(m)$  are expressed in terms of qubit operators using the Bravyi-Kitaev encoding. The hopping terms ( $t$ ) and the spin-spin interaction terms ( $J$ ) now involve the manipulation of qubits instead of fermions, which is more natural for quantum computational frameworks.

The Bravyi-Kitaev transformation offers improved scaling of quantum resources compared to the Jordan-Wigner transformation and can be crucial for implementing quantum simulations of condensed matter systems in practice.

The Bravyi-Kitaev transformation provides a significant advantage in quantum simulation by mapping fermionic algebra to qubit operations more efficiently than the Jordan-Wigner transformation. It is especially useful in the context of quantum computing, where it enables more effective resource utilization and can potentially lead to faster quantum algorithms for simulating many-particle systems in condensed matter physics.